NEDO-24757
80NED056
Class I
July 1980

MARK II CONTAINMENT SUPPORTING
PROGRAM

CAORSO SAFETY RELIEF VALVE DISCHARGE TESTS PHASE II TEST REPORT

DISCLAIMER OF RESPONSIBILITY

The only undertakings of the General Electric Company respecting information in this document are contained in the contracts for Mark II Containment Consulting Services between the General Electric Company and each of the members of the U.S. Mark II Owners Group, effective variously June 9,1975, June 13,1975, or July 29,1975, and nothing contained in this document shall be construed as changing the contracts. The use of this information by anyone other than the members of the U.S. Mark II Owners Group either themselves or through their technical consultants, or for any purpose other than that for which it is intended under the contracts, is not authorized; and with respect to any unauthorized use, the General Electric Company makes no represenation or warranty, express or implied, and assumes no liability of any kind as to the completeness, accuracy, usefulness or non-infringing nature of the information contained in this document.

REVIEW AND APPROVAL SHEET
FOR
PHASE II TEST REPORT NEDO-24757

MARK II CONTAINMENT SUPPORTING PROGRAM

CAORSO SAFETY RELIEF VALVE
DISCHARGE TESTS
PHASE II TEST REPORT

Reviewed: _____
R. J. Muzzy, Manager
Mark II Containment Design

Reviewed: _____
P. Valandani, Manager
Containment SRV
Performance Engineering

Reviewed: _____
J. D. Gilman, Manager
Dynamic and Seismic Analysis

Approved: _____
P. W. Ianni, Manager
Containment Design

Approved: _____
A. E. Rogers, Manager
Containment Technology

Approved: _____
E. O. Swain, Manager
Piping Design

Approved: _____
W. F. English, Manager
Dynamic Loads & Stress
Analysis

CONTRIBUTORS TO PHASE II TEST REPORT NEDO-24757

J. J. Holan

H. L. Hwang

C. T. Kawate

C. S. Lin

S. Mintz

D. Ashley - NUS

B. Dawson - NUS

C. Kropp - AMN

CONTENTS

CONTENTS (Continued)

CONTENTS (Continued)

APPENDICES

ILLUSTRATIONS

ILLUSTRATIONS (CONTINUED)

TABLES

ACRONYMS

SVA	-	Single Valve First Actuation
CVA	-	Single Valve Consecutive Action
MVA	-	Multiple Valve Actuation
NWL	-	Normal Water Level in Safety Relief Valve Discharge Line
EWL	-	Elevated Water Level in Safety Relief Valve Discharge Line
DWL	-	Depressed Water Level in Safety Relief Valve Discharge Line
LP	-	Low Reactor Pressure
LV	-	Leaking Valve
VB	-	SRVDL Vacuum Breaker
CP	-	Cold Pipe
WP	-	Warm Pipe
HP	-	Hot Pipe
SRV	-	Safety Relief Valve
SRVDL	-	Safety Relief Valve Discharge Line
PCM	-	Pulse Code Modulation
PSD	-	Power Spectral Density
CPSD	-	Cross Power Spectral Density
RTD	-	Resistance Temperature Detector
SG xx	-	Strain Gage xx
P xx	-	Pressure Transducer xx
PT xx	-	Pressure Transducer xx (A labeling distinction between pressure transducers P xx and PT xx is made only because the sensor at location PT xx was originally installed as a temperature sensor and then replaced with a pressure transducer prior to the start of testing.)

T xx - Temperature Sensor xx

LVDT xx - Displacement Sensor xx

L xx - Level Probe xx

TL xx - Level Probe xx
(A labeling distinction between level probes L xx and TL xx is made only because the sensor at location TL xx was originally installed as a temperature sensor and then replaced with a level probe prior to the start of testing.)

VP1 - Vacuum Breaker Position Indicator

VB2 - Vacuum Breaker Butterfly Valve Position Indicator

DFFR - Dynamic Forcing Function Information Report - Revision 3

RPV - Reactor Pressure Vessel

VAP - SRV Stem Position Indicator for Valve A

VEP - SRV Stem Position Indicator for Valve E

VFP - SRV Stem Position Indicator for Valve F

VUP - SRV Stem Position Indicator for Valve U

AC - Air Clearing

WC - Water Clearing

ABSTRACT

This report presents the results of the Phase II in-plant safety relief valve (SRV) discharge tests conducted at the Caorso Nuclear Station in Italy during January and February 1979. These tests represent the second of two phases of the Caorso SRV discharge tests which included single valve first actuations at normal and low reactor pressures, single valve first and consecutive valve actuation tests with leaking and non-leaking SRV's and multiple valve actuation tests using two, three, four and eight valves. The results of the first phase of testing, which included only single valve first and consecutive valve actuation at normal reactor pressures, were provided in a previous report.

The results of the Phase II tests show that all test data exhibit excellent repeatability and consistency within allowable limits of the acceptance criteria. Further, these results are applicable for use in the Mark II Containment Supporting Program.

1. INTRODUCTION

1.1 BACKGROUND

In-plant safety relief valve (SRV) discharge tests were performed at the Caorso Nuclear Station in Italy as part of the Mark II Containment Supporting Program. These tests were conducted in conjunction with normal plant startup testing to provide in-plant measurements of loads that may be imposed on suppression pool and containment structures, and on nuclear steam supply system components as a result of SRV actuations. A detailed description of the test plan for these tests is given in the Test Plan Document.*

This report presents the test results from the 53 test actuations conducted in January and February 1979 during the second phase of Caorso testing. The results from the first phase of Caorso testing are reported in the Phase I Test Report.**

1.2 TEST OBJECTIVES

The overall objective of the Caorso SRV test program is to obtain SRV discharge test data as applicable to Boiling Water Reactor (BWR) plants utilizing the X-quencher SRV discharge device. Figures 1-1 through 1-4 are schematics of the type of containment configuration and quencher device tested. General data on the SRV and SRVDL vacuum breakers used in Caorso are presented in Table 1-1.

The specific areas of interest addressed by the Phase II tests are:

a. Suppression pool boundary pressures
b. Containment dynamic response
c. SRV discharge line clearing and reflood transients
d. Quencher structural response
e. Submerged structure loads
f. Suppression pool thermal mixing
g. Containment liner and downcomer vent structural response

*C.T. Kawate, et al., "Caorso Relief Valve Loads Tests - Test Plan," NEDM-20988, Revision 2, Addendum 1, October 1977, Addendum 2, April 1978.
**G.M. Bjorkquist et al., "Caorso SRV Discharge Tests Phase I Test Report," NEDE-25100-P, May 1979.

Items (a) through (e) are covered in this report. Items (f) and (g) will be covered in other reports.

1.3 REPORT SUMMARY

A summary of the principal observations is presented in Section 2. Description of the test plan procedure, the data acquisition system from the sensors through the pulse code modulation (PCM) tape outputs, and the data reduction process from the PCM tape outputs through the final outputs in the form of engineering data plots are presented in Sections 3, 4 and 5, respectively.

Descriptions of the data evaluation methods, phenomenon, comparisons with data predictions or acceptance criteria as appropriate to the report, and evaluations of the data plots concerning hydrodynamic phenomenon, quencher response, and containment response are presented in Sections 6, 7 and 8, respectively.

Table 1-1

GENERAL DATA - SRV and SRVDL VACUUM BREAKER

Safety Relief Valve

Manufacturer:	Dikkers
Cat. Number:	ALS G471
Valve Type:	123 mm Pilot Operated Safety/Relief Valve
Size - Inlet:	6 inches
- Outlet:	10 inches
Throat Diameter:	4.84 inches
Design Temperature (at SRV inlet):	608°F
Set Pressure Range	1165 - 1205 psig
Capacity:	861300 - 890500 lb/hr

SRVDL Vacuum Breaker

Manufacturer:	Atwood and Morrill Co.
Model Number:	10" - 300# 13680-01
Valve Type:	Straight through with swinging disc
Line Size:	10 inches
Throat Diameter:	10 inches
Flow Area:	78.54 in.^{2}
Flow Coefficient ($A\sqrt{K}$):	0.2 feet^2
Design Conditions (at valve throat):	
Flow:	14000 ft^3/min
Pressure:	14.7 psia
Temperature:	100°F
Delta P:	-7 psi
Service Conditions (maximum conditions in SRVDL at VB location):	
Pressure:	500 psig
Temperature:	470°F
Cycles:	5000

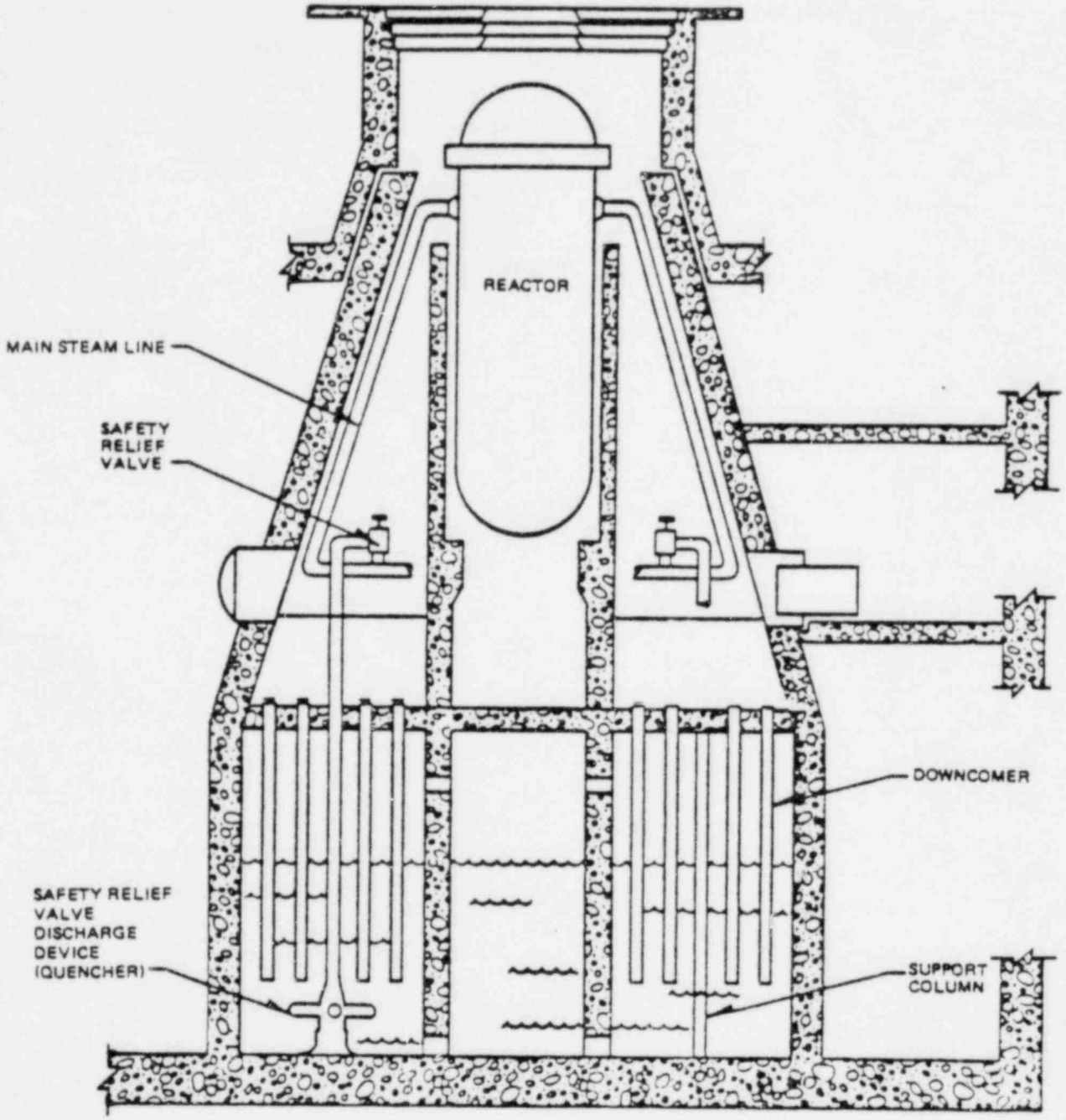

Figure 1-1. Mark II Pressure Suppression Containment

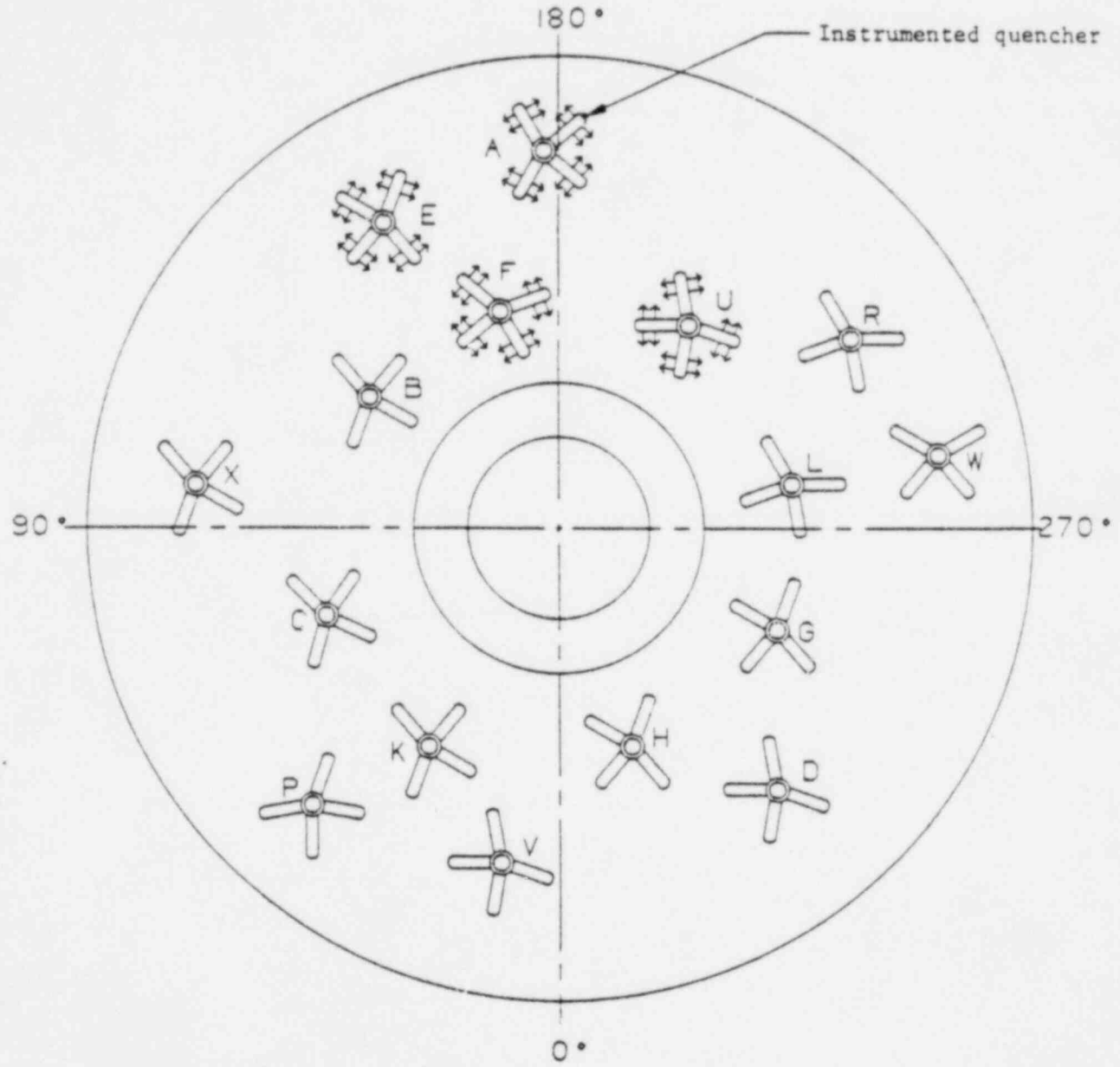

Figure 1-2. Orientation of Safety Relief Valve Discharge Quenchers Within Caorso Suppression Pool

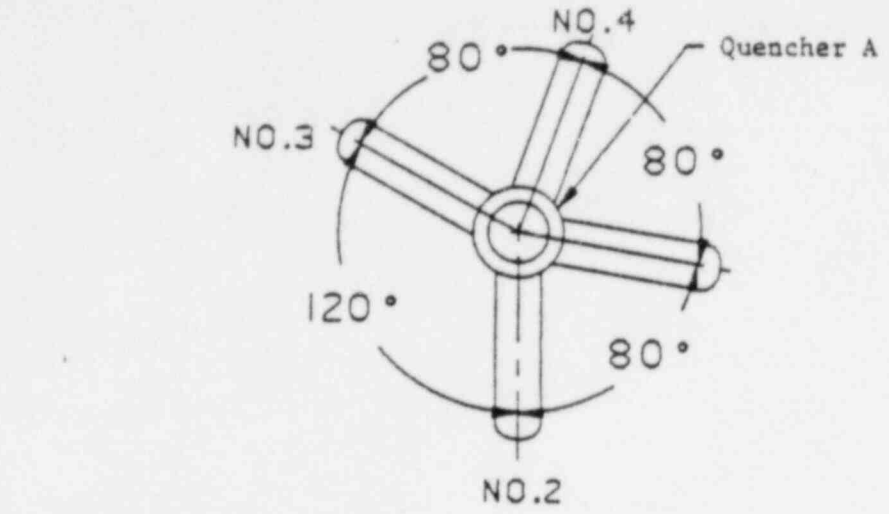

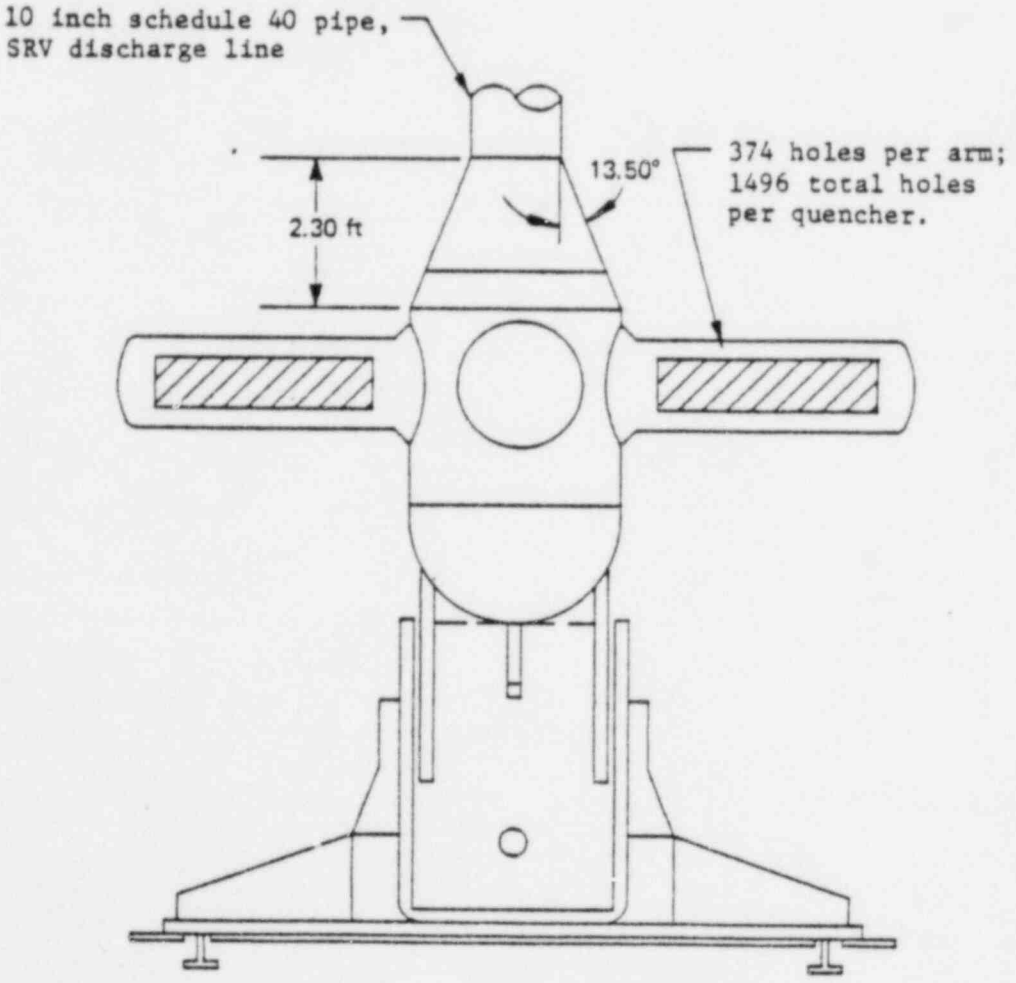

Figure 1-3. Caorso Quencher and Support

Figure 1-4. Quencher Arm
(GENERAL ELECTRIC COMPANY PROPRIETARY)

2. SUMMARY OF PRINCIPAL OBSERVATIONS

2.1 HYDRODYNAMIC

2.1.1 Internal Pressure Loads in the SRVDL and Quencher (Reference Subsection 6.3)

During Phase II testing, the highest SRVDL pressure of 345 psia was measured at a point near the SRV. The maximum internal quencher pressure of 677 psia was measured in the conical transition section between the SRVDL and quencher. Both of these pressures were recorded during CVA, WP, EWL tests. A comparison of these results with Phase I test results shows excellent repeatability for tests with similar initial conditions. As in Phase I the SRVDL and quencher internal pressures tended to increase with increased initial water leg volumes. MVA and LV tests resulted in maximum SRVDL and quencher pressures similar to those observed during SVA and CVA tests.

The low reactor pressure (LP) tests resulted in lower SRVDL and quencher internal pressures than the tests under full reactor pressure.

2.1.2 SRVDL Reflood Transient (Reference Subsection 6.4)

The reflood data of SRVDL A from the Phase II testing confirmed findings of the Phase I tests. Generally, the peak SRVDL reflood level was between 1 and 5 feet above NWL. After the first excursion, the water level dropped below NWL and remained there for the duration of the transient and oscillated about an equilibrium point for 30 to 50 seconds.

Initial test conditions did not have any apparent effects on the reflood transient, except in the LV tests where the equilibrium point seemed to be below that for non-leaking valve tests.

2.1.3 Suppression Pool Boundary Pressures Due to SRVDL Clearing (Reference Subsection 6.5)

Results from both the Phase I and II tests showed excellent repeatability of the data for tests under similar initial conditions. The maximum positive and negative pressures for any tests were 9.4 and -6.6 psid measured during a CVA, HP, DWL (Valve U). As in Phase I the CVA tests resulted in somewhat higher boundary pressures than SVA tests. The maximum floor pressures (Sensor P19) of 8.2 and -4.3 psid were measured during a CVA, HP, DWL test (Valve A), as compared to 5.0 and -4.0 psid for a SVA, CP, NWL test (Valve A). The maximum boundary pressures measured during a CVA, WP, EWL test were 5.4 and -3.9 psid.

LV tests had low positive boundary pressure peaks of 3.8 psid (maximum) on the first actuation. The negative peaks, however, were within normal range (-5.7 psid maximum). In LV, CVA tests the initial conditions did not differ significantly from initial conditions for the non-leaking valve CVA tests with the same initial pipe temperature. Consequently, the peak boundary pressures were also similar.

MVA tests resulted in peak boundary pressures no higher than those measured during SVA tests.

LP tests show that all boundary pressures obtained under the reduced RPV conditions were lower than those resulting from full reactor pressure tests.

The boundary pressure waveforms for all non-leaking valve tests observed during both Phase I and Phase II tests were characterized by one or two high frequency (25 to 30 Hz) oscillations followed by four or five lower frequency oscillations in the 5 to 10 Hz range.

During the first actuation of the LV tests the initial pressure peaks were followed by an oscillation of higher frequency than observed in non-leaking valve tests (approximately 20 Hz). The CVAs of the LV tests, however, exhibited the same waveform characteristics as the non-leaking valve tests.

The MVA tests did not result in any significantly altered waveforms, although most MVA test pressure histories were more irregular than those for the SVA tests. The most conspicuous difference was in the energy content distribution because some of the MVA tests had significant energy content in the 20 to 60 Hz range, while their dominant frequencies were still in the 5 to 10 Hz range as in SVA and CVA tests. Lower reactor pressures did not result in any change to the boundary pressure oscillation frequency.

2.1.4 SRVDL Clearing Loads on Submerged Structures (Reference Subsection 6.6)

The highest pressure difference of 4.8 psid measured across a submerged structure was recorded during a SVA, CP, NWL test. With one exception, in every test the maximum pressure difference measured across any submerged structure was less than the maximum positive boundary pressure.

2.1.5 Suppression Pool Boundary Pressures Due to Steam Condensation (Reference Subsection 6.7)

The maximum boundary pressure due to steam condensation observed during any Phase II test with normal pool water temperature was ±2.5 psid. The frequency of oscillations ranged from 65 to 95 Hz. During the extended discharge test the highest measured boundary pressures were ±3.3 psid at a pool temperature of 95°F. The boundary pressure measurements tended to increase slightly with pool temperature. Also, the range of frequency oscillation was broader for the extended discharge test (50 to 125 Hz).

Lower reactor pressures and steam flow rates produced lower steam condensation loads. During the two lowest reactor pressure tests (50 and 100 psig), intermittent condensation was observed after a brief period of smooth condensation. The maximum amplitude of the pressure oscillations during intermittent condensation was well below the maximum boundary pressures due to smooth steam condensation at full reactor pressure.

2.2 QUENCHER STRUCTURAL RESPONSE (Reference Section 7)

All dynamic vibratory stresses measured on the wetwell SRV piping, quencher hub, and quencher arms were less than 6200 psi. The maximum total stress, including dynamic vibratory stresses, weight stress and pressure stress was less than 8800 psi or two to three times less than Section III code allowable for occasional load.

There were no significant differences in measured stresses between the (SVA, CP, NWL) and (MVA, CP, NWL) tests. This indicates that blowdowns of quenchers adjacent to quencher A, i.e. quencher E, F, or U, resulted in negligible dynamic stresses on quencher A.

The average stresses in the wetwell SRV discharge piping just above quencher A for the (SVA, CP, NWL), (CVA, HP, DWL), (MVA, CP, NWL) and (LV, SVA) tests were 3220, 2910, 3110 and 3400 psi during water clearing, and 4160, 3070, 3490 and 3460 psi during air clearing.

Both air clearing and water clearing demonstrated about the same magnitude of stresses in the quencher hub. Hub stresses during air clearing were primarily due to a bending moment on the hub from loads imposed by the quencher arms. Hub stresses during water clearing were primarily due to high pressures in both the hub and the arms. The maximum measured stress was 4750 psi.

The pressure peak measured in the quencher during water clearing did not appear in the quencher hub stress measurements. This indicates that these peaks are of such short duration they do not have sufficient energy to stress the hub.

The average water clearing thrust loads for the (SVA, CP, NWL), (CVA, HP, DWL), (MVA, CP, NWL) and (LV, SVA) tests were 36 kips, 67 kips, 44 kips and 75 kips.

The linear thermal gradient stresses at the top and bottom of the quencher arms were much higher than at the quencher arm sides. After SRV closure

reflood of cold water into the SRVDL did not cause any significant negative linear thermal gradient stresses for the case studied.

Negligible responses were found in the wetwell SRVDL piping and all parts of the quencher during discharges at reactor pressures below 100 psig. At pressures above 100 psig, the responses were about in proportion to the pressures. The extended discharge test did not result in any increased stresses due to dynamic loads, because all the peak stresses occurred within 0.6 sec after SRV actuation.

2.3 CONTAINMENT DYNAMIC RESPONSE (Reference Section 8)

A significant scattering of data was observed for nearly identical SVA tests. The coefficients of variation ranged from 13 percent on the basemat to 25 percent at the top of the biological shield wall.

The repeatability of the tests was proved by the observation that responses from similar tests conducted during Phase I and Phase II agreed reasonably well in terms of magnitudes and frequency contents.

Responses to subsequent actuations generally enveloped those of the first actuations. Different structural modes were excited by the two types of actuations.

The responses increased, relative to single valve actuations, when multiple valves were actuated. However, the increase was substantially less than proportional to the number of valves actuated.

In multiple valve tests the responses were affected by the time phasing of valve actuations, but the effect was small in consideration of the scattering observed for identical single valve tests.

Leaking valve first actuation tests generally gave higher responses than SVA tests.

3. TEST PLAN AND PROCEDURE

3.1 TEST PLAN

A matrix of the SRV tests conducted during January and February of 1979 (Phase II testing) is shown in Table 3-1. Phase II testing included single valve first actuation tests at normal and low reactor pressures, single valve first and consecutive valve actuation tests with leaking and non-leaking SRVs, and multiple valve actuation tests using two, three, four and eight valves. A total of 53 tests were performed during the Phase II testing. The initial conditions for each test are shown in Table 3-2. A classification and summary of the tests according to their initial conditions is given as follows:

Test Condition		Number of tests performed
SVA, CP, NWL	Valve A, normal reactor pressure	5
	Valve A, low reactor pressure	6
	Valve U, two VBs	1
	Valve V, two VBs	1
CVA, WP, DWL	Valve A	4
CVA, WP, EWL	Valve A	1
CVA, HP, DWL	Valve A	7
	Valve U, two VBs	4
SVA, LV, DWL	Valve A	5
CVA, LV, DWL	Valve A	8

Test Conditions		Number of tests performed
CP, NWL, MVA	Valves A, F	2
	Valves A, E, F	1
	Valves A, E*, F, U	6
	Valves B, C, D, L	1
	Valves A**, B, D, H, K, L, R, V	1
	Total	53

Test conditions CP, WP and HP are qualitative descriptions of the SRV pipe temperature prior to a given SRV actuation. CP indicates that the pipe was cooled to the ambient temperature of the drywell/wetwell, which ranged from 85 to 100°F during the tests. WP indicates that one or two 5-second SRV actuations, an equivalent of 5 to 10 seconds of steady steam flow, preceded the test by less than 2 minutes and resulted in a pipe temperature between 100° and 300°F. HP indicates that the test was preceded by a steam flow through the SRVDL sufficient to heat the pipe to an average temperature above 300°F. The average SRVDL temperature before each test is given in Table 3-2.

All SRVDLs were equipped with two 10-inch vacuum breakers (VB). A typical arrangement of two VBs on an SRVDL is shown in Figure 3-2. However, for the test program one VB on line A was equipped with a butterfly valve to determine the effect of variable VB size, and instrumented to measure air flow through the VB. The other VB was blocked off as shown in the figure. The effective area ($A/\sqrt{K}$) of each VB as calculated from VB flow measurements was 0.24 ft^2.

Table 3-3 lists the timing of the SRV openings (starts of the main disc movement) for the MVA tests. The times elapsed between subsequent SRV actuations for CVA tests are listed in Table 3-1.

The duration of the valve actuations varied from 4 to 20 seconds with the exception of Test 40 which had a total discharge time of 13 minutes 7 seconds. Table 3-1 gives the actual discharge time for each test.

*Test 45-2, Valve E leaking (as determined by in-plant temperature sensors in the discharge line).
**Depressed water leg in SRVDL A due to some valve leakage.

3.2 TEST PROCEDURE

All SRVs were actuated manually by one to four persons. During each test run, on-line real time data from approximately 40 of the 236 test channels were monitored and evaluated. The brush recorder and reactor/plant data were reviewed after each test run for acceptability, and used as input for subsequent test planning.

3.2.1 Control of SRVDL Water Level

Previous experience with other in-plant SRV tests has shown that the SRVDL water level stabilizes below normal level after SRV closure due to excess air drawn it through the VB. An air bleed vent was installed on each SRVDL to ensure that the water level returned to normal level prior to each first actuation test. However, during the leaking valve tests the water level remained depressed even when the air bleed system was used. A schematic of the air bleed system is shown in Figure 3-1.

Prior to start of each first actuation (SVA or MVA) test, the air bleed system was operated for 5 minutes and closed 5 to 10 minutes before the start of testing. This system, however, was not operated between consecutive valve actuations, because this would not have been typical of a normal plant operation and would have also precluded an accurate measurement of the air volume in the discharge line. In the CVA tests the time intervals between actuations were predetermined from the reflood plots to establish the desired water level in the SRVDL, i.e. DWL, NWL or EWL.

3.2.2 Single Valve Tests

3.2.2.1 First Actuations

After verifying that all initial condition requirements were satisfied and communication had been established between the control room and the recording stations, the steady state data was collected. The actual test started with a 5-minute countdown. When the count reached 10 seconds all recording equipment was started, and the valve actuated at time zero. The valve was kept

open for a predetermined time and then closed. Reactor/plant data was recorded for at least 60 seconds, and structural and hydrodynamic data was recorded for at least 90 seconds following valve closure.

3.2.2.2 Consecutive Actuations

CVA tests were conducted in the same manner as the SVAs, except the valve was reopened after initial closure at various time intervals as specified in the test matrix (see Table 3-1) to attain the required water level in the SRVDL. Each CVA test series consisted of a first actuation followed by four subsequent valve openings. The reactor/plant data and structural and hydrodynamic data were recorded for 90 seconds after the final valve actuation in each test series.

3.2.3 Multiple Valve Tests

MVA tests were performed in much the same way as the SVA tests, except that one to four operators manually actuated the valves depending on the number of valves to be opened for any particular test. Each operator was responsible for actuating a maximum of two valves. Because synchronization depended upon the operators' skill and timing, many dry runs were performed. In every MVA test where data on the SRV main disc movement was available all the initial SRV main disc movements started within a time span of 0.15 second or less. In those tests where this data was not available, the maximum time lag between the valve actuation switch signals was 0.222 second. The exact timing sequence of the valve openings is given in Table 3-3. The valves were closed individually at approximately 5-second intervals. The recording of reactor/plant, structural and hydrodynamic data continued for at least 90 seconds after the last valve was closed.

3.2.4 Leaking Valve Tests

Following Test 2305 the outside pipe temperature measured by Sensor T21 immediately downstream of the SRV would not decrease below 220°F. Usually after the

normal 4 to 5 hour period between tests the temperature returned to 100 to 110°F. This high steady state pipe temperature indicated that steam was leaking through the SRV. The decision was made to proceed with the optional leaking valve tests as part of the test program.

The SRVDL air bleed system described in Paragraph 3.2.1 was used prior to SRV actuation for Tests 41 through 43. In spite of this, the water was depressed to a level between Sensors L9 and L6 (2.8 to 8 ft below NWL) prior to each of these leaking valve tests. Test 4401 was conducted without activating the air bleed system before the test to simulate the effect a leaking SRV would actually have during plant operation. Upon completion of the leaking valve tests the SRV seat was lapped and the normal test program resumed.

3.2.5 Low Pressure Tests

The low pressure tests are considered a part of the SVA tests described in Subparagraph 3.2.2.1, the only difference being the lower reactor operating pressure. These tests were performed to determine the dependence of the containment and SRVDL pressures on the reactor pressure during SRV discharge.

3.2.6 Extended Discharge Test

The procedure for the extended discharge test required cooling the suppression pool water to a temperature of 60°F using both loops of the RHR system.

The test was initiated about 4 hours after both loops had been turned off. The SRV remained open for 13 minutes and 7 seconds at which time the highest in-plant suppression pool temperature sensor measurement was 101.5°F.

Reactor/plant data was recorded for 90 seconds following valve closure. Recording of structural and hydrodynamic data was terminated 60 seconds after valve opening, and resumed again for approximately 90 seconds at the end of the test. Pool temperature measurements including those made by plant instrumentation were recorded during the entire test and for 20 minutes following SRV closure. The results of this test will be documented in a separate report.

3.3 ACCEPTANCE LEVEL CRITERIA

Plant safety was the primary consideration governing the performance of the Caorso test program. Assurance of plant operating conditions being maintained within safe limits during testing was controlled by key measurement points selected to constantly monitor for Level 1 and Level 2 acceptance criteria. Explanations of these criteria are given in Subsection 3.2 of the Phase I Test Report.*

A summary of the Level 1 and Level 2 criteria established for the Phase II tests is given in Table 3-4.

*G.M. Bjorkquist et al., "Caorso SRV Discharge Tests Phase I Test Report," NEDE-25100-P, May 1979.

Test[a]	Test Type	Valve	Pipe Temperature, Water Level	Reactor Pressure (psig)	Approximate Discharge Time (sec)
22A01	SVA	U	CP,NWL[b]	982	20
22A02	CVA	U	HP,DWL	982	5
22A03	CVA	U	HP,DWL	982	5
22A04	CVA	U	HP,DWL	982	5
22A05	CVA	U	HP,DWL	932	5
2301	SVA	A	CP,NWL[b]	980	5
2302	CVA	A	WP,DWL	980	5
2303	CVA	A	WP,DWL	980	5
2304	CVA	A	HP,DWL	980	5
2305	CVA	A	HP,DWL	980	5
2311	SVA	A	CP,NWL[b]	977	4
2312	CVA	A	WP,EWL	977	5
2313	CVA	A	HP,DWL	977	5
2314	CVA	A	HP,DWL	977	5
2315	CVA	A	HP,DWL	977	5
2321	SVA	A	CP,NWL[b]	967	20
2322	CVA	A	HP,DWL	967	5
2323	CVA	A	HP,DWL	967	5
2324	CVA	A	HP,DWL	967	5
2325	CVA	A	HP,DWL	967	5
24	MVA	A,F	CP,NWL[b]	982	5,10
25	MVA	A,F	CP,NWL[b]	977	5,10
26	MVA	A,E,F	CP,NWL[b]	973	5,10,15
27	MVA	A,E,F,U	CP,NWL[b]	969	5,10,15,20
28	MVA	A,E,F,U	CP,NWL[b]	970	5,10,15,20
29	MVA	A,E,F,U	CP,NWL[b]	970	5,10,15,20
30	MVA	A,E,F,U	CP,NWL[b]	980	5,10,15,20
45-1	MVA	A,E,F,U	CP,NWL[b]	980	5,10,15,20
45-2	MVA	A,E,F,U	CP,NWL[b]	982	5,10,15,20
31	MVA	B,C,D,L	CP,NWL[b]	985	5,10,15,20
32	MVA	A,B,D,H K,L,R,V	CP,NWL[b]	973	20
33	SVA	A	CP,NWL[b]	50	20
34	SVA	A	CP,NWL[b]	100	20
35	SVA	A	CP,NWL[b]	215	20
36	SVA	A	CP,NWL[b]	400	20
37	SVA	A	CP,NWL[b]	601	20
38	SVA	A	CP,NWL[b]	802	20
39	SVA	A	CP,NWL[b]	977	20
40	SVA	A	CP,NWL[b]	975	787
41	SVA	A	WP,DWL[b]	976	5
42	SVA	A	WP,DWL[b]	977	5
43	SVA	A	WP,DWL[b]	980	5

Table 3-1
CAORSO PHASE II SRV TEST MATRIX

Valve On Date	Valve On Time (hr:min:sec)	CVA Valve Closed Time (sec)	Comments
1/20/79	13:51:47	15	
1/20/79	13:52:22	15	Two 10-in. vacuum breakers
1/20/79	13:52:42	15	in use on SRVDL U[c]
1/20/79	13:53:02	15	
1/20/79	13:53:22	-	
1/20/79	18:48:00	15	
1/20/79	18:48:20	15	
1/20/79	18:48:40	15	
1/20/79	18:49:00	15	
1/20/79	18:49:20	-	
1/26/79	19:33:14	3	
1/26/79	19:33:21	2	Short valve
1/26/79	19:33:28	2	closed time
1/26/79	19:33:35	2	
1/26/79	19:33:42	-	
1/27/79	00:42:00	15	
1/27/79	00:42:35	15	
1/27/79	00:42:55	15	
1/27/79	00:43:15	15	
1/27/79	00:43:35		
1/26/79	12:14:31	-	Both valves opened within 8 ms
1/30/79	13:58:41	-	
1/30/79	20:24:24	-	3 valves opened within 106 ms
1/31/79	00:28:20	-	4 valves opened within 150 ms
1/31/79	15:24:28	-	4 valves opened within 60 ms
1/31/79	19:23:50	-	4 valves opened within 25 ms
2/1/79	09:56:00	-	4 valves opened within 80 ms
2/1/79	15:00:04	-	4 valves opened within 18 ms
2/1/79	19:51:20	-	4 valves opened within 92 ms, Valve E leaking[d]
2/1/79	23:42:06	-	4 valves actuated within 116 ms
2/2/79	12:10:00	-	8 valves actuated within 222 ms, Valve A leaking
1/24/79	6:45:21	-	Low reactor pressure
1/24/79	3:39:31	-	Low reactor pressure
1/24/79	00:06:00	-	Low reactor pressure
1/23/79	19:45:00	-	Low reactor pressure
1/23/79	15:17:43	-	Low reactor pressure
1/23/79	10:19:20	-	Low reactor pressure
1/17/79	19:44:13	-	
2/3/79	11:35:00	-	Extended discharge test
1/21/79	11:22:51	-	Valve A leaking
1/21/79	17:22:06	-	Valve A leaking
1/21/79	21:36:00	-	Valve A leaking

Test[a]	Test Type	Valve	Pipe Temperature, Water Level	Reactor Pressure (psig)
4401	SVA	A	WP,DWL	967
4402	CVA	A	WP,DWL	967
4403	CVA	A	HP,DWL	967
4404	CVA	A	HP,DWL	967
4405	CVA	A	HP,DWL	967
4401F	SVA	A	NA,DWL	979
4402F	CVA	A	NA,DWL	979
4403F	CVA	A	HP,DWL	979
4404F	CVA	A	HP,DWL	979
4405F	CVA	A	HP,DWL	979
501X	SVA	V	CP,NWL[b]	NA

[a] "F" indicates tests where incomplete data was gathered

[b] SRVDL bleed system employed prior to test

[c] All SRV lines equipped with two 10-in. vacuum breakers. However, one vacuum breaker on SRVDL A was blocked off during testing.

[d] Leakage from Valve E was determined by discharge line in-plant temperature sensor.

NA - Data not available.

Table 3-1
CAORSO PHASE II SRV TEST MATRIX (Continued)

Approximate Discharge Time (sec)	Valve On		CVA Valve Closed Time (sec)	Comments
	Date	Time (hr:min:sec)		
5	1/22/79	14:53:00	15	Valve A leaking
5	1/22/79	14:53:20	15	Valve A leaking
5	1/22/79	14:53:40	15	Valve A leaking
5	1/22/79	14:54:00	15	Valve A leaking
5	1/22/79	14:54:20	-	Valve A leaking
5	1/22/79	09:46:00	15	Valve A leaking
5	1/22/79	09:46:20	15	Valve A leaking
5	1/22/79	09:44:40	15	Valve A leaking
5	1/22/79	09:45:00	15	Valve A leaking
5	1/22/79	09:45:20	15	Valve A leaking
NA	NA	NA	-	Line V not instrumented

Test	Average Pipe Temperature (°F)	SRVDL Air Mass (lbm)	Steam Partial Pressure (psia)	Water Leg Length[g] (ft)	Pool Temperature at Quencher Elevation (°F)	Drywell Pressure (psia)
22A01[a]	86	4.84	0.62	17.7	82	14.95
22A02	NA	NA	NA	NA	82	14.95
22A03	NA	NA	NA	NA	82	14.95
22A04	NA	NA	NA	NA	82	14.95
22A05	NA	NA	NA	NA	82	14.95
2301	84	4.74	0.58	17.7	84	14.92
2302	227	1.90	11.17	13.6	84	14.92
2303	291	2.40	8.72	6.3	86	14.92
2304	325	2.30	9.47	6.1	86	14.92
2305	346	2.30	9.78	6.0	86	14.92
2311	87	4.69	0.64	17.7	79	14.92
2312	274	1.80	NA	19.7	79	14.92
2313	327	NA	NA	NA	NA	14.92
2314	342	NA	NA	NA	NA	14.92
2315	345	NA	NA	NA	NA	14.92
2321	93	4.61	0.77	17.7	86	14.94
2322	322	2.20	10.60	6.9	86	14.94
2323	345	2.30	10.35	6.4	86	14.94
2324	354	2.30	10.36	7.7	86	14.94
2325	362	2.30	9.69	6.5	86	14.94
24[b]	83	4.75	0.56	17.7	79	14.92
25[b]	83	4.76	0.56	17.7	76	14.94
26[b]	86	4.71	0.61	17.7	76	14.91
27[b]	93	4.60	0.77	17.7	77	14.92
28[b]	85	4.72	0.60	17.7	80	14.90
29[b]	95	4.60	0.82	17.7	80	14.93
30[b]	86	4.70	0.62	17.7	80	14.92
31[f]	86	4.61	0.62	17.7	80	14.92
32[d]	(133) 86	(3.80)4.53	(2.4)0.62	17.7	80	14.95
33	92	4.61	0.75	17.7	82	14.91

Table 3-2
INITIAL TEST CONDITIONS

Drywell/ Wetwell Pressure Difference (psid)	Total Pipe Pressure (psia)	SRV Steam Flow Rate (lbm/sec)	Valve(s)	Reactor Pressure (psig)	Valve Opening Time[e] (ms)
-0.01	14.95	212	U	982	42
-0.01	NA	212	U	982	40
-0.01	NA	212	U	982	42
-0.01	NA	212	U	982	46
-0.01	NA	212	U	982	43
-0.01	14.92	238	A	980	56
-0.01	18.06	238	A	980	40
-0.01	17.90	238	A	980	46
-0.01	18.70	238	A	980	50
-0.01	19.20	238	A	980	50
-0.01	14.92	238	A	977	45
-0.01	NA	238	A	977	45
-0.01	NA	238	A	977	53
-0.01	NA	238	A	977	45
-0.01	NA	238	A	977	49
-0.01	14.94	235	A	967	43
-0.01	19.45	235	A	967	49
-0.01	19.85	235	A	967	52
-0.01	19.99	235	A	967	42
-0.01	19.39	235	A	967	52
-0.01	14.92	239,244[f]	A,F	982	40,46[f]
-0.01	14.94	237,242[f]	A,F	975	46,NA[f]
-0.01	14.91	237,228,242[f]	A,E,F	973	56,60,56[f]
-0.01	14.92	236,227,241,209[f]	A,E,F,U	969	56,56,52,48[f]
-0.01	14.90	236,227,241,209[f]	A,E,F,U	970	52,56,44,34[f]
-0.01	14.93	236,227,241,206[f]	A,E,F,U	970	60,61,61,47[f]
-0.01	14.92	238,230,244,211[f]	A,E,F,U	980	48,55,60,38[f]
-0.01	14.92	224,225,248,238	B,C,D,L	985	NA
-0.01	14.95	237,221,245,242 234,230,242,243	A,B,D,H K,L,R,V	973	NA
-0.01	14.91	12	A	50	NA

Test	Average Pipe Temperature (°F)	SRVDL Air Mass (lbm)	Steam Partial Pressure (psia)	Water Leg Length[g] (ft)	Pool Temperature at Quencher Elevation (°F)	Drywell Pressure (psia)
34	91	4.63	0.73	17.7	81	14.91
35	89	4.65	0.69	17.7	81	14.88
36	90	4.64	0.70	17.7	81	14.89
37	90	4.66	0.69	17.7	82	14.91
38	90	4.64	0.70	17.7	81	14.89
39	82	4.75	0.53	17.7	80	14.86
40	84	4.73	0.58	17.7	59	14.90
41	217	0.26	16.21	12.5	80	14.92
42	218	0.03	16.53	13.3	80	14.92
43	218	0.04	16.53	13.6	80	14.92
4401F	NA	NA	NA	NA	NA	NA
4402F	NA	NA	NA	NA	NA	NA
4403F	326	NA	NA	5.6	86	14.95
4404F	345	NA	NA	5.5	86	14.95
4405F	353	NA	NA	5.3	86	14.95
4401	218	0.18	16.53	12.5	81	14.95
4402	286	2.10	11.27	3.7	82	14.95
4403	331	2.30	9.88	6.9	88	14.95
4404	347	2.30	8.73	8.3	88	14.95
4405	357	2.30	3.46	8.2	88	14.95
45-1[b]	92	4.70	0.51	17.7	80	14.92
45-2[b]	93	4.60	0.77	17.7	80	14.93
501X[h]	NA	NA	NA	NA	NA	NA

Table 3-2
INITIAL TEST CONDITIONS (Continued)

Drywell/ Wetwell Pressure Difference (psid)	Total Pipe Pressure (psia)	SRV Steam Flow Rate (lbm/sec)	Valve(s)	Reactor Pressure (psig)	Valve Opening Time[e] (ms)
-0.01	14.91	24	A	100	NA
-0.01	14.88	49	A	200	NA
-0.01	14.89	97	A	400	NA
-0.01	14.91	146	A	601	NA
-0.01	14.89	195	A	800	NA
-0.01	14.86	238	A	977	39
-0.01	14.90	237	A	975	30
-0.01	17.17	237	A	976	NA
-0.01	16.64	237	A	977	NA
-0.01	16.68	238	A	980	NA
NA	NA	238	A	979	NA
NA	NA	238	A	979	NA
-0.01	20.18	238	A	979	NA
-0.01	19.18	238	A	979	NA
-0.01	19.38	238	A	979	NA
-0.01	17.18	235	A	967	NA
-0.01	19.32	235	A	967	NA
-0.01	19.22	235	A	967	NA
-0.01	18.32	235	A	967	NA
-0.01	18.29	235	A	967	NA
-0.01	14.92	238,230,240,209[f]	A,E,F,U	980	46,50,50,55[f]
-0.01	14.93	239,230,244,209[f]	A,E,F,U	982	40,41,48,42[f]
NA	NA	NA	V	NA	NA

Table 3-2
INITIAL TEST CONDITIONS (Continued)

The methods of obtaining initial conditions are explained in the Phase I Test Report, Appendix D. For LV, first actuations, saturated steam at average temperature in the SRVDL was assumed.

a. Tests 22A01 through 22A05 were performed on Valve U. Except for the SRV flowrate, the initial conditions for SRVDL U prior to Test 22A01 were obtained by determining the initial conditions for SRVDL A because SRVDL U was not instrumented. The initial conditions for Tests 22A02 through 22A05 were incomplete as the necessary data was not available.

b. Initial conditions indicated are for Valve A only. Except for steam flow rates, and valve opening times, other conditions are dependent on line geometry and since all lines had similar geometries, they all had similar initial conditions.

c. The initial conditions are those of Valve A. Although A was not actuated it was assumed that the initial conditions for Valve A were similar to those in the other valves. The SRV flow rates are for the indicated valves.

d. The values in parentheses are the initial conditions for Valve A only. Temperature readings indicated there was some leakage in the valve. The other initial conditions shown - not in parentheses - were determined by the method used for Test 22A01.

e. Valve opening time is defined as time elapsed between the start of the main disc movement and the fully open position. Sensor VAP (SRV A position indicator) was used to determine the times.

f. Order shown corresponds to the order given under "valve(s)."

g. Water leg length is defined as the distance between the initial gas/water interface and the X-quencher arms centerline.

h. Test 501X was performed on Valve V whose SRVDL and quencher were not instrumented. Only the containment pressure and temperature histories are available from this test.

NA - Data not available

Table 3-3

TIMING* OF VALVE OPENINGS DURING THE MULTIPLE VALVE ACTUATION TESTS

(All Values in Milliseconds)

Test No.	Safety Relief Valve											Time Lag Between First and Last SRV Actuated
	A	B	C	D	E	F	H	K	L	R	U	V	
24	0	-	-	-	-	8	-	-	-	-	-	-	8
25**	22	-	-	-	-	0	-	-	-	-	-	-	22
26	0	-	-	-	106	106	-	-	-	-	-	-	106
27	0	-	-	-	119	115	-	-	-	-	150		150
28	0	-	-	-	40	40	-	-	-	-	60		60
29	0	-	-	-	0	0	-	-	-	-	25		25
30	80	-	-	-	70	70	-	-	-	-	0		80
45-1	18	-	-	-	10	14	-	-	-	-	0		18
45-2	0	-	-	-	85	92	-	-	-	-	82		92
31**	-	87	0	52	-	-	-	-	116	-	-	-	116
32**	222	61	-	68	-	-	0	69	194	6	-	111	222

*The valve actuated first (first to move main disc) in any given test has a zero time assigned to it.

**Only time between actuations of SRV operation switch was available for this test.

Table 3-4

CAORSO TEST SENSORS SELECTED FOR LEVEL CRITERIA MONITORING

Measurement	Level 1 Criteria	Level 2 Criteria	Maximum Measured Value
SRV discharge pressure, PT25[a]	625 psig	550 psig	330 psig
Quencher pressure, P5	890 psig	535 psig	662 psig
Containment response:			
Reactor flange, A1Z	Sensor failed.	Backup sensor A42 used.	
Reactor pedestal, A3Z	Sensor failed.	Backup sensor A42 used.	
Reactor pedestal, A4Z	0.55g	0.44g	0.033g
Quencher inlet nozzle dynamic stress, SG33, SG35 and SG36	17320 psi	11160 psi	6700 psi
Quencher arm dynamic stress			
Arm top and bottom, SG2/6	31800 psi	25380 psi	NA[b]
Arm sides, SG4/8	31800 psi	25380 psi	NA[b]
Containment floor liner strains			
SG44A	2500 μs	1100 μs	50 μs[c]
SG46A	2500 μs	1500 μs	80 μs[c]
Containment wall liner strain			
SG48A	1000 μs	250 μs	20 μs[c]
Downcomer vent strain			
SG51/53	1100 μs	70 μs	59 μs[c]
SG52/54	1100 μs	70 μs	59 μs[c]

[a] Subsequent to the Phase I tests it was determined that the sensor originally specified for SRVDL pressure monitoring was giving erroneous readings. Sensor PT25 was used as backup during the Phase II tests.

[b] Not available. Review of SG2/6 and SG4/8 data after the conclusion of testing indicated the readings were inaccurate.

[c] Real time data.

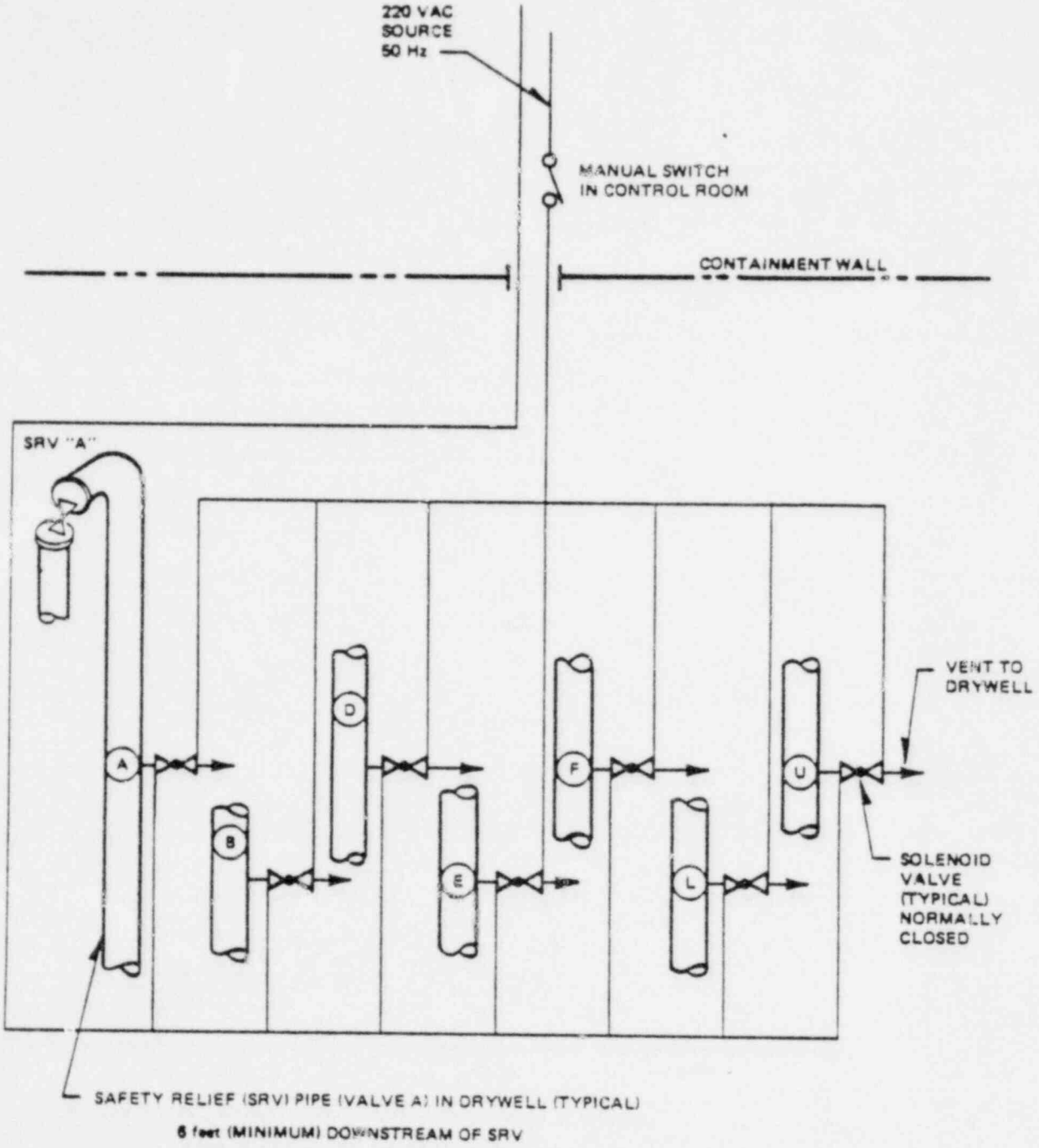

Figure 3-1. SRV Discharge Line Air Bleed System Schematic Diagram

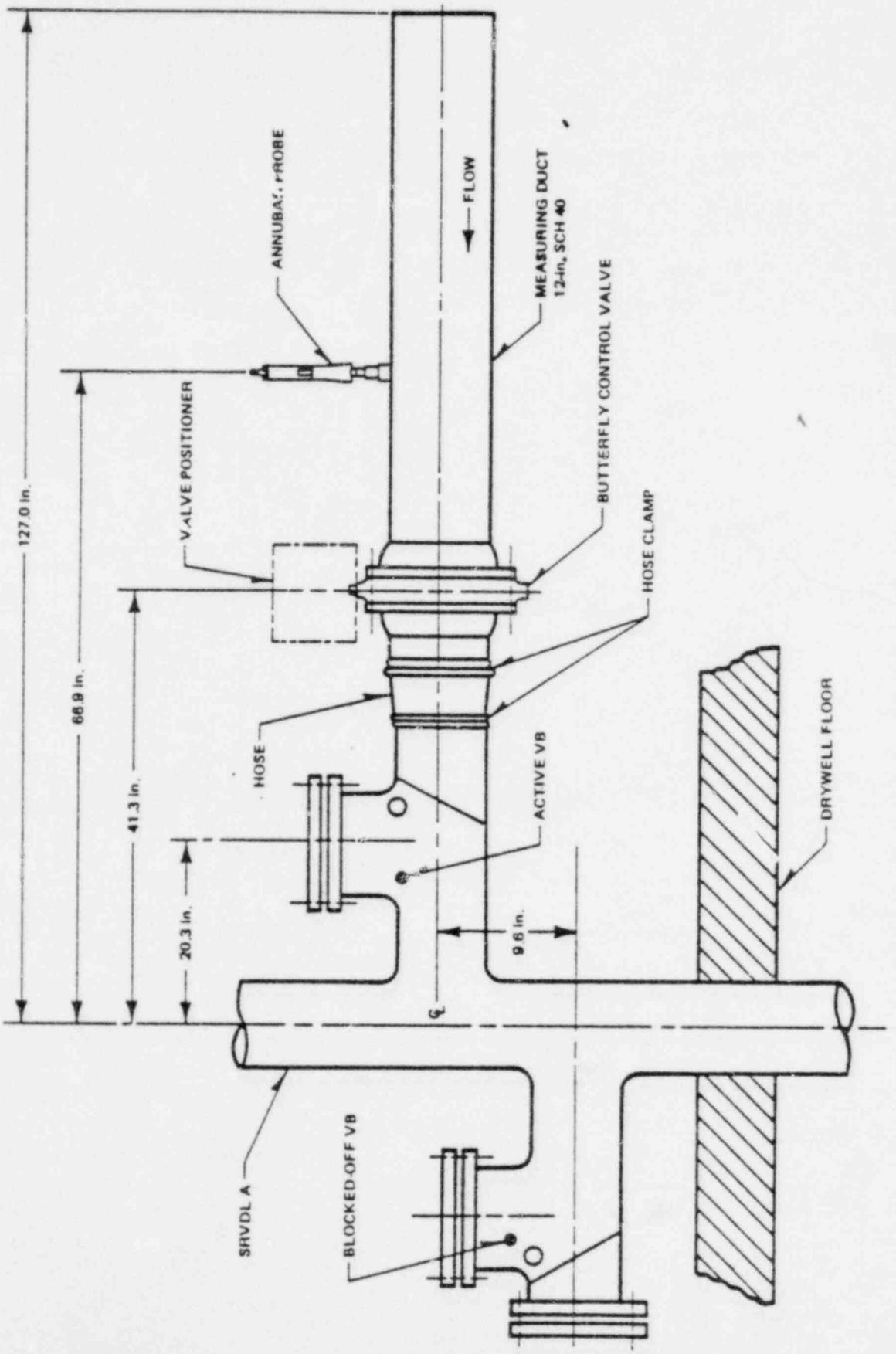

Figure 3-2. SRVDL A Vacuum Breaker and VB Measurement Assembly

4. DATA ACQUISITION SYSTEM

4.1 INTRODUCTION

A total of 236 signal channels were used to collect test data during the Caorso test program. In order to accommodate both this volume of data and the frequency resolution requirements placed on the instruments, the PCM system was selected for reading the output of the individual sensors and storing the information on magnetic tapes for further processing. A description of this system is given in Subsection 4.1 of the Phase I Test Report.

4.2 [illegible] SENSORS

A complete list of the 186 sensors installed at Caorso is given in Table 4-1 with references to Figures 4-2 through 4-22 showing their locations. Specifications for these sensors are given in Appendix A of the Phase I Test Report. Figure 4-1 shows quencher locations in the suppression pool. Figure 4-23 is a detailed illustration of SRVDL U.

As noted in Table 4-1, several sensors failed before or during testing. However, the basic objectives of the tests were not compromised in any of these cases because:

a. There were sufficient direct or indirect backups to the failed sensors.

b. The data to have been obtained for these sensors were of a secondary nature.

c. Sufficient data were obtained prior to the sensor failure.

The alternative applicable in each case is specified in Table 4-1..

4.3 DATA ERROR ANALYSIS

In assessing the quality of the data obtained from the Caorso tests, a data accuracy evaluation was performed on the data acquisition system from the sensors to the final system output (engineering computer plots). The results of the complete evaluation performed on the data acquisition system and the Phase I test data are reported in Appendix B of the Phase I Test Report.

In assessing the applicability of the data accuracy evaluation results to the Phase II test data, evaluations were made of statistical samples of test data from the Phase II tests. The results of these evaluations show that the end-to-end accuracies reported in the Phase I Test Report are also valid for the Phase II tests. Although some measurements were of greater magnitude in Phase II than the corresponding measurements in Phase I, the increase did not result in any significant accuracy differences. The report on the results of the evaluations performed in the Phase II test data is included in Appendix B.

Table 4-1

CAORSO TEST SENSORS

Sensor Designation	Type	Location	Reference Figure	Remarks
P1	Pressure transducer	Inside SRVDL A	4-7	Failed during Test 4 of Phase I. Comparison of P1 and PT25 for the first three Phase I tests showed sufficient consistency that PT25 was acceptable as a backup.
P2	Pressure transducer	Inside SRVDL A	4-7	Failed prior to start of testing. Intended as backup to P1.
P3	Pressure transducer	Inside SRVDL A	4-7	Failed during Test 4 of Phase I. P55 used as backup.
P4	Pressure transducer	Inside SRVDL A	4-7, 4-8	-
P5	Pressure transducer	Inside quencher A	4-7, 4-8	-
P6	Pressure transducer	Inside quencher A arm	4-7, 4-8	-
P7	Pressure transducer	Inside SRVDL A	4-7	Failed prior to start of testing. P4 used as backup.
P8	Pressure transducer	Inside SRVDL A	4-7	
P9	Pressure transducer	On suppression pool wall	4-2, 4-3	
P10	Pressure transducer	On suppression pool wall	4-2, 4-3	Failed prior to start of testing. P9, P13, P14 used as indirect backups.
P11	Pressure transducer	On suppression pool wall	4-2, 4-3	
P12	Pressure transducer	On suppression pool wall	4-2, 4-3	
P13	Pressure transducer	At intersection of suppression pool wall and floor	4-2, 4-3	-

Table 4-1

CAORSO TEST SENSORS (Continued)

Sensor Designation	Type	Location	Reference Figure	Remarks
P14	Pressure transducer	On suppression pool wall	4-2, 4-3	-
P15	Pressure transducer	On suppression pool wall	4-2, 4-3	-
P16	Pressure transducer	On suppression pool wall	4-2, 4-3	Failed prior to start of testing. P15 was used as indirect backup.
P17	Pressure transducer	On suppression pool wall	4-2, 4-3	-
P18	Pressure transducer	On suppression pool wall	4-2, 4-3	Failed during Test 11 of Phase 1. P15, P17 used as indirect backups.
P19	Pressure transducer	On suppression pool floor	4-2	-
P20	Pressure transducer	On suppression pool floor	4-2	Failed prior to start of testing. P19, P42 used as indirect backups.
P21	Pressure transducer	On suppression pool floor	4-2	Failed prior to start of testing. P19, P35 used as indirect backups.
P22, P52	Pressure transducer	Outside of quencher A arm	4-2	Sensors located in area of high vibration and appeared to show an acceleration response of the sensor diaphragm.
P23	Pressure transducer	On suppression pool floor	4-2	-
P24, P53	Pressure transducer	Outside of quencher F arm	4-2	-

Table 4-1

CAORSO TEST SENSORS (Continued)

Sensor Designation	Type	Location	Reference Figure	Remarks
P25	Pressure transducer	On suppression pool floor	4-2	-
P26	Pressure transducer	On pedestal wall	4-2, 4-3	-
P27	Pressure transducer	On pedestal wall	4-2, 4-3	-
P28	Pressure transducer	On pedestal wall	4-2, 4-3	Failed prior to start of testing. P31, P32, P27 used as backups.
P29	Pressure transducer	On pedestal wall	4-2, 4-3	
P30	Pressure transducer	On pedestal wall	4-2, 4-3	
P31	Pressure transducer	On pedestal wall	4-2, 4-3	-
P32	Pressure transducer	On pedestal wall	4-2, 4-3	-
P33	Pressure transducer	On downcomer vent 9	4-2, 4-4	-
P34	Pressure transducer	On downcomer vent 9	4-2, 4-4	-
P35	Pressure transducer	On suppression pool floor	4-2	-
P36	Pressure transducer	On suppression pool floor	4-2	-
P37	Pressure transducer	On suppression pool floor	4-2	-
P38	Pressure transducer	On suppression pool floor	4-2	Failed before Test 22A01. P36, P37 and P51 used as indirect backups.
P39	Pressure transducer	On column 7	4-2, 4-4	-
P40	Pressure transducer	On column 7	4-4, 4-4	-
P41	Pressure transducer	On column 7	4-2, 4-4	-
P42	Pressure transducer	On column 7	4-2, 4-4	-

Table 4-1

CAORSO TEST SENSORS (Continued)

Sensor Designation	Type	Location	Reference Figure	Remarks
P43	Pressure transducer	Upstream of quencher A VB	4-17	Failed prior to start of testing. P44 used as backup.
P44	Pressure transducer	Upstream of quencher A VB	4-17	-
P45	Flow probe pressure transducer	In suppression pool	4-6	Sensors located in areas of high vibration and appeared to show acceleration response of sensor diaphragm.
P46	Flow probe pressure transducer	In suppression pool	4-6	
P47	Flow probe pressure transducer	In suppression pool	4-6	
P48	Pressure transducer	Inside quencher A pedestal	4-5	-
P49	Pressure transducer	Inside quencher A pedestal	4-5	-
P50	Pressure transducer	On suppression pool floor	4-2	-
P51	Pressure transducer	On suppression pool floor	4-2	-
P54	Pressure transducer	Inside SRVDL A	4-7	-
P55	Pressure transducer	Inside SRVDL A	4-7	Failed before Test 22A01. P54 used as indirect backup.
P56	Pressure transducer	On suppression pool floor	4-2	Failed before Test 22A01. P50 used as indirect backup.
P57	Pressure transducer	On suppression pool	4-2	Failed before Test 22A01. P51 used as indirect backup.

Table 4-1

CAORSO TEST SENSORS (Continued)

Sensor Designation	Type	Location	Reference Figure	Remarks
PT25	Pressure transducer	Inside SRVDL A	4-7	-
T1	Resistance temperature detector	Inside SRVDL A	4-9	Failed during Test 12 of Phase I. T21, T24 used as indirect backups.
T2	Resistance temperature detector	Inside SRVDL A	4-9	Failed during Test 22 of Phase I. T21, T24 used as indirect backups.
T3	Resistance temperature detector	Inside SRVDL A	4-9	-
T4	Resistance temperature detector	Inside SRVDL A	4-9	Failed during Test 22 of Phase I. T5 used as indirect backup.
T5	Resistance temperature detector	Inside quencher A	4-9, 4-10	-
T7	Resistance temperature detector	Inside quencher A arm	4-9, 4-10, 4-11	Failed prior to start of testing. T8 used as backup.
T8	Resistance temperature detector	Inside quencher A arm	4-9, 4-10, 4-11	-
T9	Resistance temperature detector	Inside quencher A arm	4-9, 4-10, 4-11	-
T10	Resistance temperature detector	Inside quencher A arm	4-9, 4-10, 4-11	Failed during Test 22A01. T9 used as backup.
T11	Resistance temperature detector	In suppression pool	4-16	-
T12	Resistance temperature detector	In suppression pool	4-16	-
T13	Resistance temperature detector	In suppression pool	4-16	-
T14	Resistance temperature detector	In suppression pool	4-10	-

Table 4-1

CAORSO TEST SENSORS (Continued)

Sensor Designation	Type	Location	Reference Figure	Remarks
T15	Resistance temperature detector	In suppression pool	4-16	-
T16	Resistance temperature detector	In suppression pool	4-16	-
T17	Resistance temperature detector	In suppression pool	4-16	-
T18	Resistance temperature detector	In suppression pool	4-16	-
T19	Resistance temperature detector	In suppression pool	4-16	-
T20	Resistance temperature detector	In suppression pool	4-16	-
T21	Resistance temperature detector	Outer surface of SRVDL A	4-9	-
T22	Resistance temperature detector	Outer surface of SRVDL A	4-9	-
T23	Resistance temperature detector	Outer surface of SRVDL A	4-9	-
T24	Resistance temperature detector	Within pipe wall of SRVDL A	4-9	-
T26	Resistance temperature detector	Within pipe wall of SRVDL A	4-9	-
T27	Resistance temperature detector	Inside SRVDL A	4-9	
T28	Resistance temperature detector	Inside SRVDL A	4-9	Failed during Test 4 of Phase I. Intended as backup for L9.

Table 4-1

CSORSO TEST SENSORS (Continued)

Sensor Designation	Type	Location	Reference Figure	Remarks
L1	Level probes	Inside SRVDL A	4-12, 4-13	-
L2	Level probes	Inside SRVDL A	4-12, 4-13	Operable only during Tests 4 and 501-505 of Phase I. L1, L3 and T27 used as indirect backups.
L3	Level probes	Inside SRVDL A	4-12, 4-13	-
L4	Level probes	Inside SRVDL A	4-12, 4-13	-
L5	Level probes	Inside SRVDL A	4-12, 4-13	-
L6	Level probes	Inside SRVDL A	4-12, 4-13	-
L7	Level probes	Inside SRVDL A	4-12, 4-13	-
L8	Level probes	Inside quencher A arm	4-12, 4-13	-
L9	Level probes	Inside SRVDL A	4-12, 4-13	-
L10	Level probes	Inside SRVDL A	4-12	-
L11	Level probes	Inside SRVDL A	4-12	-
L12	Level probes	Inside SRVDL A	4-12, 4-13	Failed prior to start of testing. T8, T9 and T10 used as indirect backups.
TL6	Level probes	Inside quencher A arm	4-12, 4-13	
LVDT1	Displacement sensors	On quencher A pedestal	-	-
LVDT2	Displacement sensors	On quencher A pedestal	-	Failed prior to start of testing. Data to have been obtained would be of secondary importance.

Table 4-1

CAORSO TEST SENSORS (Continued)

Sensor Designation	Type	Location	Reference Figure	Remarks
VB1	Vacuum breaker position indicator	On SRVDL A VB	-	Failed prior to start of testing. Data to have been obtained would be of secondary importance.
VB2	Vacuum breaker butterfly valve position indicator	Upstream of SRVDL A VB	-	-
VAP	SRV position indicator	On SRV A	-	
VEP	SRV position indicator	On SRV E	-	-
VFP	SRV position indicator	On SRV F	-	-
VUP	SRV Position indicator	On SRV U	-	-
A1	Biaxial accelercmeter	On RPV shield wall	4-14, 4-15	-
A2	Biaxial accelerometer	On RPV shield wall	4-14, 4-15	-
A3	Triaxial accelerometer	On RPV pedestal		Vertical axis failed prior to start of testing. A4 used as backup.
A4	Triaxial accelerometer	On RPV pedestal	4-14, 4-15	-
A5	Triaxial accelerometer	Center of operating floor	4-14, 4-15	-
A6	Triaxial accelerometer	On diaphragm floor	4-14, 4-15	-
A7	Triaxial accelerometer	On pedestal wall	4-14, 4-15	-

Table 4-

CAORSO TEST SENSORS (Continued)

Sensor Designation	Type	Location	Reference Figure	Remarks
A8	Triaxial accelerometer	On pedestal wall	4-14, 4-15	-
A9	Triaxial accelerometer	On suppression pool floor	4-14, 4-15	-
A10	Triaxial accelerometer	On suppression pool floor	4-14, 4-15	-
A11	Triaxial accelerometer	On RPV at flange	4-14, 4-15	Range of all 3 axes saturated for all Phase I tests. A4 used as backup. Vertical axis was corrected for Phase II tests. The correction for the other two axis was not successful.
A12	Biaxial accelerometer	On containment wall in drywell	4-14, 4-15	-
A13	Uniaxial accelerometer	On basemat between primary and secondary containments	4-14, 4-15	-
A14	Uniaxial accelerometer	On basemat between primary and secondary containments	4-14, 4-15	-
A15	Triaxial accelerometer	On quencher A hub	4-18	-
A16	Biaxial accelerometer	On quencher A hub	4-18	-
A17	Biaxial accelerometer	On end of quencher A arm	4-19	-
A18	Biaxial accelerometer	On end of quencher A arm	4-19	-

Table 4-1

CAORSO TEST SENSORS (Continued)

Sensor Designation	Type	Location	Reference Figure	Remarks
A19	Biaxial accelerometer	On end of quencher A arm	4-19	-
A20	Biaxial accelerometer	On end of quencher A arm	4-19	-
A21	Uniaxial accelerometer	On suppression pool floor	4-21	-
A22	Uniaxial accelerometer	On suppression pool floor	4-21	-
A23	Uniaxial accelerometer	On suppression pool floor	4-21	-
SG1	Uniaxial strain gage	On quencher arm	4-18, 4-19	-
SG3	Uniaxial strain gage	On quencher arm	4-18, 4-19	-
SG5	Uniaxial strain gage	On quencher arm	4-18, 4-19	-
SG7	Uniaxial strain gage	On quencher arm	4-18, 4-19	-
SG9	Uniaxial strain gage	On quencher arm	4-18, 4-19	-
SG11	Uniaxial strain gage	On quencher arm	4-18, 4-19	-
SG13	Uniaxial strain gage	On quencher arm	4-18, 4-19	-
SG15	Uniaxial strain gage	On quencher arm	4-18, 4-19	-

Table 4-1

CAORSO TEST SENSORS (Continued)

Sensor Designation	Type	Location	Reference Figure	Remarks
SG17	Uniaxial strain gage	On quencher arm	4-18, 4-19	-
SG19	Uniaxial strain gage	On quencher arm	4-18, 4-19	-
SG21	Uniaxial strain gage	On quencher arm	4-18, 4-19	-
SG23	Uniaxial strain gage	On quencher arm	4-18, 4-19	-
SG25	Uniaxial strain gage	On quencher arm	4-18, 4-19	-
SG27	Uniaxial strain gage	On quencher arm	4-18, 4-19	-
SG29	Uniaxial strain gage	On quencher arm	4-18, 4-19	-
SG31	Uniaxial strain gage	On quencher arm	4-18, 4-19	-
SG2/6	Strain gage bridge	On quencher arm	4-18, 4-19	Two uniaxial strain gages coupled to join a bending moment bridge.
SG4/8	Strain gage bridge	On quencher arm	4-18, 4-19	Two uniaxial strain gages coupled to join a bending moment bridge.
SG10/14	Strain gage bridge	On quencher arm	4-18, 4-19	Two uniaxial strain gages coupled to join a bending moment bridge.
SG12/16	Strain gage bridge	On quencher arm	4-18, 4-19	Two uniaxial strain gages coupled to join a bending moment bridge.
SG18/22	Strain gage bridge	On quencher arm	4-18, 4-19	Two uniaxial strain gages coupled to join a bending moment bridge.

Table 4-1

CAORSO TEST SENSORS (Continued)

Sensor Designation	Type	Location	Reference Figure	Remarks
SG20/24	Strain gage bridge	On quencher arm	4-18, 4-19	Two uniaxial strain gages coupled to join a bending moment bridge.
SG26/30	Strain gage bridge	On quencher arm	4-18, 4-19	Two uniaxial strain gages coupled to join a bending moment bridge.
SG28/32	Strain gage bridge	On quencher arm	4-18, 4-19	Two uniaxial strain gages coupled to join a bending moment bridge.
SG33	Uniaxial strain gage	SRVDL A at quencher inlet	4-18	-
SG34	Uniaxial strain gage	SRVDL A at quencher inlet	4-18	Failed prior to start of testing. SG33, SG35, SG36 used as indirect backups.
SG35	Uniaxial strain gage	SRVDL A at quencher inlet	4-18	-
SG36	Uniaxial strain gage	SRVDL A at quencher inlet	4-18	-
SG37	Uniaxial strain gage	On quencher A hub	4-18	-
SG38	Uniaxial strain gage	On quencher A hub	4-18	-
SG39	Uniaxial strain gage	On quencher A hub	4-18	-
SG40	Uniaxial strain gage	On quencher A hub	4-18	-
SG41	Strain rosette	On suppression pool floor liner	4-18	-
SG42	Strain rosette	On suppression pool floor liner	4-21	-

Table 4-1

CAORSO TEST SENSORS (Continued)

Sensor Designation	Type	Location	Reference Figure	Remarks
SG43	Strain rosette	On suppression pool floor liner	4-21	-
SG44	Strain rosette	On suppression pool floor liner	4-21	-
SG45	Strain rosette	On suppression pool floor liner	4-21	-
SG46	Strain rosette	On suppression pool floor liner	4-21	-
SG47	Strain rosette	On suppression pool floor liner	4-21	Axis B failed prior to start of testing. SG46A, SG46B, SG46C, SG47A, SG47C used as indirect backup.
SG48	Strain rosette	On suppression pool wall liner	4-22	-
SG49	Strain rosette	On suppression pool wall liner	4-22	-
SG50	Strain rosette	On suppression pool wall liner	4-22	-
SG51	Uniaxial strain gage	On downcomer vent 1 at upper bracing	4-20	-
SG52	Uniaxial strain gage	On downcomer vent 1 at upper bracing	4-20	-
SG53	Uniaxial strain gage	On downcomer vent 1 at upper bracing	4-20	-
SG54	Uniaxial strain gage	On downcomer vent 1 at upper bracing	4-20	-

Table 4-1

CAORSO TEST SENSORS (Continued)

Sensor Designation	Type	Location	Reference Figure	Remarks
SG55	Uniaxial strain gage	On downcomer vent 9 at upper bracing	4-20	-
SG56	Uniaxial strain gage	On downcomer vent 9 at upper bracing	4-20	Failed prior to start of testing. SG55 used as backup.
SG57	Uniaxial strain gage	On downcomer vent 9 at upper bracing	4-20	-
SG58	Uniaxial strain gage	On downcomer vent 9 at upper bracing	4-20	-

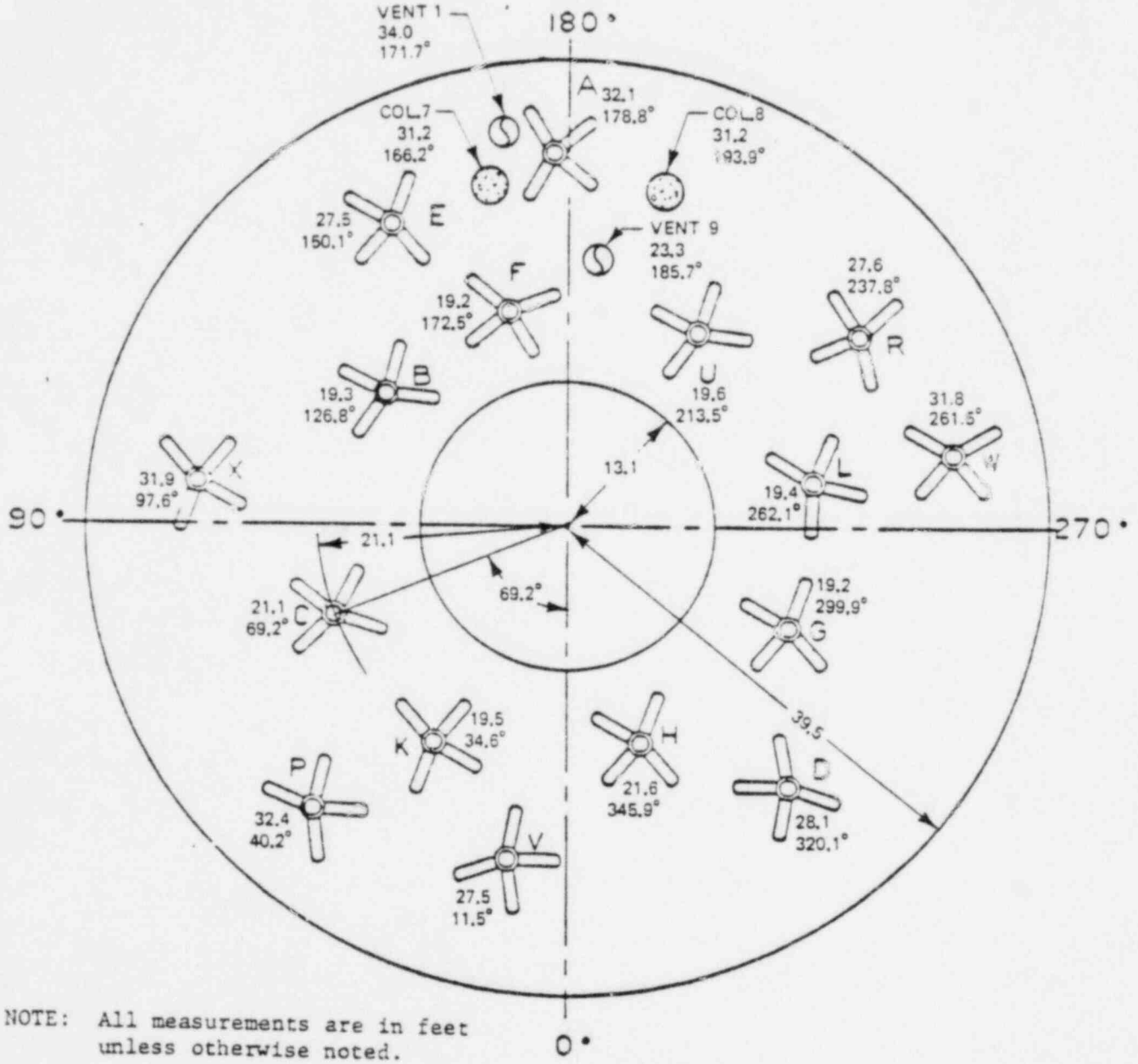

NOTE: All measurements are in feet unless otherwise noted.

Figure 4-1. Caorso Quencher Locations

NOTES:

1. ALL MEASUREMENTS ARE IN INCHES UNLESS OTHERWISE NOTED.
2. SENSORS P13, 19, 23, 35, 36 37, 50, 51, 56, 57 ON FLOOR LINER.
3. SENSORS P20, 21, 25 ON PEDESTAL BASE AT EL 128.6 FT (39.20M)
4. SENSORS P12, 14, 15, 17, 18 AT EL 133.5 FT (40.70M) P16 AT EL 141.7 FT (43.19M)
5. SENSORS P22, 24, 52, 53 ON QUENCHER ARM.
6. SENSORS P50 AND P56 ON STRAIGHT LINE CONNECTING ℄'s OF QUENCHERS "A" AND "E".
7. SENSORS P51 AND P57 ON STRAIGHT LINE CONNECTING ℄'s OF QUENCHERS "A" AND "U".
8. SENSORS P39 THRU P42 ON STRAIGHT LINE CONNECTING ℄'s OF QUENCHER "A" AND COL. 7
9. SENSORS P33 AND P34 ON STRAIGHT LINE CONNECTING ℄'s OF QUENCHER "A" AND DOWNCOMER VENT 9

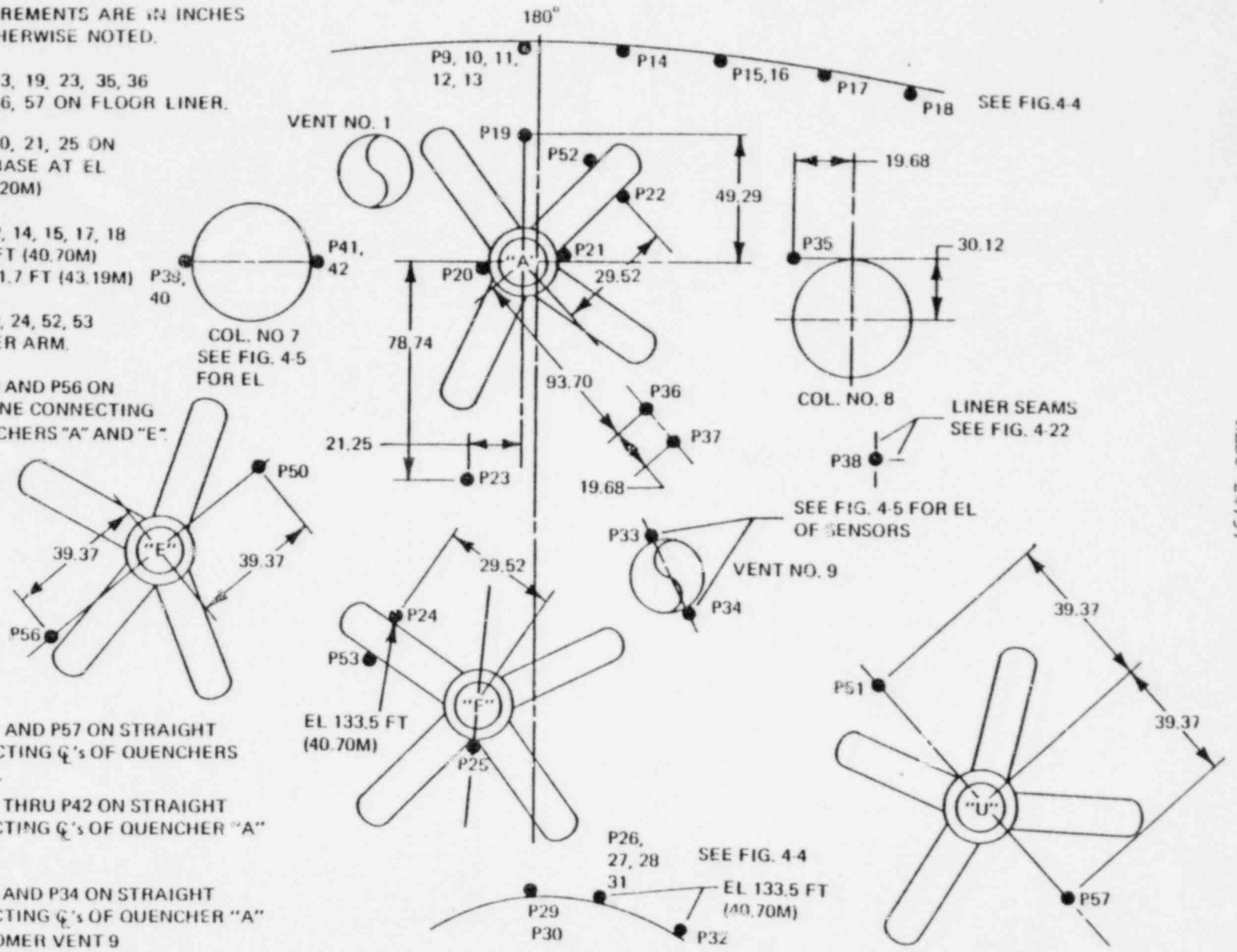

Figure 4-2. Pool Pressure Sensors

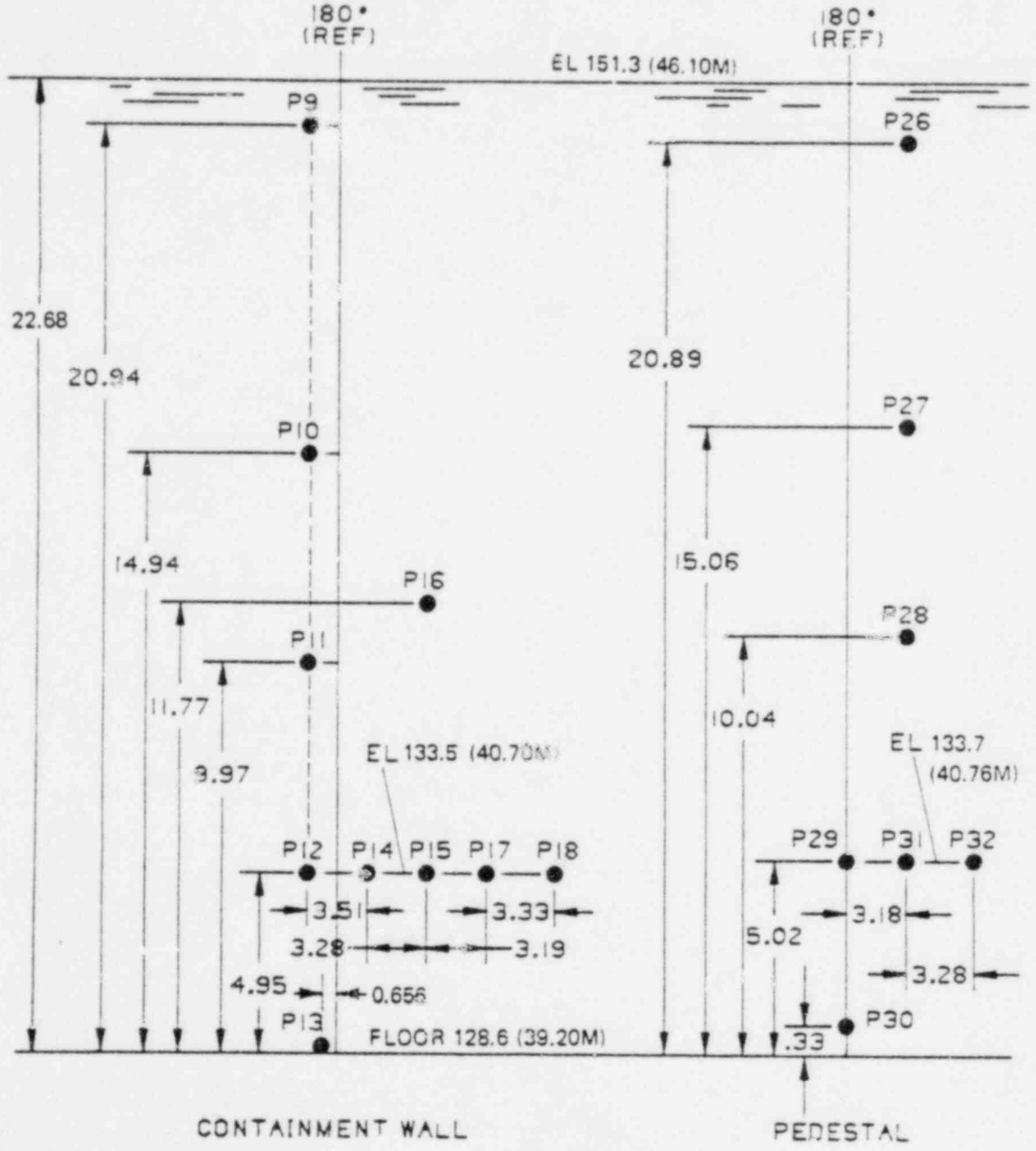

NOTE: All measurements are in feet unless otherwise noted.

Figure 4-3. Pool Pressure Sensors on Containment Wall and Pedestal (Detail)

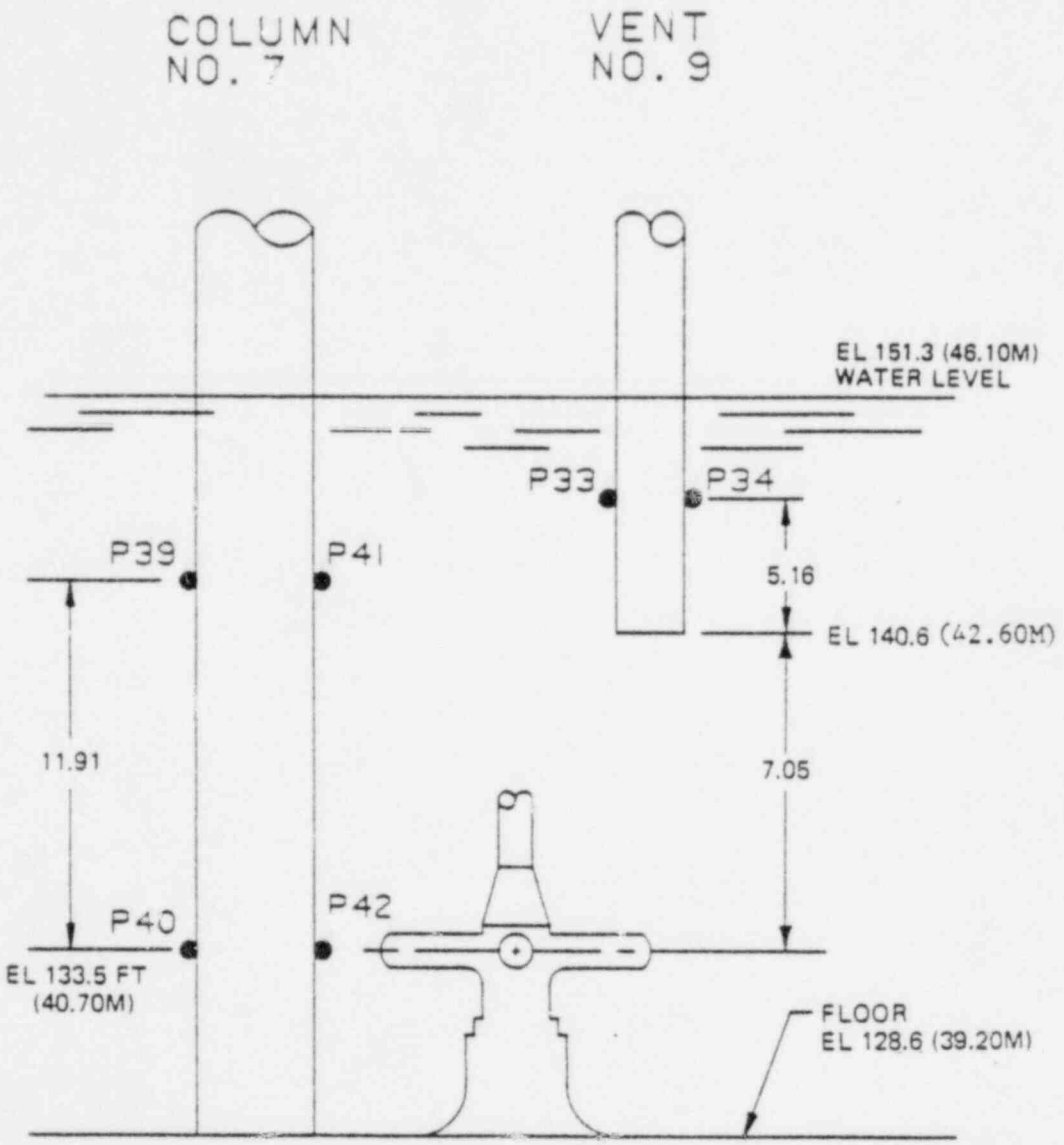

NOTE: All measurements are in feet unless otherwise noted.

Figure 4-4. Pressure Sensors on Column and Downcomer Vent

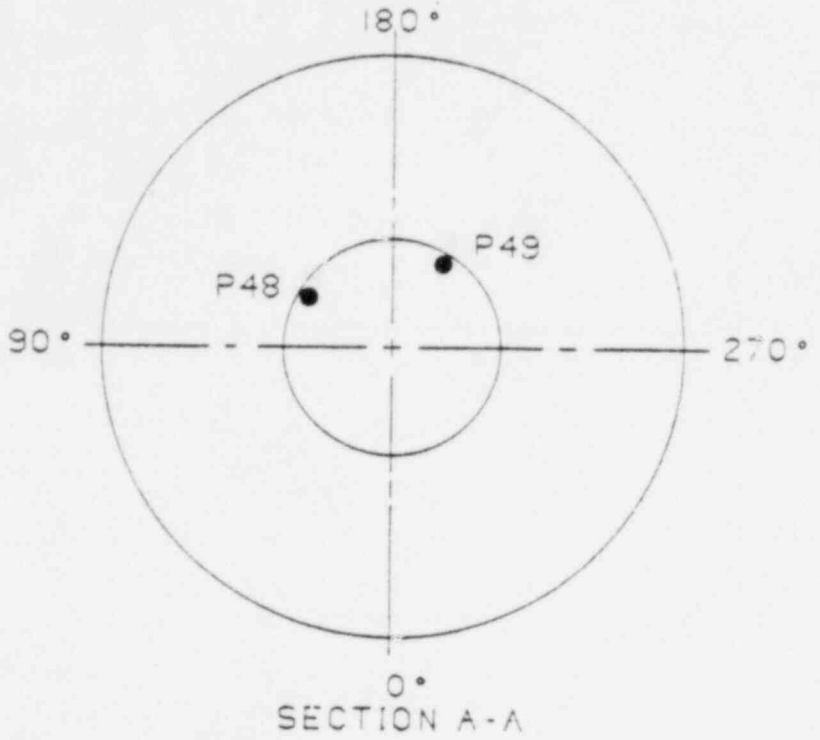

NOTE: Pressure sensors to read pressure within pedestal support.

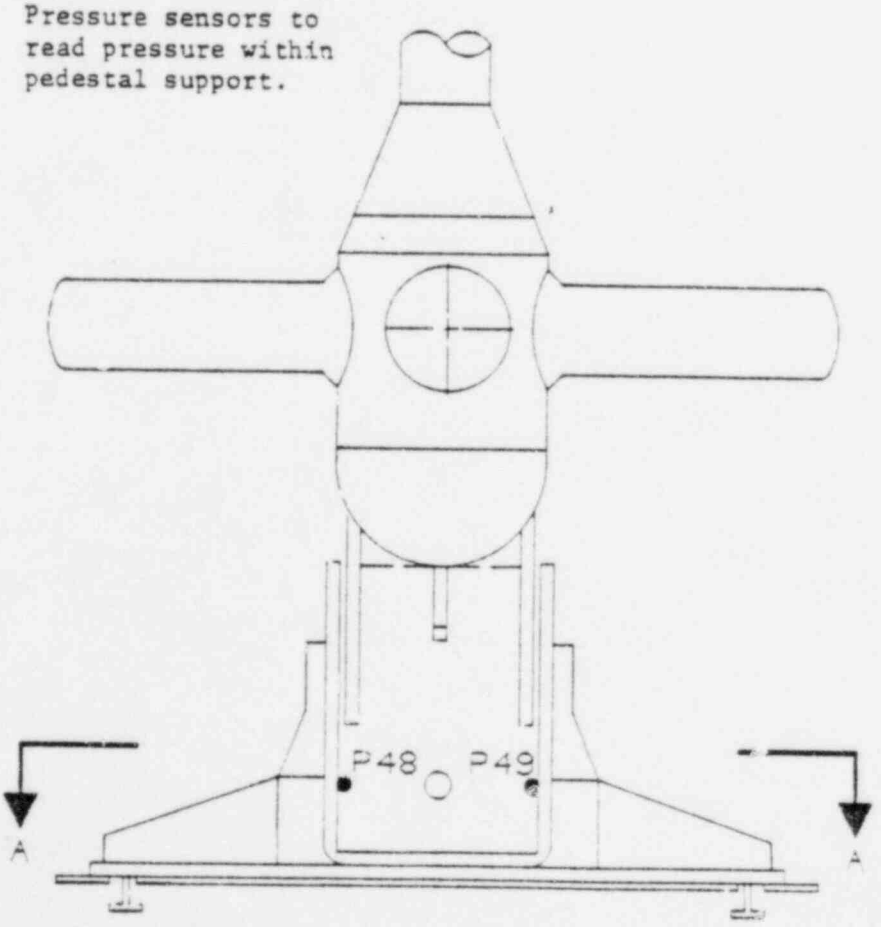

Figure 4-5. Pressure Sensors in Quencher A Support

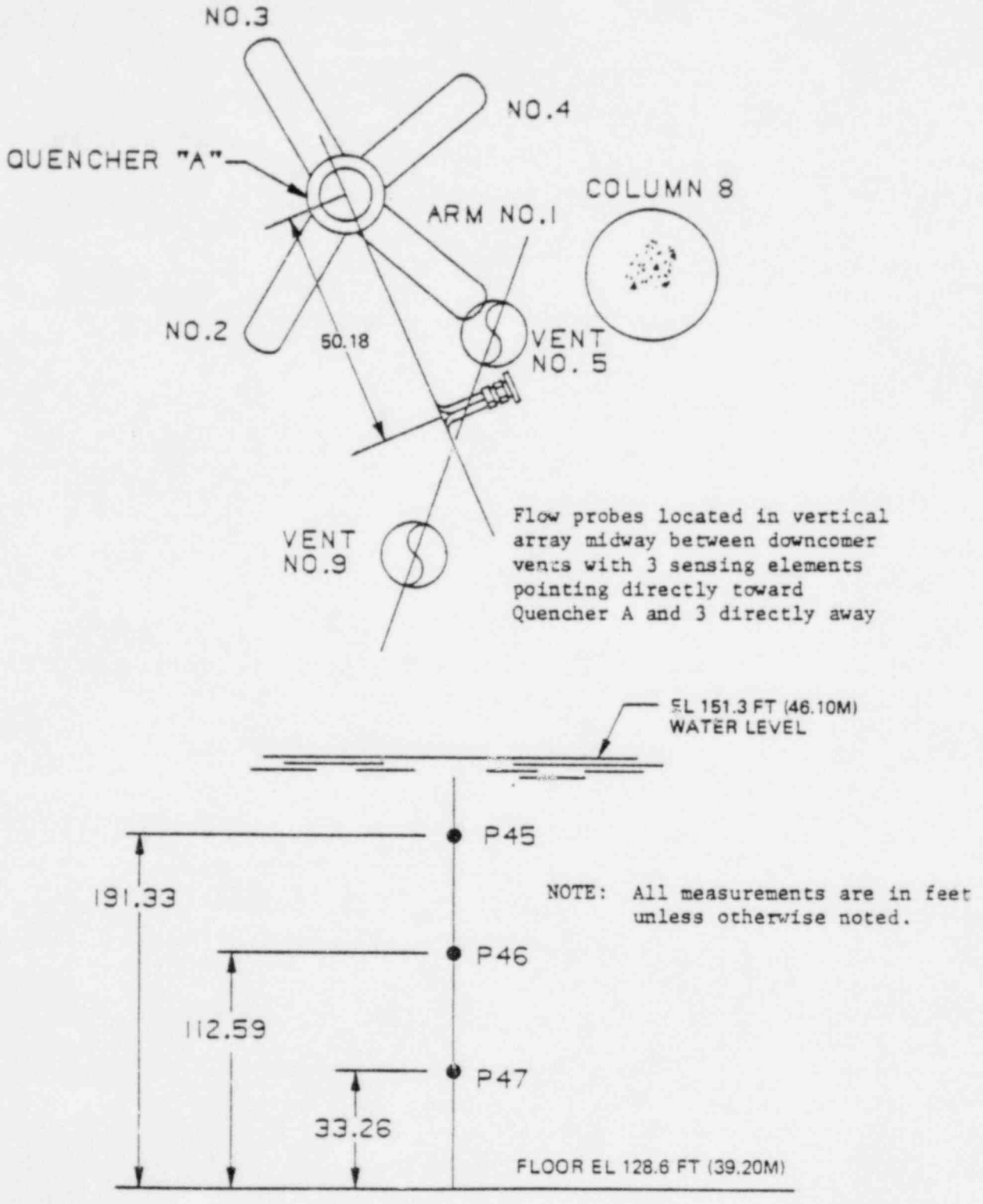

Figure 4-6. Elevation of Flow Probes and Pressure Transducers Assembly

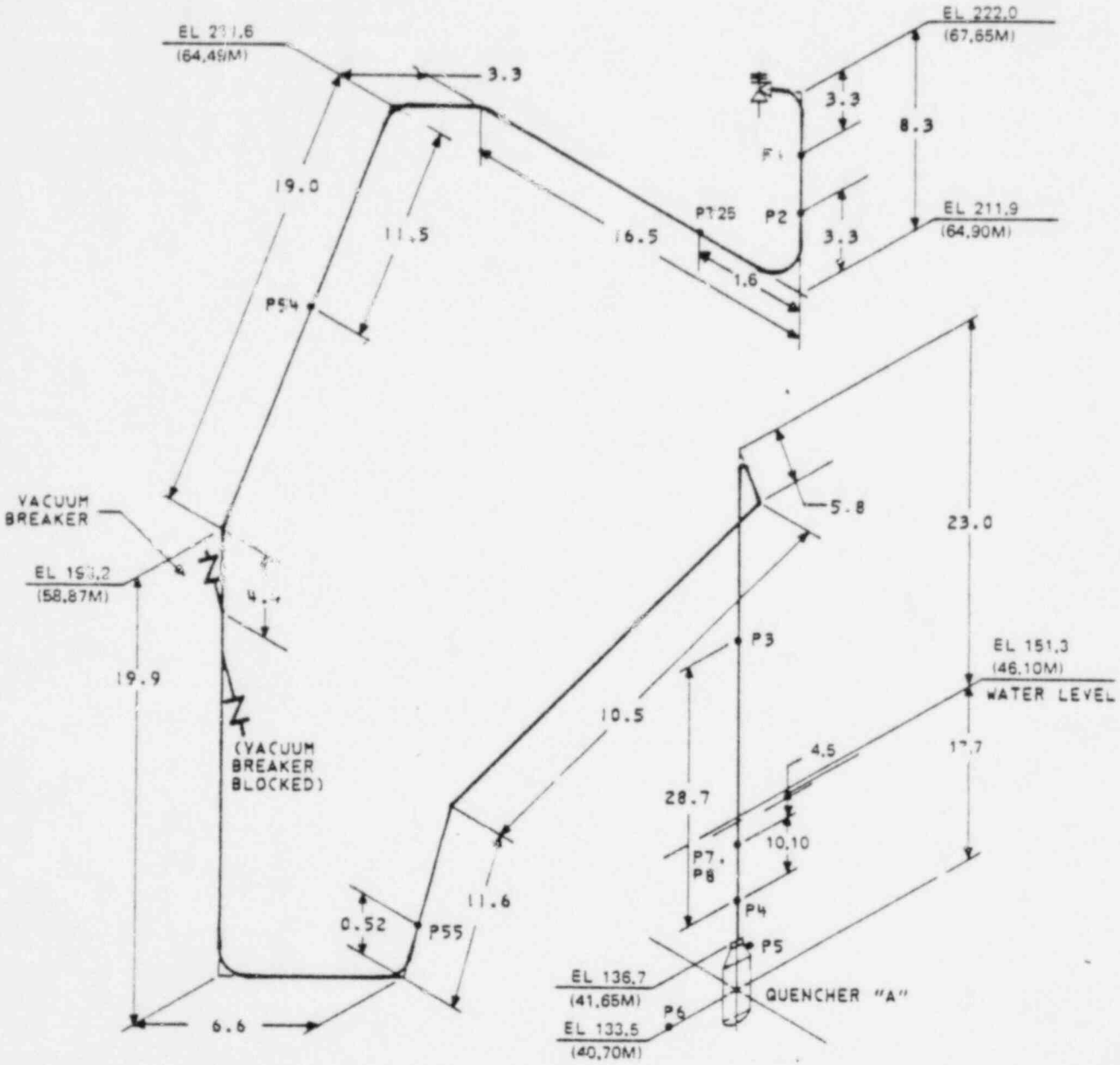

NOTE: All measurements are in feet unless otherwise noted.

Figure 4-7. SRV A Discharge Line and Quencher Configuration Pressure Sensors

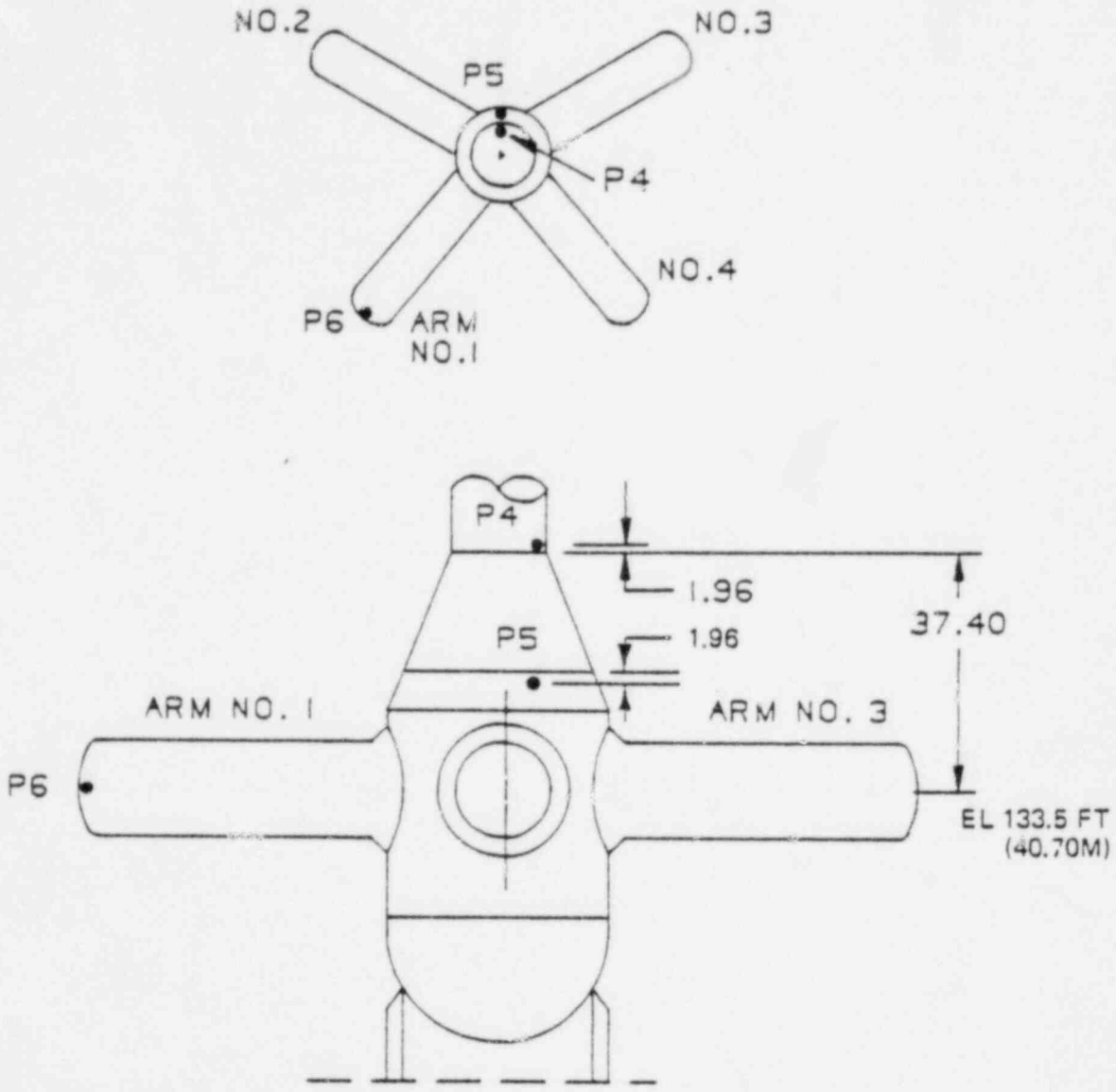

NOTES:

1. All sensors located inside piping or quencher.

2. All measurements are in inches unless otherwise noted.

Figure 4-8. SRV A Discharge Line and Quencher Pressure Sensors

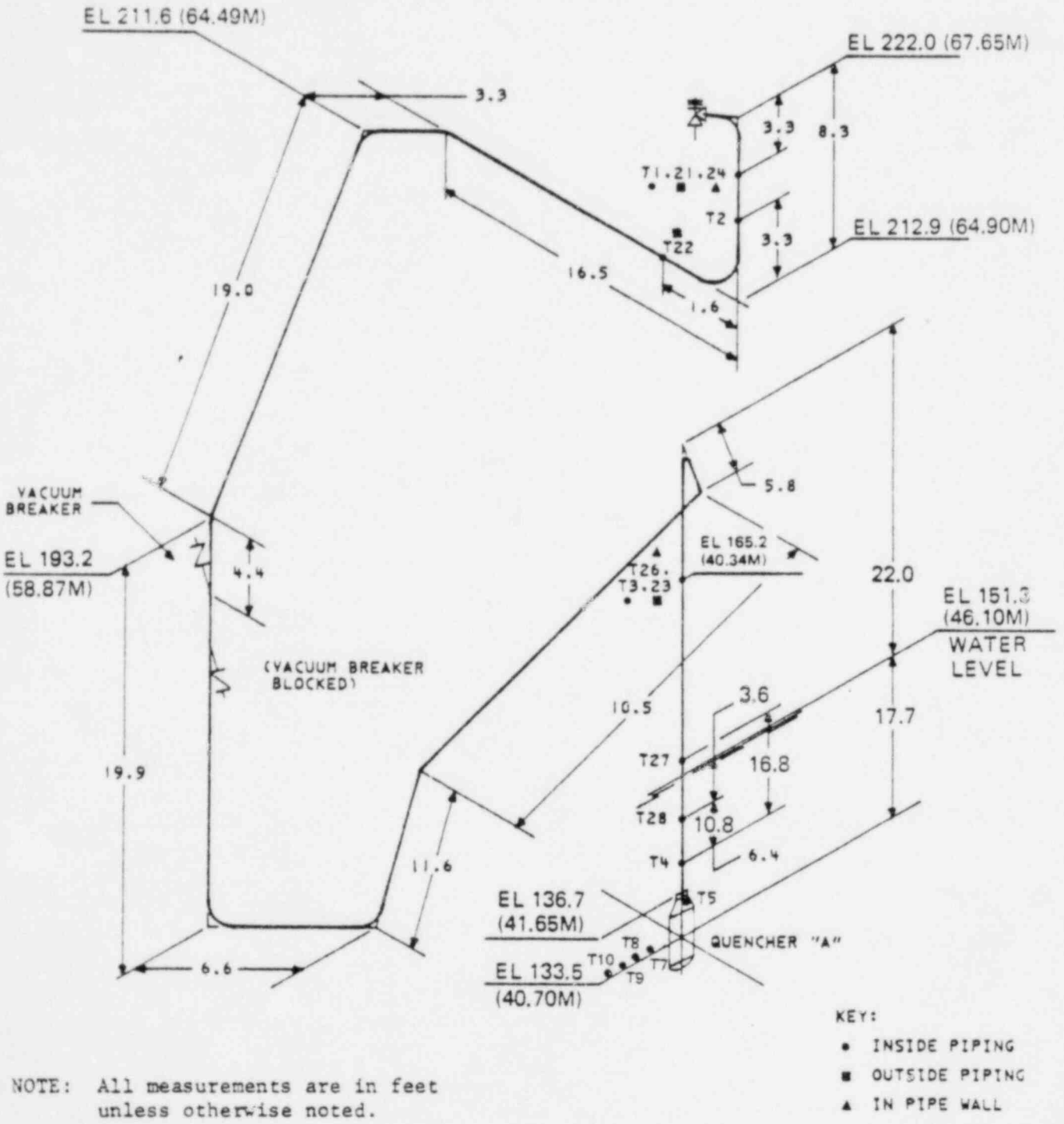

NOTE: All measurements are in feet unless otherwise noted.

Figure 4-9 . SRV A Discharge Line and Quencher Configuration Temperature Sensors

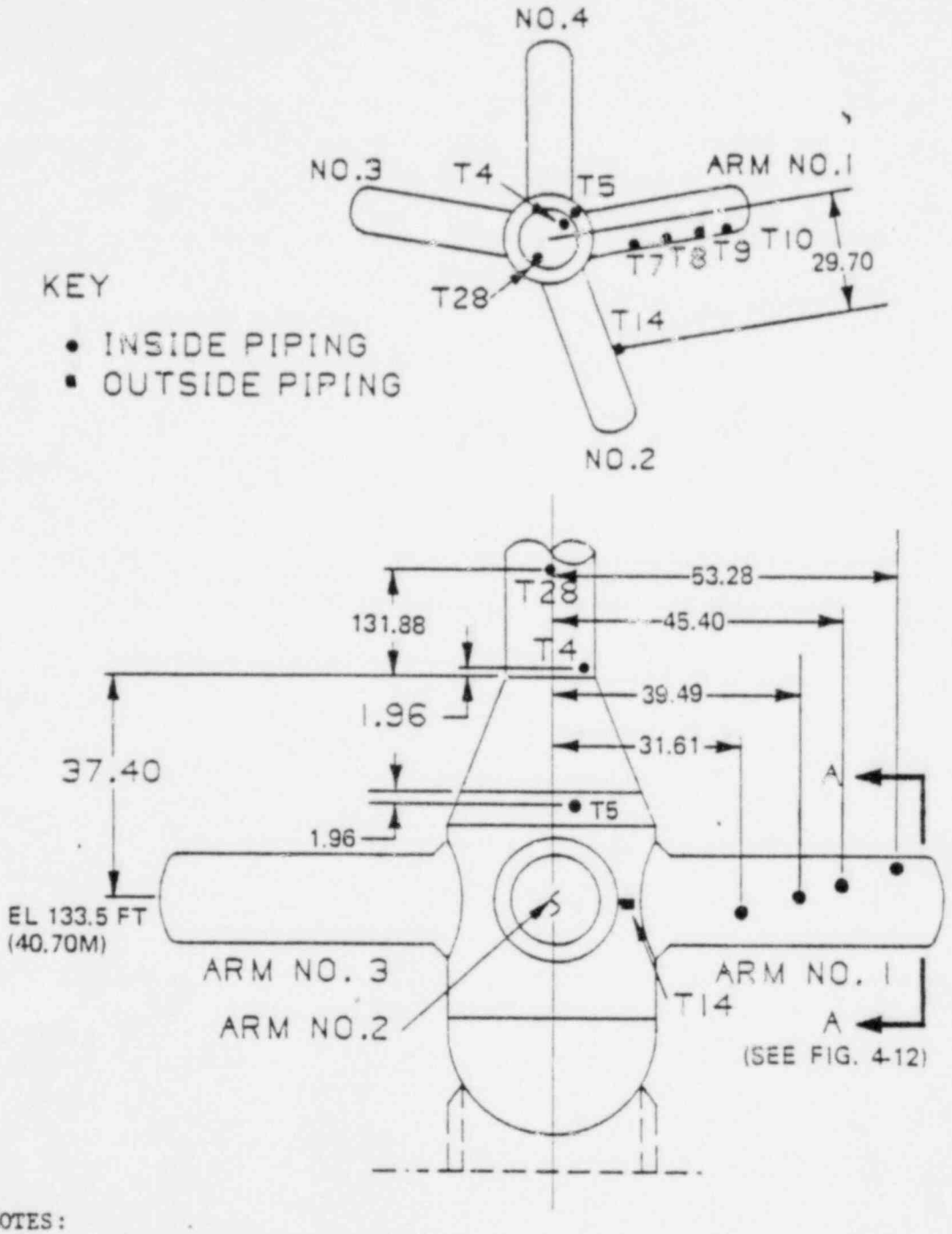

NOTES:

1. T4 and T5 rotated into view.
2. All measurements are in inches unless otherwise noted.

Figure 4-10. SRV A Discharge Line and Quencher Temperature Sensors

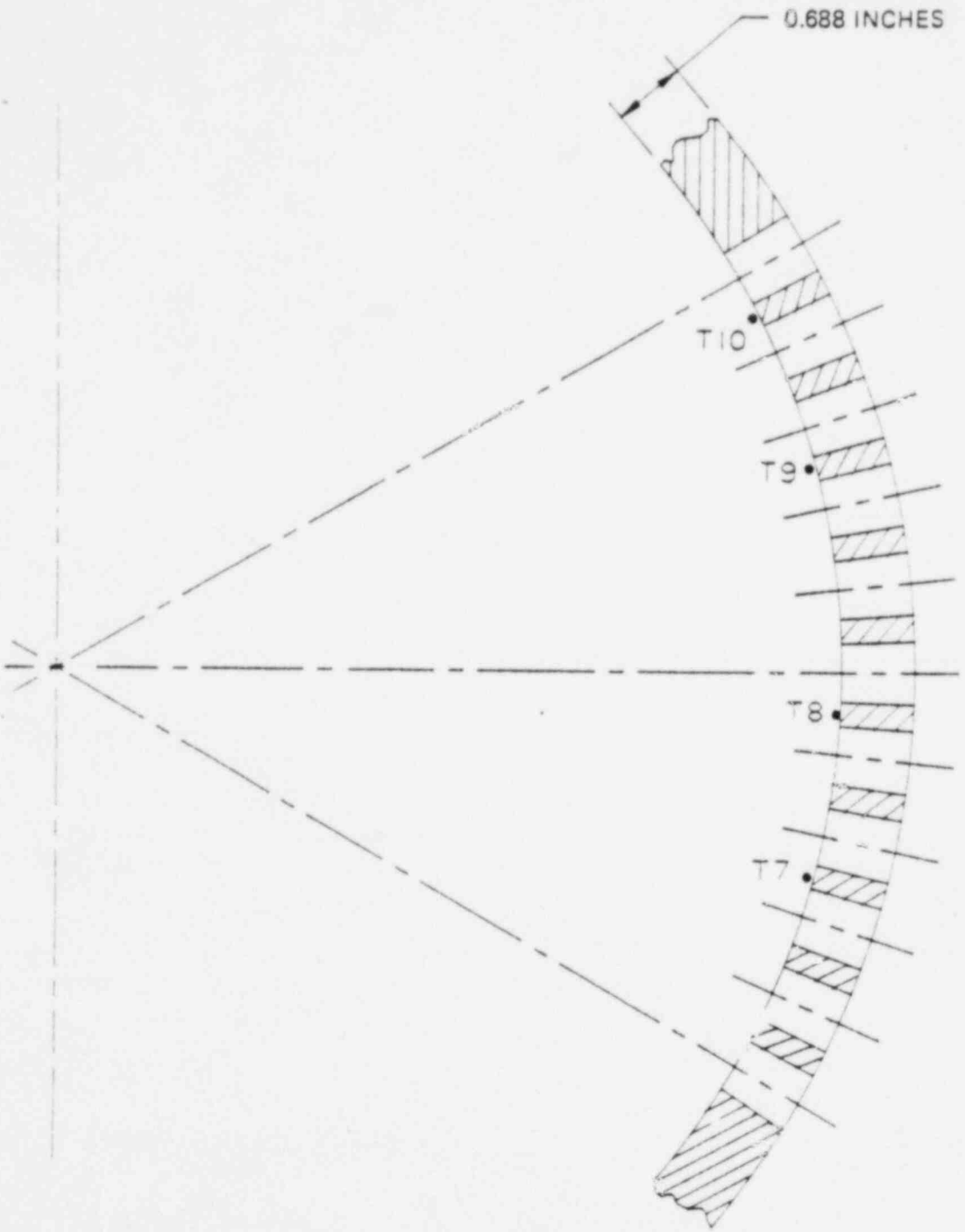

QUENCHER ARM CROSS SECTION A–A
(SEE FIGURE 4-11)

Figure 4-11. Quencher A Arm No. 1 Temperature Sensors

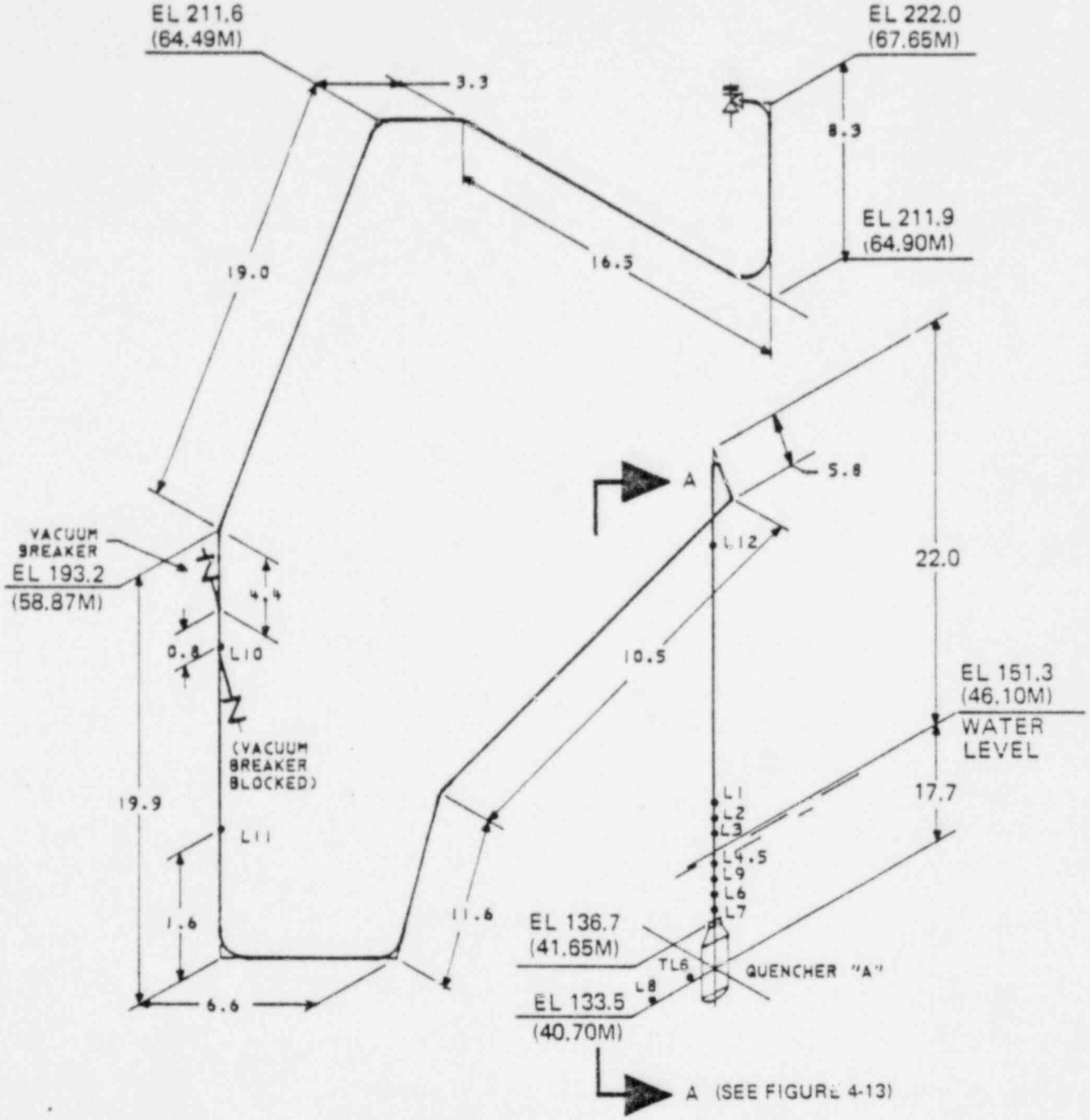

NOTE: All measurements are in feet unless otherwise noted.

Figure 4-12. SRV A Discharge Line and Quencher Water Level Sensors

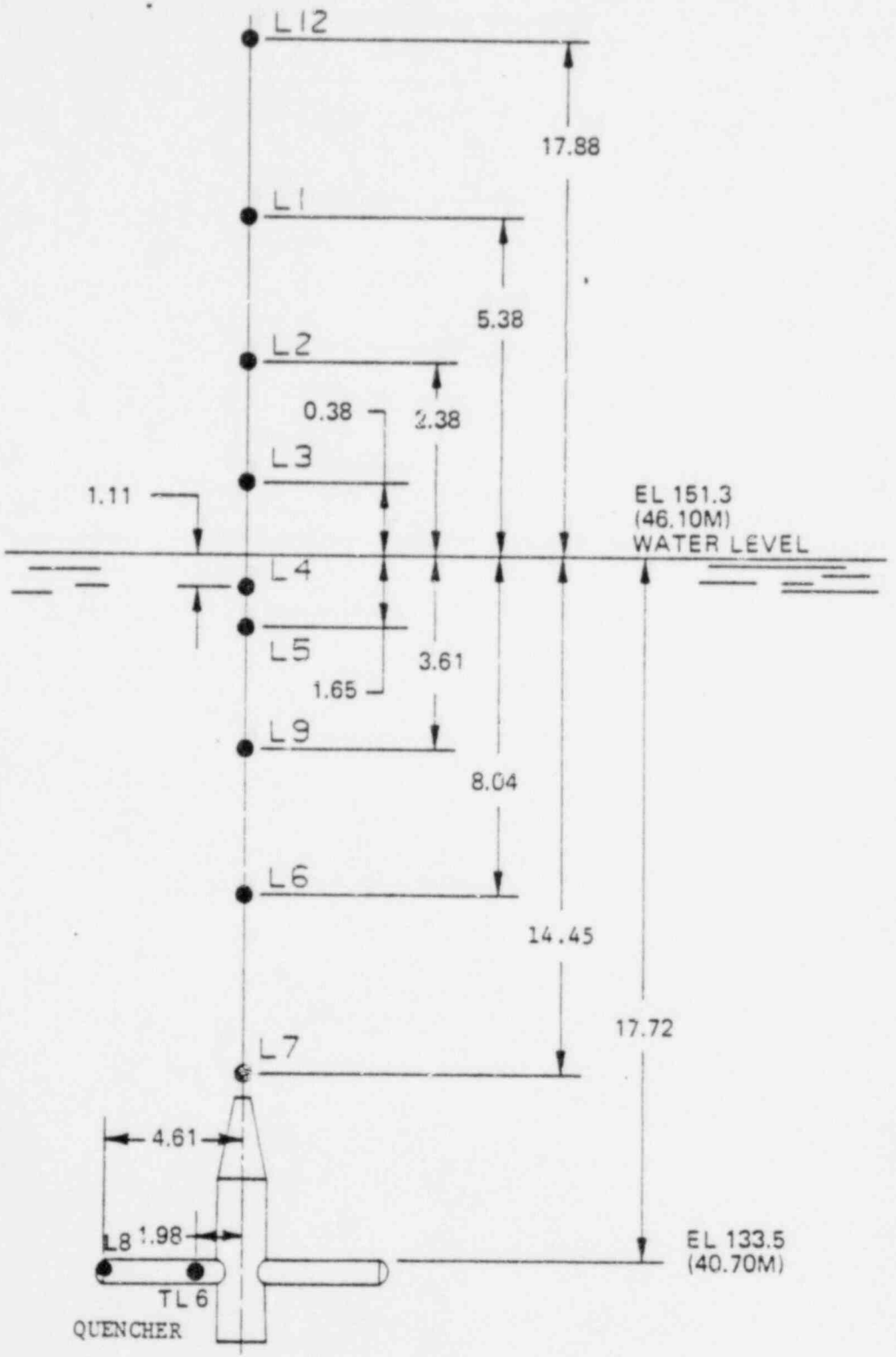

NOTE: All measurements are in feet unless otherwise noted.

Figure 4-13. Level Sensors-Section A-A

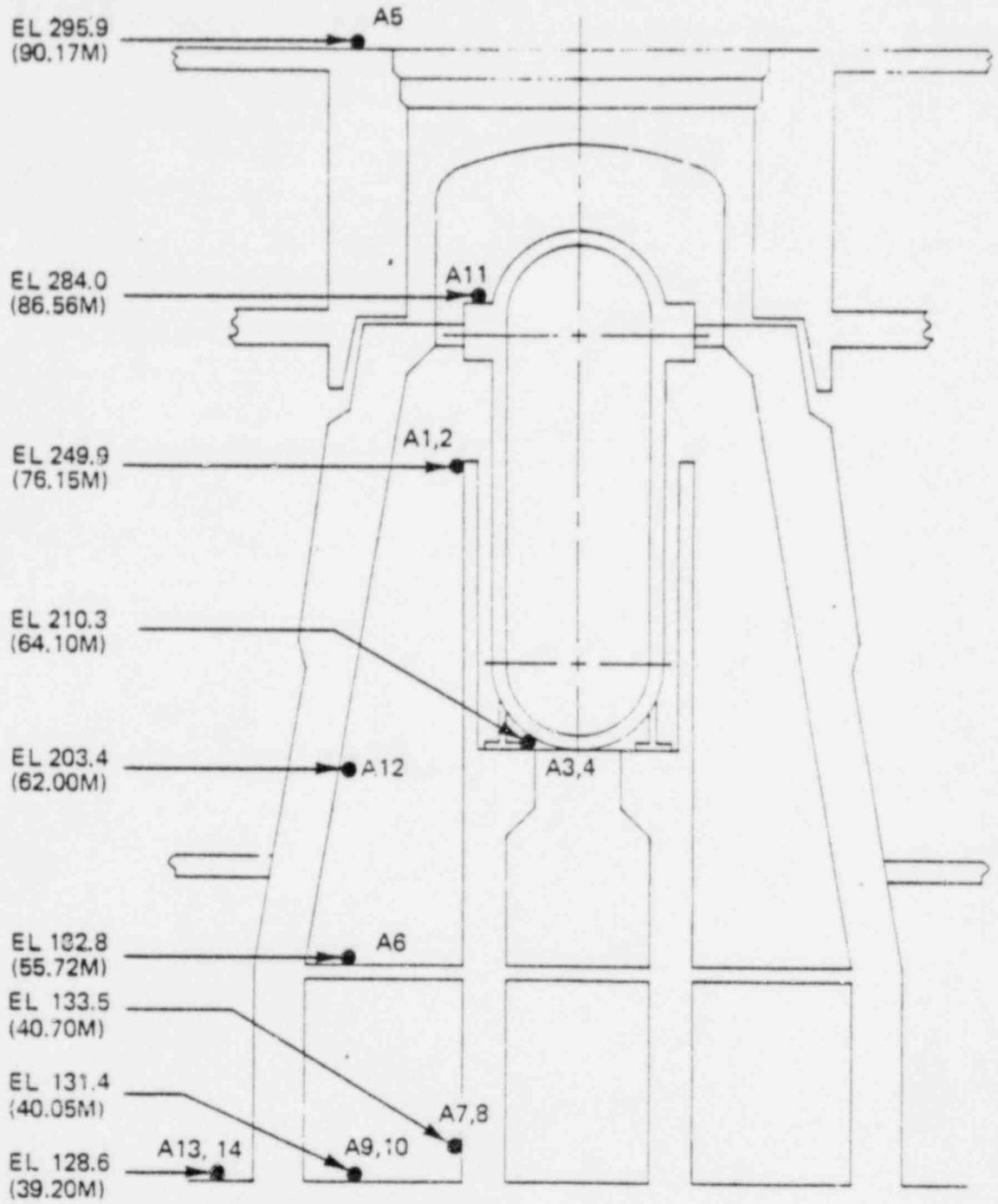

NOTE:

1. Accelerometers have been rotated into plane of paper (see Figure 4-15 for locations).

2. All measurements are in feet unless otherwise noted

Figure 4-14. Containment Accelerometer Location (View From 90° Azimuth)

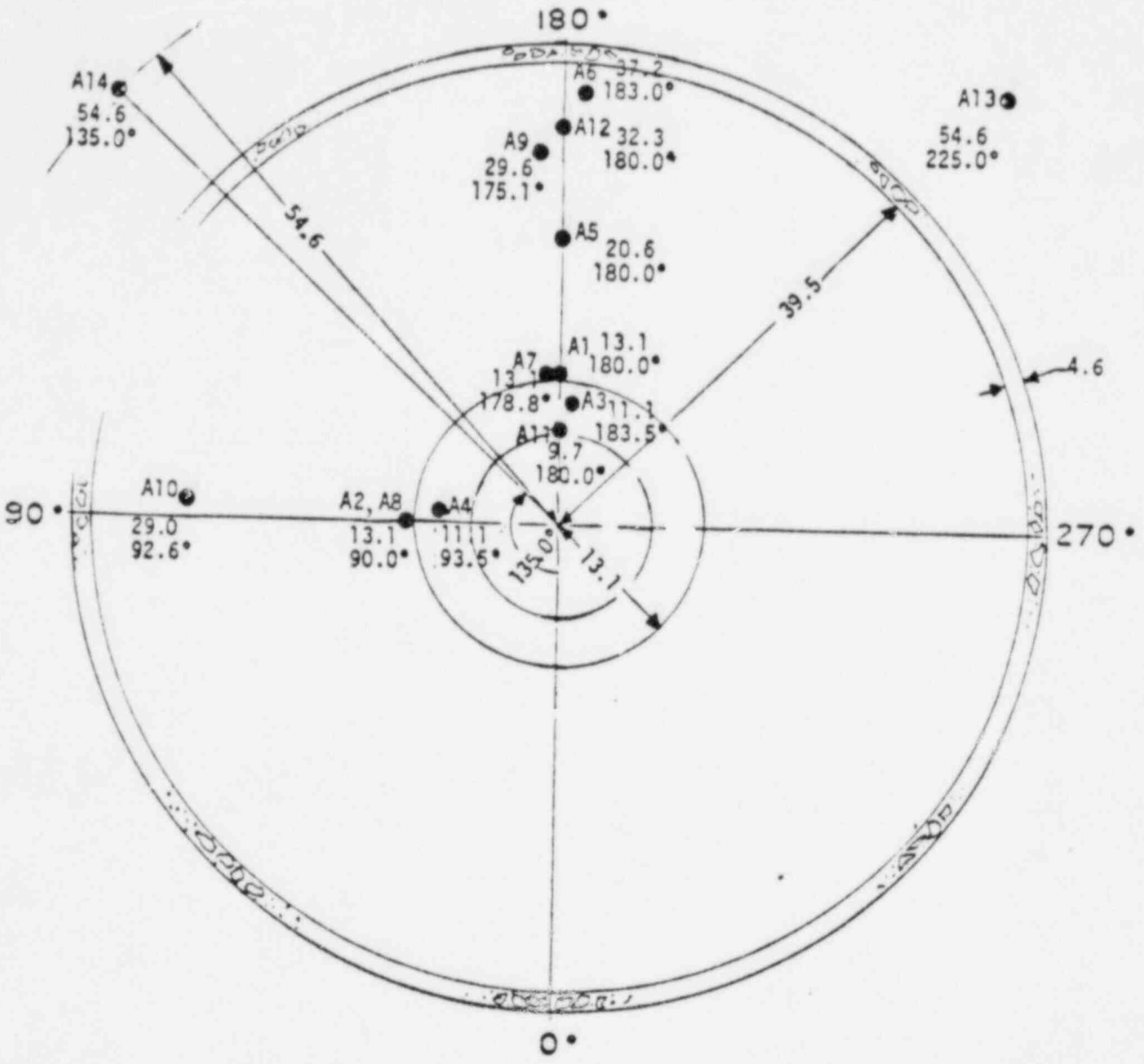

NOTE:

1. All measurements are in feet unless otherwise noted.

2. Accelerometers elements X, Y and Z are oriented tangentially, radially, and vertically to the pedestal wall, except A13 and A14 which are uniaxial accelerometers oriented vertically.

Figure 4-15. Containment Accelerometers

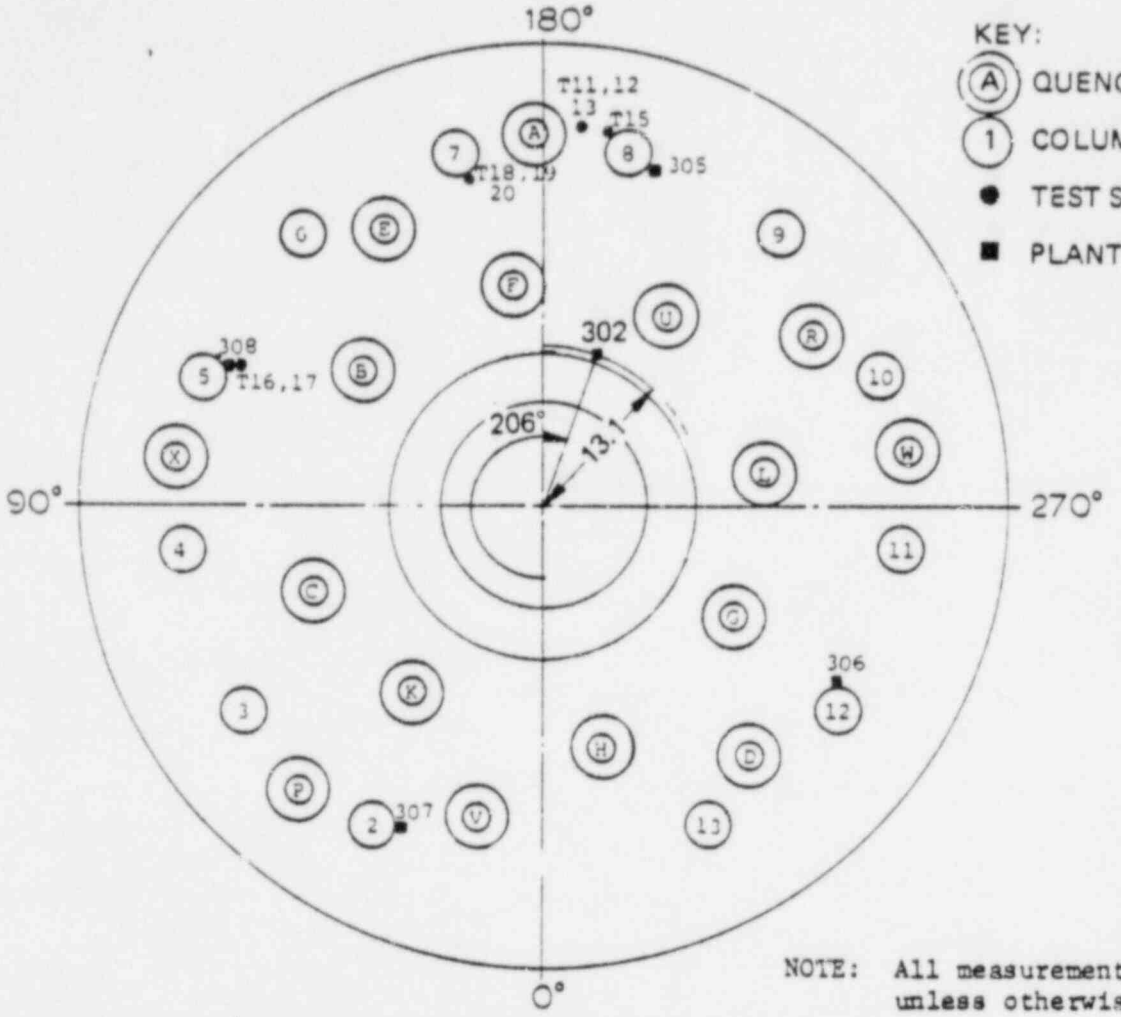

NOTE: All measurements are in feet unless otherwise noted.

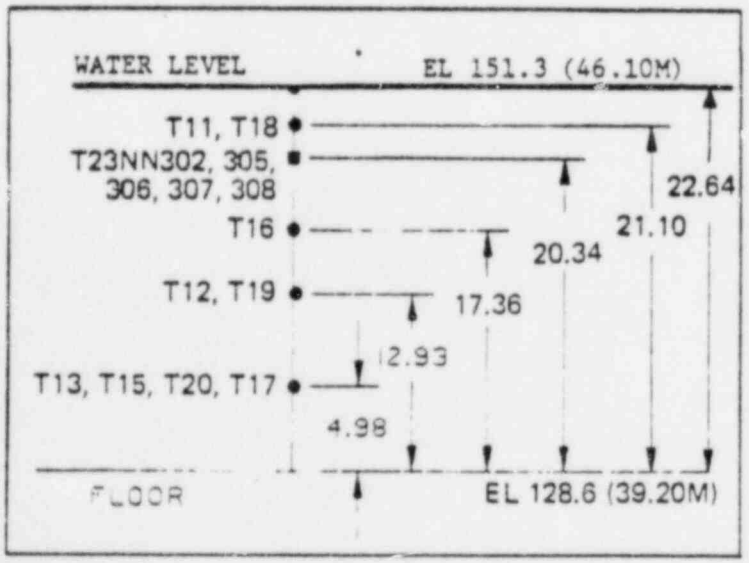

SENSOR NO.	LOC. FROM ℄ OF PEDESTAL
T11, T12, T13	32.2, 183°
T15	32.1, 190°
T16, T17	30.2, 115°
T18, T19, T20	29.2, 167°
T23NN302	13.1, 206°
T23NN305	30.3, 197°
T23NN306	30.2, 300°
T23NN307	30.2, 24°
T23NN308	30.2, 115°

Figure 4-16. Pool Temperature Sensor Location

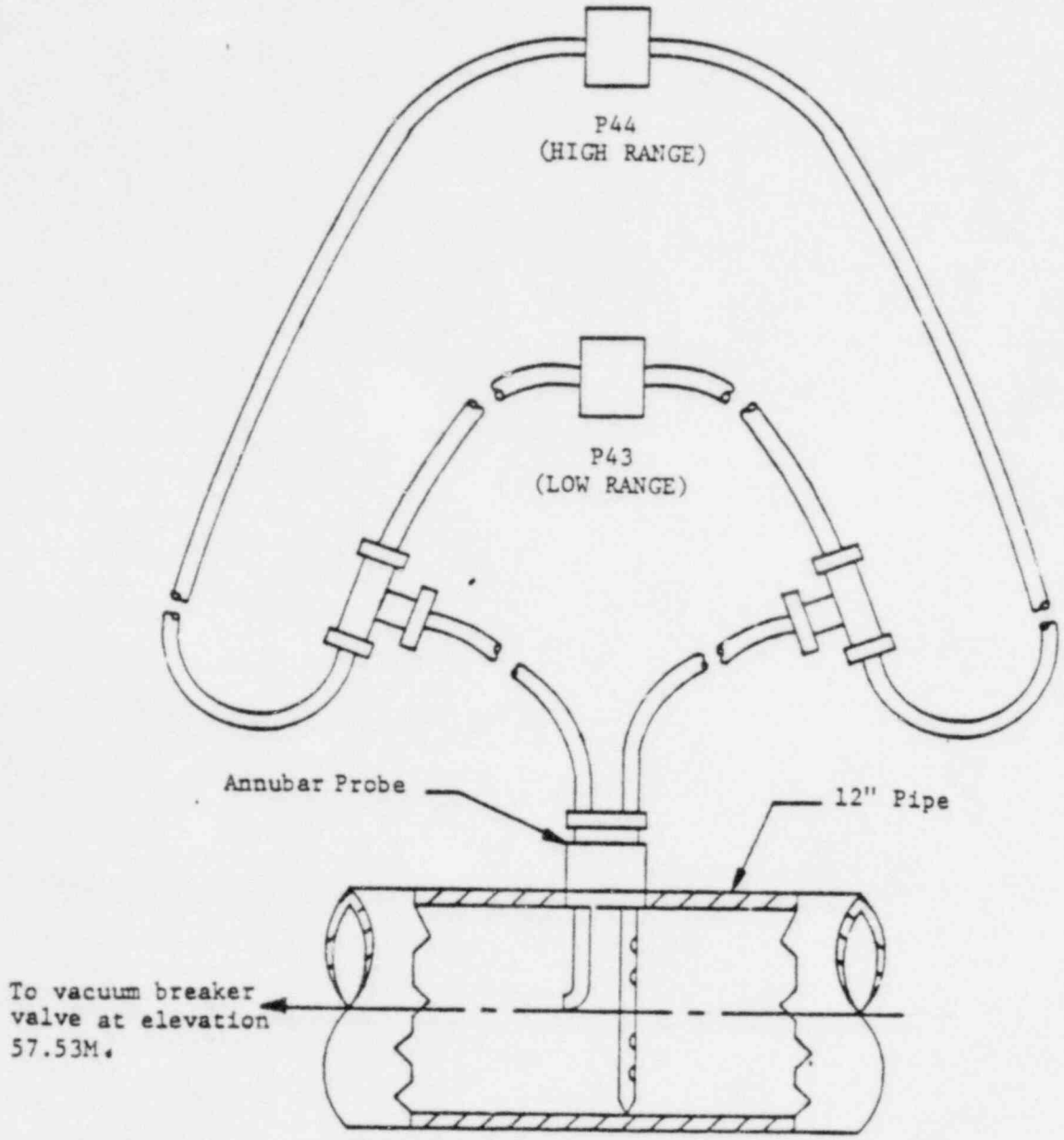

NOTE: Vacuum breaker valve at elevation 57.10M blocked.

Figure 4-17. Vacuum Breaker Flow Measuring Probe

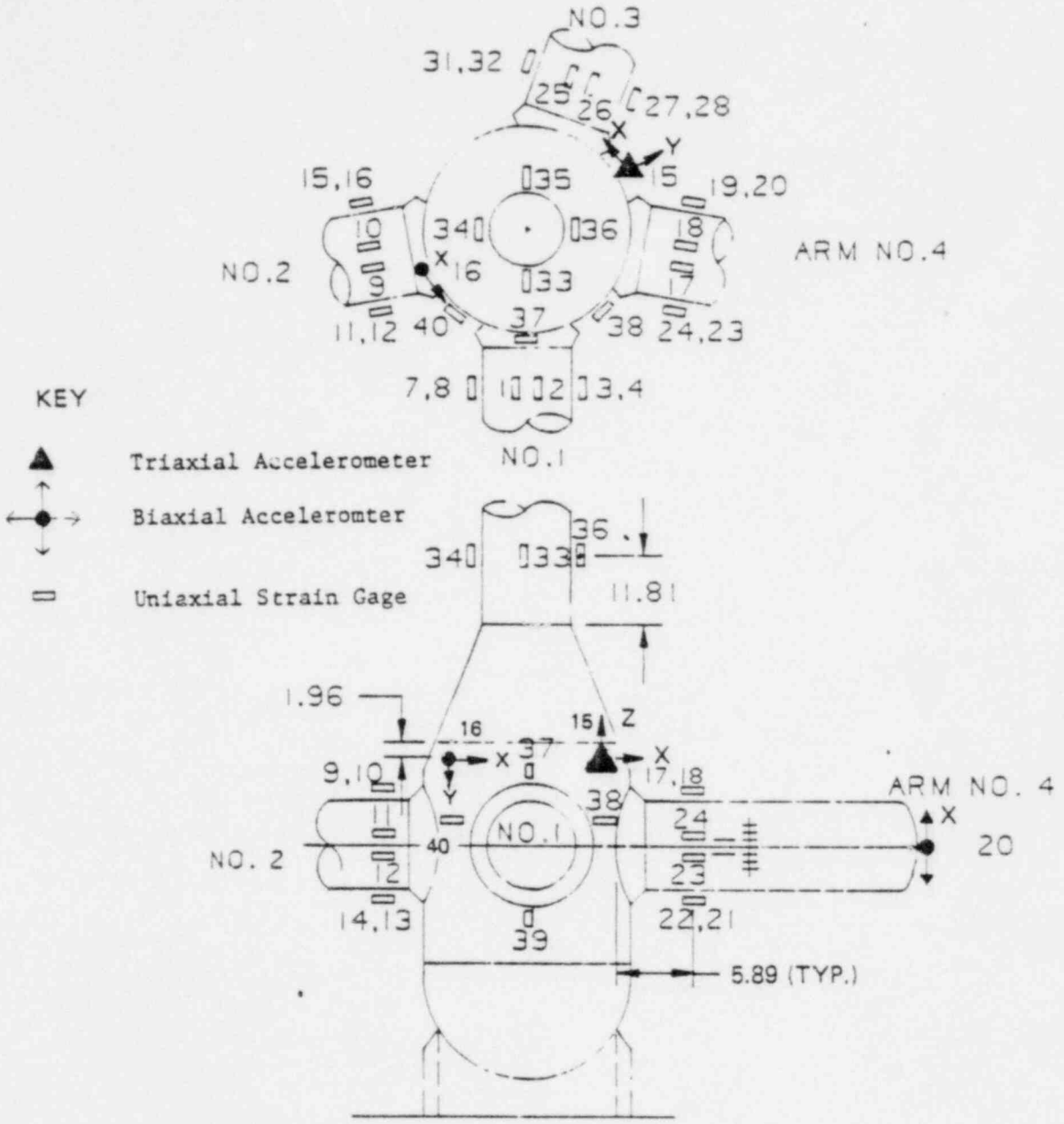

NOTE:

1. All measurements are in inches unless otherwise noted.

2. Positive strain readings correspond to tension on all strain gages.

Figure 4-18. Quencher A Strain Gages and Accelerometers

Figure 4-19 View of Each Quencher Arm with Strain Gages and Accelerometers - Looking Toward the Hub (General Electric Company Proprietary)

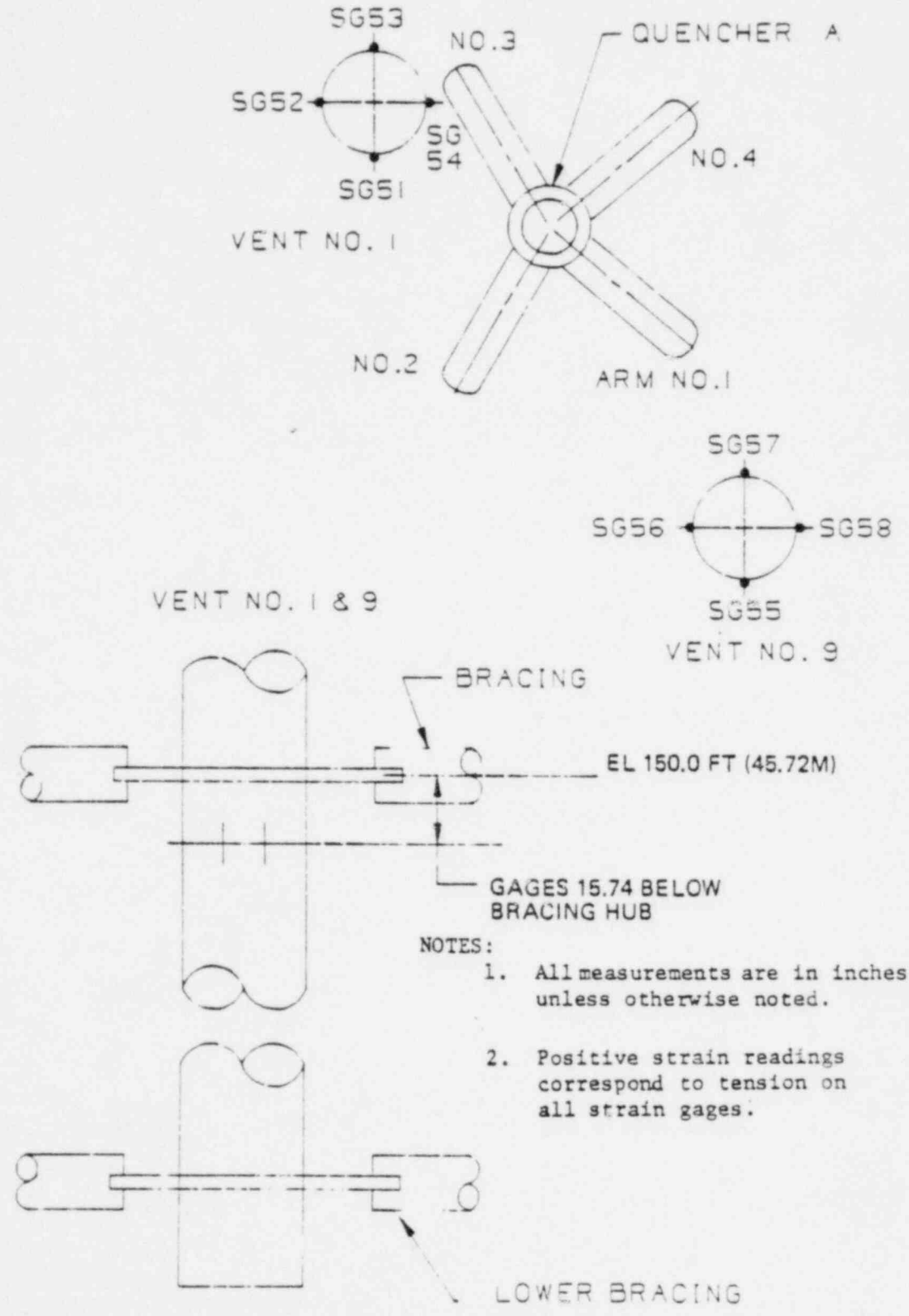

Figure 4-20. Strain Gage Locations on Downcomer Vents

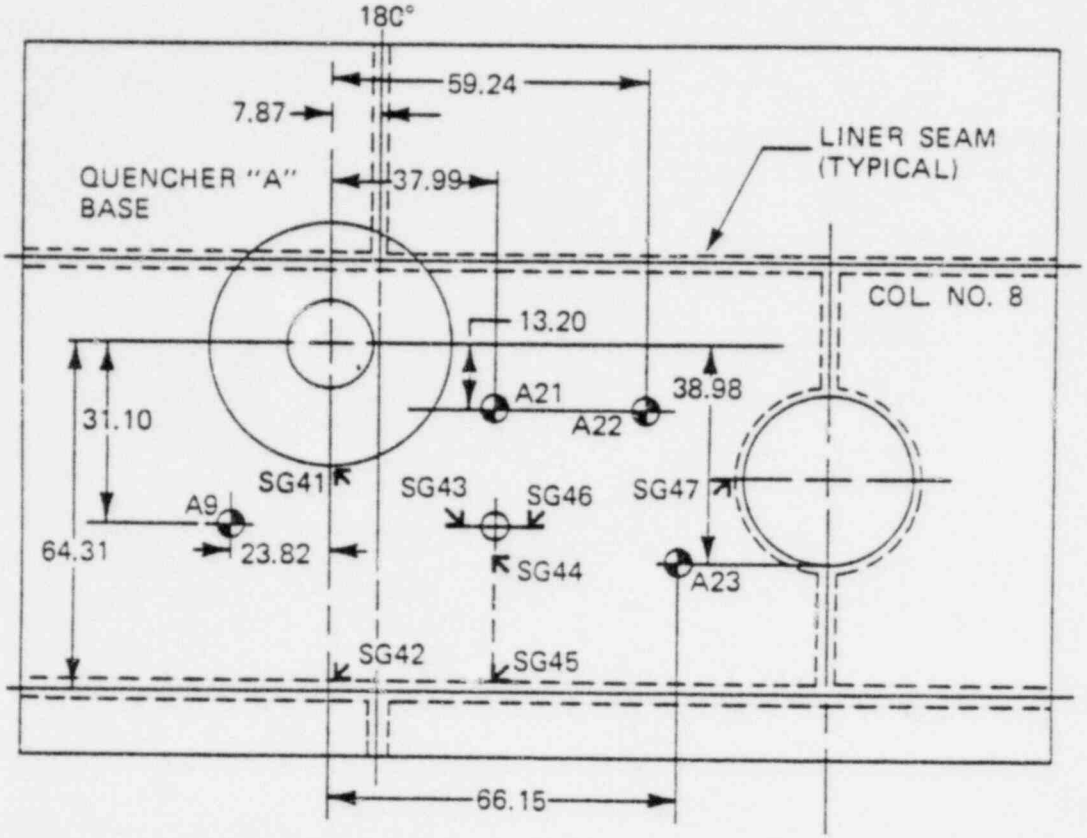

KEY

↙ STRAIN GAGE ROSETTE

◒ UNIAXIAL ACCELEROMETER

○ FASTENER

NOTES:

1. Weldable strain gages are placed in rectangular rosette patterns oriented so one of the perpendicular elements is parallel to a liner seam.

2. All accelerometers and strain gages shown are fastened to liner plate.

3. Positive strain readings correspond to tension on all strain gages.

4. All measurements are in inches unless specified otherwise.

Figure 4-21. Pool Floor Liner Strain Gages and Accelerometers

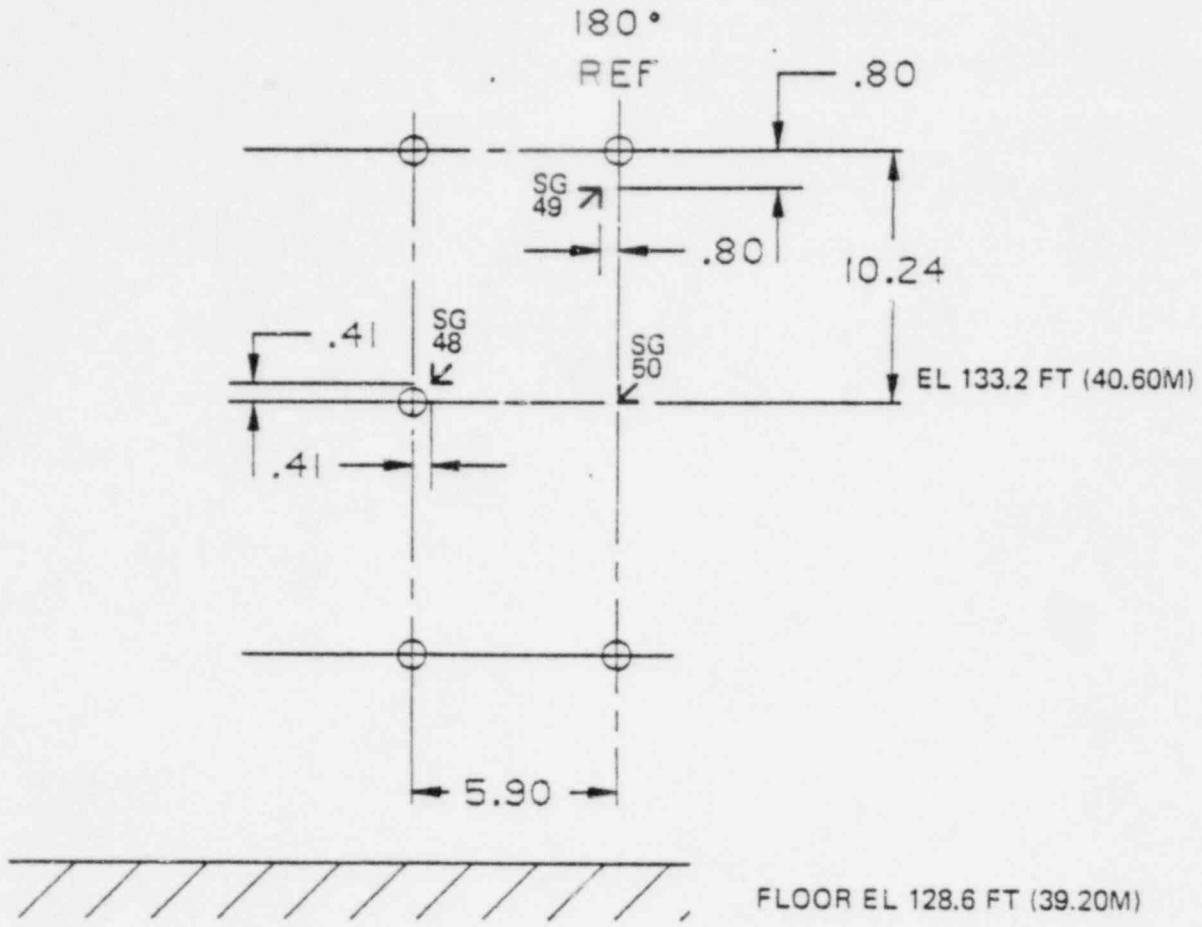

KEY

○ FASTENER

↙ STRAIN GAGE ROSETTE

NOTES:

1. Weldable strain gages to be placed in rectangular rosette patterns oriented with one of the elements horizontal.

2; All measurements are in inches unless otherwise noted.

Figure 4-22. Pool Wall Liner Strain Gages

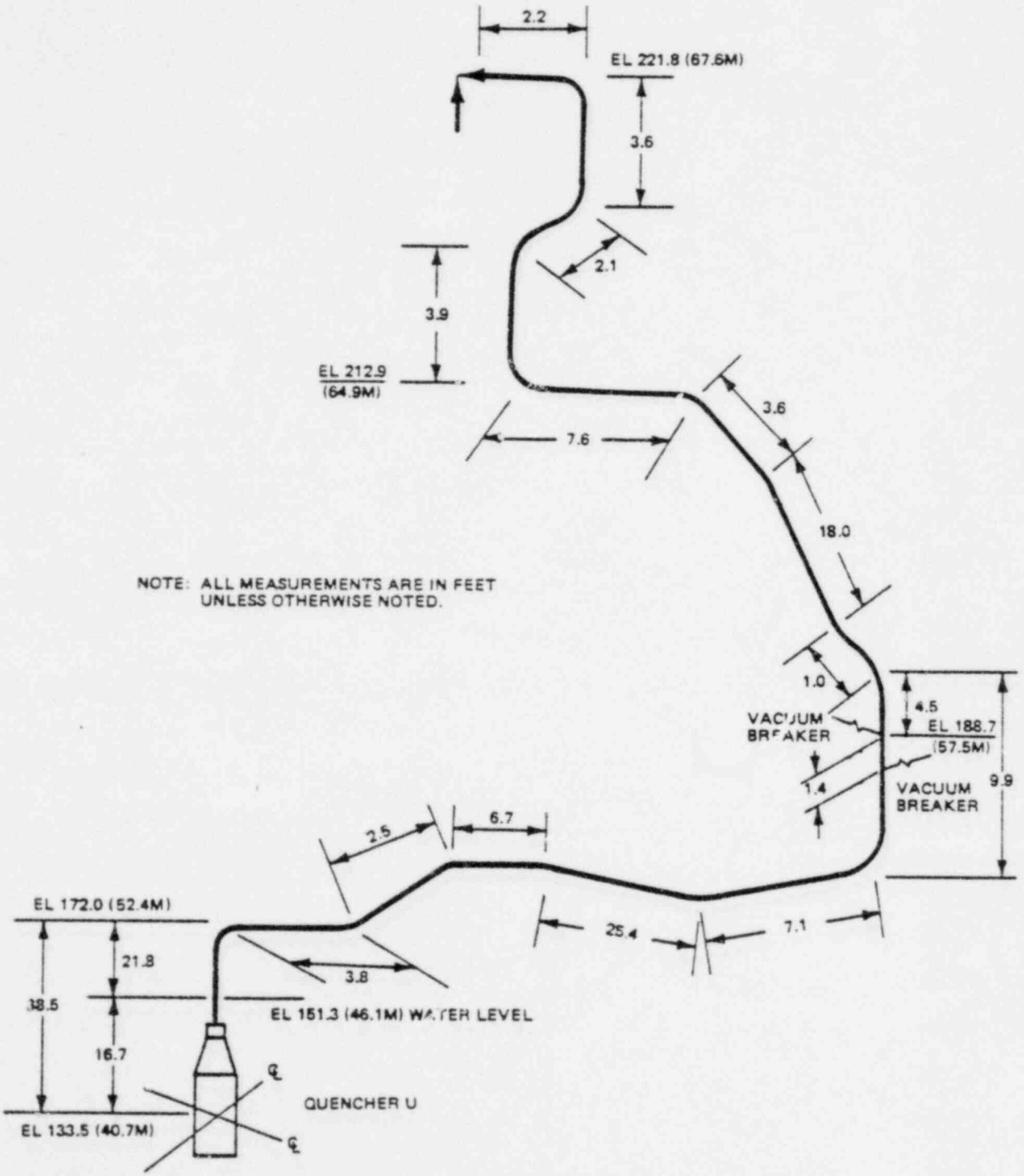

Figure 4-23. SRV U Discharge Line and Quencher Configuration

5. DATA REDUCTION

After the test data had been collected by the PCM data acquisition system, the resulting data tapes required further reduction before the test data engineering plots or data edits could be evaluated. A description of the data reduction system and the various software programs comprising this system is given in Section 5 of the Phase I Test Report.

6. HYDRODYNAMIC PHENOMENA

6.1 INTRODUCTION

Emphasis during Phase II testing was on MVA tests, tests at low reactor pressures, optional LV tests, and the extended discharge test.

The extended discharge test (Test 40) was performed to evaluate the thermal mixing characteristics of the suppression pool. The results of this test will be presented in a separate report. The SVA tests and CVA tests will only be discussed briefly in this report as they are mostly reiterations from the Phase I tests with exception of Test 501X in Phase II. This test involved an actuation of Valve V located opposite to the instrumented SRVDL A in the suppression pool.

Measurements recorded include SRVDL and quencher internal pressures and temperatures, air flow through the vacuum breaker, SRV stroke time, water reflood level in the SRVDL following valve closure, suppression pool temperatures and boundary pressures, and pressure differentials across submerged structures.

A summary of the principal hydrodynamic data is presented in Table 6-1. The maximum SRVDL pressures, quencher internal pressures and pool boundary pressures together with the means ($\bar{x}$), standard deviations (s) and the ratios $s/\bar{x}$ are tabulated for the various test conditions and selected sensors. As appropriate, data from both Phase I and Phase II tests were used in the statistical calculations. The hydrodynamic data from all operative sensors and all tests in Phase II are tabulated in Appendix B.

6.2 DATA REDUCTION AND EVALUATION METHODS

6.2.1 Data Sampling Rates

The data acquisition system used to record the hydrodynamic data during the Phase II tests sampled and recorded data at one-millisecond intervals. Most hydrodynamic data (e.g., SRV pipe and suppression pool pressures) were reduced

at this rate. Any data that did not require as high a resolution (e.g., pipe and suppression pool temperature, and water level measurements) were reduced at greater time intervals.

6.2.2 Zero Shifts in Pressure Measurements

After completion of some test runs some pressure sensors did not return to their initial base value (zero signal). Such zero shifts are not caused by the property being measured, but are attributable to possible changes in ground potential and/or thermal effects on the pressure sensors.

The values for those sensors that did show some zero shift were read from the data plots with an estimated zero reference point at the approximate center of the pressure oscillations. Those sensor readings based on assumed zero references are identified by an asterisk (*) in the pressure tabulations of Appendix B together with an estimated uncertainty which was assumed equal to the magnitude of the zero shift.

6.2.3 Manual Manipulation of SRV Pipe and Quencher Pressure Data

The SRVDL pressure data recorded near the SRV contained high frequency oscillations (approximately 200 Hz) superimposed on the pressure transient. The peak and steady state pressures reported for these sensors were read from the data plots as mean values of these oscillations to obtain the bulk pressurization of the line.

6.2.4 Filtering of Submerged Structures Pressure Data

High frequency oscillations were also observed in pressure data for the submerged structures. This was attributed to vibration of the structures on which the pressure transducers were mounted. Frequencies of above 100 Hz were filtered out to obtain the plot of the forcing function. This was for sensor pairs P24-P53 and P33-P34.

6.3 SRV PIPE AND QUENCHER PRESSURE

6.3.1 Description of Phenomenon

Following SRV actuation, the pressure within the SRVDL increases. Pressurization continues until the inertia of the initial water slug located in the submerged portion of the piping and quencher is overcome and the water and air initially located in the SRVDL are cleared.

6.3.2 Instrumentation and Test Data Summary

Nine pressure transducers (Sensors P1 through P6, PT25, P54 and P55) were installed on SRVDL A to measure pipe and quencher pressures during line clearing and steady state steam flow. Locations of each sensor on the SRVDL and quencher are shown in Figures 4-7 and 4-8.

Sensor P3 failed prior to testing, and Sensor P55 had to be excluded because its ambient pressure reading was negative. Readings from Sensors P1 and P2 were also excluded from the results because they showed more than 10 percent calibration error during testing. The remaining sensors mounted on the SRVDL provided adequate indirect data to compensate for these failed sensors.

Representative peak SRVDL and quencher pressures, the mean values, and standard deviations if appropriate for the various test conditions are shown in Table 6-1. The table also shows the result of both Phase I and Phase II tests with equivalent conditions. Selected plots of the SRVDL and quencher pressures from these tests are shown in Figures 6-1 through 6-3. The peak pressures magnitudes measured by each sensor from every test are reported in Appendix B.

6.3.3 Results

The maximum pipe pressure measured during any test was 345 psia as recorded by Sensor PT25 located 7 ft downstream from the SRV. Sensor P5 measured the maximum recorded quencher pressure of 677 psia. Both of these maximum pressures were measured during Test 2312, a CVA, WP, EWL test. Generally, this test had the maximum values for most sensors. As in the Phase I tests, the SRVDL internal pressures tended to be higher with a higher initial water leg. The dependency of the SRVDL pressure at PT25 and the quencher pressure at P5 on the reactor pressure is shown in Figure 6-4. Generally, both of these pressures increased with increasing reactor pressure while none of the pressures under LP conditions were higher than the corresponding pressure resulting from a full reactor pressure test. The maximum SRVDL pressure recorded for all first actuation tests of 315 psia was measured by PT25 during the two-valve actuation Test 24. The maximum quencher pressure of 522 psia for all first actuation tests was measured by Sensor P5 during SVA Test 2301. The SRVDL pressure did not appear to depend on the number of valves actuated or the amount of steam in the SRVDL prior to valve actuation in LV tests.

The SRV pipe and quencher pressures observed are consistent with the Phase I test results, and confirm the findings from tests with similar initial conditions. Also, the MVA and LV tests did not exhibit any major deviations from the pattern.

Typical traces for Sensors PT25, P5 and P6 (quencher arm pressure) from MVA, LV, and LP tests are shown in Figures 6-1, 6-2 and 6-3. The SVA trace at full reactor pressure is included for comparison.

6.4 SRVDL WATER REFLOOD

6.4.1 Description of Phenomenon

Following SRV closure, the pressure in the discharge line decreases and the steam inside the line begins to condense as water rushes back into the quencher and SRV line. This condensation rapidly reduces the pressure of the line

even further, and draws in more water. Finally, the discharge line pressure drops to a point where the discharge line vacuum breaker (VB) opens and allows air to reenter the line causing more condensation. The maximum height to which the water refloods the discharge line is dependent on vacuum breaker dynamics and flow area, i.e. the amount of air which enters the discharge line. Furthermore, the quencher volume minimizes the water level overshoot by acting as a reservoir for the incoming water.

6.4.2 Instrumentation and Test Data Summary

Conductivity probes and temperature sensors mounted on SRVDL A measured the water level. Ten of the twelve conductivity probes (except Sensors L10 and L11) and temperature Sensors T3, T27 and T28 were used to measure the water level in SRVDL A. Level Sensor L2 was inoperable during testing.

The conductivity probes reacted with a step change when the water rose or fell past a probe location, and the temperature sensor reacted with a slope change. To obtain a plot of the reflood transient, the time of sensor activation was plotted against the conductivity probe height. Pressure Sensor P19 located on the pool floor near quencher A was used in determining the time of valve closure (t = 0 on the plot). The return of the pressure at Sensor P19 to its base value was assumed to coincide with the SRV closure. Water reflood data is shown in Table 6-2.

6.4.3 Results

The maximum water level overshoot above NWL with one 10-inch VB was approximately 5.4 feet as shown in Table 6-2. The VB lets in enough air for the equilibrium point of the oscillating water level to remain from 6 to 10 feet below normal water level after the initial overshoot. These observations are in agreement with Phase I test results.

After LP Test 33 (reactor pressure of 50 psig) the steady state reflood level returned to normal water level following SRV closure (see Figure 6-5); while in nearly all other tests the steady state reflood level ranged from 6 to

10 feet below normal water level. The test data for Sensor P44 indicate that the vacuum breaker did not open during LP Test 33. Otherwise the low reactor pressure tests had little effect on the water reflood levels. Figure 6-6 shows a reflood plot for the LP Test 36 (400 psig).

The reflood plot for LV Test 4401 is shown in Figure 6-7. A trend toward lower steady state recover levels was noted in the SVA leaking valve tests which had recovery levels between 10 and 14 feet below normal water level. The LV, CVA tests resulted in normal reflood levels between actuations.

6.5 SUPPRESSION POOL BOUNDARY PRESSURES DUE TO SRVDL CLEARING

6.5.1 Description of Phenomenon

On SRV actuation the water and air content of the SRVDL is forced into the suppression pool by high pressure steam. The water leg initially at rest is rapidly accelerated until the water clears the quencher. The water leg is immediately followed by an air/steam mixture that is also forced through the holes in the quencher arms. The air/steam mixture forms several air bubbles that oscillate as they rise toward the pool surface. As a result of these phenomena, pressure loadings on the suppression pool boundary were observed.

6.5.2 Instrumentation and Test Data Summary

Thirty pressure transducers (P9 through P21, P23, P25 through P32, P35 through P38, P50, P51, P56 and P57) were mounted on the suppression pool wall, floor and pedestal beneath the water level in that quadrant containing quenchers A, E, F and U. Locations of these transducers are shown in Figure 4-2.

Sensors P12, P16, P20, P21, P29 and P30 failed prior to testing. Calibrations of P10, P11, P18, P28, P38, P56 and P57 drifted more than 10 percent during testing. Consequently, the data from these sensors is not included in the results. Enough sensors remained operable to provide backup data for the failed sensors.

Peak positive and negative pressures measured by selected sensors, including oscillation frequencies, mean values and standard deviations for each test condition are presented in Table 6-1. The means and standard deviations from Phase I and Phase II data have been combined wherever appropriate. Peak positive and negative pressures measured by each operable sensor in every Phase II test are contained in Appendix B. Representative plots of boundary pressure versus time from several locations are given in Figures 6-8 through 6-14.

6.5.3 Results

The maximum pool boundary pressures measured during Phase II testing were 9.4 psid and -6.6 psid. These pressures were recorded during a CVA, HP, DWL (Test 22A02). The maximum pool boundary pressures for SVA, CP, NWL tests were 5.0 psid and -4.0 psid (Tests 39/2311). This compares well with the Phase I results of 5.0 and -4.3 psid. The maximum pool boundary pressures for CVA, HP, DWL (Valve A) tests were 8.2 psid and -5.0 psid (Tests 5324/2313), compared with Phase I values of 7.5 psid and -5.2 psid. The maximum pool boundary pressures for CVA, EWL tests were 5.4 psid and -3.9 psid (Test 2312). Similar Phase I tests produced pressures of 8.0 psid and -5.7 psid. First actuations of the LV tests resulted in maximum boundary pressures of 3.8 and -5.7 psid (Test 42). The maximum values for Phase I and Phase II testing with means, standard deviations, and boundary pressure frequencies for various test conditions are compared in Table 6-1 which shows consistent results between the two test phases. Subsequent actuations of LV tests showed results similar to non-leaking valve tests with comparable initial conditions (i.e., CVA, HP, DWL, Valve A). The maximum boundary pressures recorded during the LV tests were 8.9 and -5.9 psid (Test 4402). MVA tests can be grouped into two-valve, three-valve, four-valve, and eight-valve tests. The maximum pool boundary pressures for these groups were 5.3 psid/-3.8 psid (Test 24), 4.2 psid/-5.3 psid (Test 26), 7.0 psid/-5.3 psid (Test 45-2) and 5.6 psid/-4.6 psid (Test 32), respectively. Reduced reactor pressure tests resulted in lower boundary pressures. Figure 6-15 shows the relationship between RPV pressures and the suppression pool boundary pressures.

6.5.4 Boundary Pressure Waveform Characteristics

6.5.4.1 Initial Boundary Pressure Spikes

Pool boundary pressure oscillations in the 5 to 10 Hz range were usually preceded by higher magnitude/higher frequency oscillations. Generally, the frequency of the initial pool boundary pressure peaks was 25 to 30 Hz.

The SVA, LV tests had lower positive peaks than the CVA, LV tests. CVA, HP, DWL tests had higher initial positive pressures than CVA, WP, DWL tests, however, the negative peaks did not differ significantly. The effect of MVA actuation did not result in any significant variations in the pressure peaks.

6.5.4.2 Boundary Pressure Oscillation Frequency Content

PSD is used as a measure of the energy content versus frequency of a given signal. First actuation and consecutive actuation analyses are discussed in the Phase I test report. PSD analyses of MVA, LP and LV tests are addressed in this subparagraph. The PSDs of Tests 2301 (SVA, Valve A), 2305 (CVA, Valve A), 22A01 (SVA, Valve U) and 22A05 (CVA, Valve U) are included in this subparagraph as representative of the SVA and CVA tests in Phase II. Sensor P23 located on the containment floor midway between Quenchers A and F was chosen for PSD comparison of the tests given in Table 6-3.

In the Valve U actuations (Tests 22A01 and 22A05) Sensor P51 located on the containment floor directly under Quencher U was selected for the PSD analysis (see Figures 6-24 and 6-25).

Comparing the PSDs from Sensor P23 shows that with the exception of LV Test 43 there is little difference in the signal frequency content of these various tests at this particular location. The dominant frequencies are located in the interval between 0 to 10 Hz. Also, in almost all cases, over 60 percent of

the signal energy (over 90 percent for the LP tests) is concentrated in this interval. Due to large higher frequency initial pressure peaks in Test 2301 a greater portion (almost 50 percent) of the signal energy is distributed above 10 Hz. Similar phenomenon can be observed for the Valve U actuations by comparing the PSDs of Tests 22A01 (SVA) and 22A05 (CVA) at Sensor P51 location. In either case, however, the dominant frequencies of the forcing function are still in the normal 0 to 10 Hz range.

The PSD for LV Test 43 shows that boundary pressure energy is distributed in a bell shaped fashion from 0 to 60 Hz with a "dead zone" in the 30 to 40 Hz range. Other LV tests have similar energy distributions. Waveforms from the LV, SVA tests are highly irregular compared to waveforms of other tests.

6.5.4.3 Boundary Pressure Phasing

Appendix B contains a discussion on the phasing of the pool boundary pressure at various locations about the quencher. The pressure traces and the cross-correlations between different pressure measurements in this Appendix show that the boundary pressures around the quencher are essentially in phase during the LV, LP and most MVA tests.

6.5.5 Boundary Pressure-Distance and Pressure-Time Attenuation

Discussions on pool boundary pressure-distance and pressure-time attenuation for the SVA and CVA tests are presented in Subparagraphs 6.6.3.2 and 6.6.3.3 of the Phase I Test Report. Detailed discussion of MVA, LP, and LV test boundary pressure-distance and pressure-time attenuation is presented in Subsection 6.8.

6.6 SRVDL CLEARING LOADS ON SUBMERGED STRUCTURES

6.6.1 Description of Phenomenon

Loads on submerged structures in the suppression pool are caused by the water/air clearing phenomenon discussed in Paragraph 6.5.1. This discharge of water

and air creates velocity and acceleration fields in the suppression pool causing drag loads on submerged structures. Pressure sensors were located in the pool to measure the pressure differential across the submerged structures.

6.6.2 Instrumentation and Test Data Summary

Pairs of pressure transducers were installed on opposite sides of various submerged structures to measure the pressure differential (ΔP) across these structures. The ΔP across each structure was calculated by taking the difference between the two readings at each time step.

Sensors were installed at the following locations:

P24 and P53 - on the arm of Quencher F

P33 and P34 - on downcomer vent 9, 7.1 feet above the horizontal centerline of Quencher A

P39 and P41 - on diaphragm floor column 7 (adjacent to Quencher A), 11.9 feet above the horizontal centerline of Quencher A

P40 and P42 - on the diaphragm floor column 7 at Quencher elevation

See Figure 4-2 for the sensor locations. All sensors performed well except for zero shift in P42 (see Paragraph 6.2.1). Sensors P24, P53, P33 and P34 recorded high frequency oscillations superimposed on the pressure transient because of the vibrations in the structures on which they were mounted. These data were filtered at 100 Hz (see Paragraph 6.2.4) prior to evaluation. The maximum ΔP readings for each sensor group in each test is shown in Appendix B. Velocity probes were installed to measure local suppression pool water motion, but vibrations in their support structures dominated the velocity readings and rendered them useless.

6.6.3 Results

The maximum ΔP across the submerged structures was always less than the corresponding maximum boundary pressure for all the tests, except ΔP readings for Sensors P24 and P53 (across quencher arm on SRV F) during MVAs in which SRV F was actuated. The highest ΔP of 4.8 psid was recorded during SVA, CP, NWL (Test 39) and MVA (Test 29) tests.

Figure 6-26 shows a typical plot obtained from Sensors P40 and P42 during SVA Test 2301 and MVA Tests 26 and 32. The maximum ΔPs across submerged structures for all tests are tabulated in Appendix B.

6.7 SUPPRESSION POOL BOUNDARY PRESSURES DUE TO STEAM CONDENSATION

6.7.1 Description of Phenomenon

After clearing the initial air/steam mixture a steady flow of steam (approximately 240 lbm/sec at a reactor pressure of 940 psig) passes through the quencher holes. Condensation of this steam in the pool results in high frequency, low magnitude pressure loads.

6.7.2 Instrumentation and Test Data Summary

The instrumentation used to record the steam condensation loads is the same as that used to measure pool boundary pressures during SRVDL clearing (see Subparagraph 6.5.2).

6.7.3 Results

The maximum pool boundary pressure measured at normal pool temperature due to steam condensation was ±2.5 psid (5.0 psid peak-to-peak) during Test 40. The frequency of these oscillations ranged from 65 to 95 Hz.

During the extended discharge test (Test 40) steam condensation boundary pressures were recorded over an average temperature range from 50° to 100°F in the immediate vicinity of the discharging quencher. Sensors T11 through T15 were used to determine the average temperature. Because of fluctuations in the measured values, pool temperatures and corresponding boundary pressures and frequencies were averaged over a time interval of 10 seconds in 70-second steps. Figures 6-28 and 6-29 present the average pressures and frequencies, respectively, as a function of the average temperature. The maximum boundary pressure measured during this test was 6.6 psid peak-to-peak at a temperature of 95°F. The frequencies of the pressure oscillations for this range of temperature varied from 50 to 125 Hz.

During the LP Tests 33 and 34 (reactor pressures of 50 psig and 100 psig, respectively) intermittent condensation oscillations with frequencies ranging from 25 to 50 Hz were observed. The period of these oscillations ranged from 0.3 to 0.4 second during Test 34 and approximately 0.6 second during Test 33. In either case the maximum amplitude of these oscillations was less than maximum boundary pressures due to steam condensation at normal reactor pressures. Also, the remaining low pressure tests produced normal steam condensation loads of lower magnitude than those resulting from full reactor pressure tests.

6.8 DFFR (REVISION 3)/DATA COMPARISON

The suppression pool boundary loads measured at Caorso can be directly compared with loads predicted by the current Mark II containment methodology. Only pool boundary pressure loads during the SRV discharge transient are considered here. The methodology for the SRV boundary loads discussed in the DFFR consists of independent calculations which are combined to describe the boundary loads. These calculations include the peak positive and negative boundary pressures, the distance attenuation of the peak pressures, and the determination of an idealized time history. Each is compared separately with measured data from the Caorso test.

6.8.1 Peak Positive and Negative Pressure Loads

In the DFFR the peak loads are obtained from a statistically derived correlation based on earlier small scale and full scale X-quencher test data. The correlation allows the loads to be calculated as mean values or with a confidence level. The DFFR recommends a 90-90 confidence level for the design value. In Table 6-4 the predicted mean and 90-90 confidence level bubble pressures for the corresponding test conditions are compared with observed peak pressures from the multiple valve, leaking valve, and low pressure tests. No measured pressures exceed the predicted mean bubble pressures, and the 90-90 design pressures generally exceed the measured pressures by a factor of 2 to 3. This demonstrates that design loads calculated with the DFFR methodology are conservative for the design of Mark II plants.

6.8.2 Distance Attenuation of Peak Loads

Comparisons of predicted versus measured attenuation were performed using predicted bubble pressures in the attenuation prediction model. Table 6-4 presents single and multiple valve model/data comparisons. The model was used to predict pressures corresponding to actual Caorso pressure sensor locations. Sensors P9, P13, P14, P15 and P17 were located on the suppression pool wall. Sensors P23, P35, P36, P37, P50 and P51 were located on the pool floor, while Sensors P26, P27 and P31 were located on the pedestal wall. Table 6-5 shows that in nearly all cases the model also over-predicts boundary pressures by a factor of 2 to 3. The results indicate a high degree of conservatism in the DFFR methodology for predicting maximum pool boundary pressures.

6.8.3 Time History

When comparing the DFFR time history with the Caorso data, the time attenuation and frequency content must be considered.

The DFFR specifies an idealized waveform which has a constant period where the maximum amplitude occurs in the second cycle, the first peak is 3/4 of the maximum, and the duration of the positive part of the cycle is 40% of the period.

The total duration is 0.75 second and the amplitude of the last cycle is 1/3 of the maximum. In general, the data showed faster time attenuation than predicted by the idealized waveform.

Figures 6-8 through 6-14 show time histories for the MVA, LV and LP tests. The well defined waveform observed in previous SVA and CVA tests becomes less distinguishable in the MVA tests. The exception is Test 32, an eight-valve test where greater distances between discharging lines causes less waveform distortion. In the MVA tests the bubble pressure for SRV A is represented by Sensor P19, SRV F is represented by Sensor P25, SRV U is represented by Sensor P51, and SRV E is represented by Sensor P50.

LP Test 36 (reactor pressure of 400 psig) is a single valve actuation test which exhibited waveform characteristics most closely approximating those specified in the DFFR. Conversely, Test 43 was a single leaking valve actuation test, and resulted in waveforms characterized by higher frequency oscillations (20 to 25 Hz) following the initial peak. Pressure frequencies of the MVA tests tended to be lower (in the 4 to 5 Hz range).

The following Tables are GENERAL ELECTRIC COMPANY PROPRIETARY and have been removed from this document in their entirety.

Table 6-1	Summary of Principal Hydrodynamic Data
Table 6-2	Summary of SRVDL Reflood Data
Table 6-3	PSD Comparison - Sensor P23
Table 6-4	DFFR (Revision 3)/Data Bubble Pressure Comparisons
Table 6-5	Caorso Model/Data Comparisons Model Predictions Based on Predicted Bubble Pressure

The following Figures are GENERAL ELECTRIC COMPANY PROPRIETARY and have been removed from this document in their entirety.

Figure 6-1a SRVDL Pressure Time Histories, Sensor PT25, Tests 2321, 36 and 34

Figure 6-1b SRVDL Pressure Time Histories, Sensor PT25, Tests 4401 , 4402, 27 and 32

Figure 6-2a Quencher Pressure Time Histories, Sensor P5, Tests 2321, 36 and 34

Figure 6-2b Quencher Pressure Time Histories, Sensor P5, Tests 4401, 4402, 27 and 32

Figure 6-3a Quencher Arm Pressure Time Histories, Sensor P6, Tests 2321, 36 and 34

Figure 6-3b Quencher Arm Pressure Time Histories, Sensor P6, Tests 4401, 4402, 27 and 32

Figure 6-4 Peak SRVDL and Quencher Internal Pressure versus Reactor Pressure

Figure 6-5 SRVDL Reflood Transient, Test 33

Figure 6-6 SRVDL Reflood Transient, Test 36

Figure 6-7 SRVDL Reflood Transient, Test 4401

Figure 6-8 Maximum Floor Pressure Time Histories, Sensor P19, SVA Tests 2301, 36, 34, 4401 and 4402

Figure 6-9 Maximum Floor Pressure Time Histories, Sensor P19, and P25, Two-Valve MVA Test 24

Figure 6-10 Maximum Floor Pressures and Phasing, Sensors P19, P25 and P50, Three-Valve MVA Test 26

Figure 6-11 Maximum Floor Pressures and Phasing, Sensors P19, P25, P50 and P51, Four-Valve MVA Test 27

Figure 6-12 Maximum Floor Pressure Time History, Sensor P19, Eight-Valve MVA Test 32

Figure 6-13 Floor Pressure SVA and MVA Comparison, Sensor P23, Tests 2301, 24 and 27

Figure 6-14 Boundary Pressure SVA and MVA Comparison, Sensor P18, Tests 2301, 24, 27 and 32

The following Figures are GENERAL ELECTRIC COMPANY PROPRIETARY and have been removed from this document in their entirety.

Figure 6-15 Pool Boundary Pressure versus Reactor Pressure
Figure 6-16 PSD, Test 2301 (SVA, CP, NWL). Sensor P23
Figure 6-16 PSD, Test 2301 (SVA, CP, NWL), Sensor P23

Figure 6-17 PSD, Test 2305 (CVA, HP, DWL), Sensor P23

Figure 6-18 PSD, Two-Valve Test 24 (MVA, CP, NWL), Sensor P23

Figure 6-19 PSD, Three-Valve Test 26 (MVA, CP, NWL), Sensor P23

Figure 6-20 PSD, Four-Valve Test 30 (MVA, CP, NWL), Sensor P23

Figure 6-21 PSD, Eight-Valve Test 32 (MVA, CP, NWL), Sensor P23

Figure 6-22 PSD, Test 36 (LP, SVA, 400psig), Sensor P23

Figure 6-23 PSD, Test 43 (LV, SVA), Sensor P23

Figure 6-24 PSD, Four-Valve Test 22A01 (SVA, CP, NWL), Sensor P51

Figure 6-25 PSD, Four-Valve Test 22A05 (CVA, HP, DWL), Sensor P51

Figure 6-26 ΔP Across a Submerged Structure (Column 7) SVA and MVA Comparison, Sensors P40 and P42, Tests 2301, 26 and 32

Figure 6-27 Intermittent Condensation Oscillation at Low Reactor Pressure (100 psig), Sensor P19, Test 34

Figure 6-28 Peak-to-Peak Condensation Oscillation versus Average Pool Temperature in the Quencher Area, Test 40

Figure 6-29 Condensation Oscillation Frequencies versus Pool Temperature in the Quencher Area, Test 40

7. QUENCHER STRUCTURAL RESPONSE

7.1 INTRODUCTION

The SRV discharge piping is 10-inch, Schedule 40, in the drywell and 10-inch, Schedule 80, in the wetwell. The material of the SRV piping is A106, Grade B, carbon steel. The configuration of SRVDL A is shown in Figure 7-1.

The four quencher arms attached to the quencher hub are 12-inch, Schedule 80. The material is A312 TP304, stainless steel. Each quencher arm has a total length of 46.5 inches.

The quencher is supported from the diaphragm floor by a rigid hanger in the vertical direction. The hanger is located at 37.85 feet above the center of the quencher arm on the SRV piping. The quencher support on the wetwell floor, as shown in Figure 7-2, provides horizontal restraint as well as moment restraint, but the quencher is free to move in the vertical direction.

The water clearing load associated with the SRV discharge acts downward on the quencher and is taken by the rigid hanger through the quencher reducer and the SRV pipe.

The horizontal loads associated with air clearing are taken by the quencher support on the wetwell floor.

7.2 DATA REDUCTION AND EVALUATION METHODS

7.2.1 Separation of Dynamic Stresses and Thermal Stresses

The stresses discussed in this section were calculated directly from the measured strains. The strains on the SRV piping resulted from the superposition of dynamic bending strain, dynamic axial strain, thermal expansion bending strain, pipe wall thermal gradient strain and pipe pressure strain. The strains caused by the different loads have different characteristics, as

illustrated in Figures 7-3 and 7-4. The differences in characteristics of strains caused by the different types of loading were used to evaluate the recorded strain time histories in the following manner.

Using SG33 and SG35 as examples, the following procedure was used to evaluate any given stress time history for loading components due to pipe temperature and dynamic loading effects.

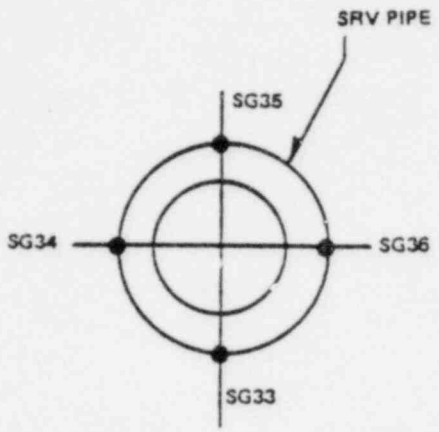

A mean stress line was first drawn through the stress time history. A sample line is shown on Figure 7-5 for SG33. This line represents the approximate stress component due to pipe temperature effects, S_{M33}. Deviations of the actual trace above and below the mean value line represent the stress component due to dynamic loading, S_{D33}. Using a similar procedure, a dynamic stress component was obtained for SG35.

Before the mean stress line was drawn on Figure 7-5, the magnitude and shape of the dynamic stresses were studied. In order to obtain conservative measurements, the mean stress line was drawn low when the maximum dynamic stress was in a positive direction; and high when the maximum dynamic stress was in a negative direction.

For the purpose of separating the dynamic axial stresses from the dynamic bending stresses, all the stress values at the same cross-section of the pipe should be taken at the same instant. This is illustrated by line A-A in Figure 7-5.

Given these two stress components, the dynamic axial stress component, S_{axial}, and the bending stress components, S_{DB33} and S_{DB35}, in the plane of SG33 and SG35 were calculated using the following equations:

$$S_{axial} = \frac{S_{D33} + S_{D35}}{2} \qquad (7\text{-}1)$$

$$S_{DB33} = S_{D33} - S_{axial}$$

$$S_{DB35} = S_{D35} - S_{axial}$$

$$= -S_{DB33}$$

Temperature induced stresses are comprised of two components, expansion stresses, S_E, and thermal gradient stresses, S_{DT}. Given the values of the temperature induced stresses, S_{M33} and S_{M35}, from the traces for SG33 and SG35, the expansion and thermal gradient stress components were calculated:

$$S_E = \frac{S_{M33} - S_{M35}}{2} \qquad (7\text{-}2)$$

$$S_{DT} = \frac{S_{M33} + S_{M35}}{2} \qquad (7\text{-}3)$$

Because the expansion stresses and the thermal gradient stresses were secondary stresses and not of primary interest in the test, the values were tabulated for only one test (see Table 7-1) to aid in understanding the piping response due to blowdown.

Figures 7-6 through 7-25 are computer output plots representative of the type of data acquired during Tests 24, 26, 27, 31, 32, 33, 36, 4401 and 4402. Utilization of the plots is described as follows:

P1 - Indicates time the SRV opened (Test 24 only).

P4 - Indicates time following SRV actuation when the pressure wave reached the water surface (Test 24 only).

P5 - Indicates peak pressure in the quencher hub (Test 24 only),

SG35 - Strain gage on the SRVDL just above the quencher to indicate the beginning of stresses in the wetwell piping (Test 24 only).

A15Z - Indicates vertical acceleration on the quencher hub.

A6Z - Indicates vertical acceleration on the diaphragm floor from which the quenchers are supported. The timing of the signals from A15Z and A6Z was used to decide the source of the indicated vibrations. Whether the quencher caused the diaphragm floor to vibrate or the diaphragm floor caused the quencher to vibrate, depended on which one reached peak value first. The results showed that the quencher caused the diaphragm floor to vibrate, because the accelerometer on the quencher reached its peak value first.

SG33 - Shows stress in the SRVDL above the quencher.

SG1 - Shows typical stresses on the top and bottom of the quencher arm.

LVDT1 - Indicates displacements of the quencher hub.

DYN PED SUP - Shows thrust loads on the quencher due to water clearing and air clearing.

7.2.2 Consideration of Pressure Effect in the Quencher Hub

Basically, the characteristics of the stresses measured on the quencher hub are similar to the characteristics of stresses measured on the discharge line. The difference being that the pressure strain is an important consideration in the evaluation of data for the hub. This is shown in the following equations.

Let

S_c be circumferential stress

S_ℓ be longitudinal stress

The longitudinal stress can be evaluated as

$$S_c \cong \frac{PD}{2t} \quad , \quad S_\ell \cong \frac{PD}{4t}$$

$$\varepsilon_\ell \cong \frac{PD}{E4t}(1 - 2\mu)$$

$$= \frac{PD}{10tE} \qquad (7\text{-}4)$$

$$S_\ell = 2.5E\varepsilon_\ell$$

where

P = internal pressure
D = outside diameter of the hub
E = modulus of elasticity of the hub material
t = hub wall thickness
μ = Poisson ratio

The circumferential stress can be evaluated as

$$\varepsilon_c \cong \frac{PD}{E2t}\left(1 - \frac{\mu}{2}\right)$$

$$S_c = 1.177E\varepsilon_c \qquad (7\text{-}5)$$

The hub stresses due to the high internal quencher pressure are associated with the water clearing phenomenon.

A conservative estimate of the maximum stress in the hub can be made from the following equations

$$S_c = 1.2E\varepsilon_c \quad \text{for time} > 0.0 \text{ sec} \tag{7-6}$$

$$S_\ell = 2.5E\varepsilon_\ell \quad \text{for time } 0 < + \leq 0.3 \text{ sec} \tag{7-7}$$

$$S_\ell = 1.2E\varepsilon_\ell \quad \text{for time} > 0.3 \text{ sec} \tag{7-8}$$

After the water clearing phenomenon (approximately 0.3 second after SRV actuation), the quencher arm bending moment predominated the stresses in the hub.

7.2.3 Separation of Dynamic Loads

7.2.3.1 General Description of Load

The SRV discharge transient results in various loads on the quencher and the submerged piping. These loads are identified as follows:

a. Transient wave load.

b. Internal pressure load.

c. Water clearing thrust load.

d. Air clearing plus uneven air-water clearing load.

e. Steady state steam condensation load.

f. Adjacent valve actuation loads.

The transient wave load occurred before the water had cleared the quencher. Because the quencher and submerged SRV piping stresses due to transient wave loads were relatively unimportant, they were not tabulated.

The internal pressure load caused small amounts of strain in the longitudinal direction, as indicated in Paragraph 7.2.2. Therefore, the logitudinal strain could not be separated from the axial load.

The internal pressure effect on the circumferential strain of the quencher hub could be separated from the local bending effect of the quencher arm, as outlined in Paragraph 7.2.1. In each test Sensor P5 indicated the time of peak pressure effect on the hub.

Consideration was given to the load imposed on both sides of the SRV pipe or quencher arms that occurred as a result of the pressure transient caused by air clearing plus uneven air-water clearing.

The load imposed on both sides of the quencher arms by the steady state steam condensation was much smaller than water clearing and air clearing, therefore, it was not tabulated.

There were no significant differences in measured stresses between the (SVA, CP, NWL) and (MVA, CP, NWL) tests. This indicates that blowdowns of quenchers adjacent to Quencher A resulted in negligible dynamic stresses on Quencher A.

7.2.3.2 Time Sequence of Dynamic Loads

The approximate time sequence of dynamic loads and blowdown events was as follows; data was obtained from Test 24 (MVA, CP, NWL) (see data plots on Figures 7-6, 7-7, 7-8 and 7-17).

		Approximate Time (sec)
a.	SRV opened	0.0
b.	Internal pressure increase started	0.0
	Peak pressure in quencher	0.27
c.	Significant water clearing load started	0.24
d.	Air clearing load started	0.3
e.	Steady state steam condensation started	0.62

7.2.4 Water Clearing Load Evaluation and Quencher Support Moments

Equation 7-1 in Paragraph 7.2.1 was used to evaluate the axial load transferred through the SRV pipe to the upper hanger.

Water clearing imparted an axial load to the SRVDL and also accelerated the mass of the quencher hub and the quencher arms. The movement of the quencher hub pressurized the water under the quencher hub as measured by Sensors P48 and P49. These pressure values (see Table 7-4) were found to be small. However, the effect of the pressure was included in the actual calculation but not in Equation 7-9 to simplify the expression.

The water clearing thrust load can be expressed as the following equation

$$T = A_p\left(\frac{S_{D33} + S_{D35}}{2}\right) + MA_{16y} + mc(A_{17x} + A_{18x} + A_{19x} + A_{20x}) \quad (7\text{-}9)$$

in which

T = Total water clearing thrust load

A_p = Metal area of SRV pipe at SG33 and SG35

= 18.92 in.^{2}

S_{D33}, S_{D35} definition, see Paragraph 7.2.1

M = Mass of quencher body + mass of the cone + mass of the nozzles + mass of steel attached to quencher body = 3427 lb

A_{16y} = Vertical accelerometer on quencher body

m = Mass of quencher arm + mass of water

= 2488 lb

c = Coefficient of equivalent mass for cantilever beam
= 0.363

A_{17x} = Vertical accelerometer at the end of the quencher arm. A_{18x}, A_{19x} and A_{20x} are on the other arms.

The peak thrust load was assumed to occur approximately at the time when the water was cleared from the quencher hub.

The total moments acting on the quencher support were evaluated in a similar manner by summing all strain gage measurements and accelerometer measurements.

7.2.5 Test Condition Categorization

The test data was separated into the following six test condition categories for evaluation:

SVA, CP, NWL
CVA, DWL
MVA, CP, NWL
LV
CVA, HP, EWL
Miscellaneous Cases

Two dynamic loading effects were evaluated for each strain gage as follows:

Water Clearing Loads (WC)
Air Clearing Loads (AC)

7.3 QUENCHER ARM RESPONSE

7.3.1 Instrumentation and Test Data Summary

There are 32 uniaxial strain gages and 4 biaxial accelerometers on the quencher arms. The arrangement of the sensors is shown in Figures 4-18 and 4-19.

The even-numbered strain gages were connected in a bending bridge in order to exclude the thermal effects. However, test results indicated there were still some differences of temperature between each side of the quencher arm.

The dynamic bending stresses calculated from the bending bridge measurements were only about 70 percent of the dynamic bending stress calculated from single gages. This is discussed in Appendix B of the Phase I Test Report. In the stress evaluations, the results from the single gages were used rather than the bending bridge measurements.

The tests results are tabulated in Tables 7-2 through 7-5. The results of SG19 located on the side of the quencher arm are not consistent with SG23 located 180° from SG19. Because the measurements from SG19 were determined to be unreasonable they were not tabulated. The accelerations at the end of each quencher arm are tabulated in Tables 7-16 and 7-17. Measurements from A19 were about 3 to 5g, which were inconsistent with the other arms and the results from the Phase I tests. Therefore, the results of A19 were not tabulated.

7.3.2 Results of Quencher Arm Response

Tables 7-6 through 7-9 are tabulations of the maximum, minimum, mean and standard deviation values for all the sensor measurements. These values were divided into six test condition categories: SVA, CP, NWL; CVA, HP, DWL; MVA, CP, NWL; LV; CVA, HP, EWL and miscellaneous cases.

The maximum stress of 5000 psi measured at the top and the bottom of the quencher arm was measured by SG21 during Test 2323.

The maximum stress of 2500 psi measured on either side of the quencher arm was measured during Tests 2313, 2323, 4401F and 4402F by several gages.

The stresses on either side of the quencher arms were caused by air clearing plus uneven air-water clearing loads.

Test condition LV caused 40 percent higher stresses on the top and bottom of quencher arms than the SVA, CP, NWL condition. In addition, the LV stresses are comparable to the CVA, HP, DWL test results.

The stresses measured on the top and bottom of the quencher arms were 60 percent higher than the stresses measured on the side of the quencher arms. The magnitudes of the quencher arm responses were approximately proportional to the initial reactor pressures. When reactor pressure was lower than 250 psig the responses were negligible.

Since the maximum stresses in the quencher arms occurred within the first second after SRV actuation, the extended discharge did not affect the stresses in the quencher arms.

No significant increases in stresses were measured in MVA tests.

The linear thermal gradient stresses in the quencher arm are plotted in Figure 7-26 for Test 45-2 starting from SRV actuation to about 1 minute after SRV closure.

Data in the figure shows that the linear thermal gradient stresses in the top and bottom of the quencher arms were much greater than the sides. The reflood of cold water after SRV closure did not cause any significant linear thermal gradient stresses for the test investigated.

7.4 SRV PIPE RESPONSE

7.4.1 Instrumentation and Test Data Summary

Four uniaxial strain gages (SG33, SG34, SG35 and SG36) were installed on the SRV pipe 1 foot above the reducer on the hub of the quencher. Sensor SG34 failed prior to start of testing. The dynamic stress data is tabulated in Table 7-10.

7.4.2 Result of SRV Pipe Response

Table 7-11 contains the maximum, minimum, mean, and standard deviation for each sensor categorized according to the test conditions.

Table 7-1 contains detailed stress evaluation results from SG33, SG35 and SG36 measurements for Test 39 in accordance with the equations outlined in Paragraph 7.2.1.

The maximum dynamic vibratory stress of 6700 psi was recorded during Test 45-2 (MVA, CP, NWL). The maximum total stress resulting from dynamic, weight and pressure effects was 8752 psi, as shown in Table 7-1. This stress was measured during the air clearing portion of the discharge transient. The stresses in the SRV pipe were about proportional to the test pressures. Since the maximum stresses in the SRV pipe occurred within the first second after SRV actuation the duration of discharge did not affect the stresses in the SRV pipe. No significant increases in stresses were measured in MVA tests as compared to SVA, CVA, or LV tests. The LV pipe stresses are comparable to the CVA, HP, DWL test results.

7.5 QUENCHER HUB RESPONSE

7.5.1 Instrumentation and Test Data Summary

Sensors SG37 and SG39 located on the quencher hub adjacent to the top and bottom of the quencher arm nozzle measured the longitudinal stress of the nozzle connection. Sensors SG38 and SG40 located on the quencher hub in the lateral direction measured the circumferential stresses of the nozzle connection. The total stresses which include pressure stresses and dynamic stress for all the tests are listed in Table 7-12.

There were five accelerometers and two LVDTs installed in the quencher hub to measure accelerations and displacements of the quencher hub. These sensors are A15X, A15Y, A15Z, A16X, A16Y, LVDT1 and LVDT2. LVDT2 failed prior to start of testing. The LVDT1 results are tabulated in Tables 7-16 and 7-17. The response spectra plotted for A15X, A15Y and A15Z from Test 45-1 are shown in Figures 7-27, 7-28 and 7-29, respectively. The responses are very low for frequencies below 10 Hz, and much higher for frequencies between 20 and 40 Hz.

Vertical displacement of the quencher hub caused by water clearing loads was much higher than air clearing. The average displacement for SVA, CP, NWL tests was 0.25 in.

7.5.2 Results of Quencher Hub Response

Table 7-13 contains the maximum, minimum, mean and standard deviation values for each sensor measurement and test condition.

The maximum stress of about 4800 psi was measured in the circumferential direction of the hub during air clearing in Test 2323. The maximum stress of 3000 psi was measured in the longitudinal direction of the hub during Tests 25, 41 and 4401.

The pressure peak which appeared in the quencher hub pressure time history did not appear in the stress measurement, i.e., a pressure peak of very short duration does not have enough energy to stress the hub. The stresses in the quencher hub were about proportional to the initial reactor pressures. Since the maximum stresses in the quencher hub occurred with the first second after SRV actuation, the extended discharge test did not affect the hub stresses.

No significant increases in hub stresses were measured in MVA tests as compared to SVA, CVA or LV tests. The LV hub stresses are comparable to the CVA, HP, DWL tests results.

7.6 WATER CLEARING THRUST LOADS AND QUENCHER SUPPORT MOMENTS

7.6.1 Data Summary

A summary of the WC loads, AC loads, and the total bending moments on the quencher support, M_x, M_y and M_z are presented in Tables 7-14 and 7-15.

The acceleration measurements used in the evaluation are listed in Tables 7-16 and 7-17.

7.6.2 Results of Water Clearing Thrust Load and Quencher Support Moments

The maximum water clearing thrust load of 98 kips was measured during Test 4405, (LV, CVA). The plots of the water clearing thrust for some selected tests are shown in Figures 7-17 to 7-25. The maximum air clearing thrust load was 110 kips measured during Test 45-2 (MVA, CP, NWL). The average water clearing thrust load obtained from SVA, CP, NWL tests was 37 kips. Test conditions for LV tests produced results which showed the load to be about twice the values of SVA, CP, NWL.

No significant increases in thrust loads and quencher support moments were measured in MVA tests as compared to SVA, CP, NWL tests. The LV thrust loads and quencher support moments are comparable to the CVA, HP, DWL test results.

The following Tables are GENERAL ELECTRIC COMPANY PROPRIETARY and have been removed from this document in their entirety.

Table 7-1	Detailed Stress Evaluation for the SRVDL SG33, SG35 and SG36 Measurements
Table 7-2	Data Summary of Quencher Arm Responses for Sensors SG1, SG2, SG5 and SG7
Table 7-3	Data Summary of Quencher Arm Responses for Sensors SG9, SG11, SG13 and SG15
Table 7-4	Data Summary of Quencher Arm Responses for Sensors SG17, SG21, SG23, P48 and P49
Table 7-5	Data Summary of Quencher Arm Responses for Sensors SG25, SG27, SG29 and SG31
Table 7-6	Quencher Arm Response Results for Sensors SG1, SG3, SG5 and SG7
Table 7-7	Quencher Arm Response Results for Sensors SG9, SG11, SG13 and SG15
Table 7-8	Quencher Arm Response Results for Sensors SG17, SG21, P48 and P49
Table 7-9	Quencher Arm Response Results for Sensors SG25, SG27, SG29 and SG31
Table 7-10	Data Summary of SRVDL Responses for Sensors SG33, SG35 and SG36
Table 7-11	SRVDL Response Results for Sensors SG33, SG35 and SG36
Table 7-12	Data Summary of Quencher Hub Responses for Sensors SG37, SG38, SG39 and SG40
Table 7-13	Hub Response Results for Sensors SG37, SG38, SG39 and SG40
Table 7-14	Data Summary of Forces and Support Moments
Table 7-15	Forces and Support Moments Results
Table 7-16	Data Summary of Quencher Accelerations
Table 7-17	Quencher Acceleration Results

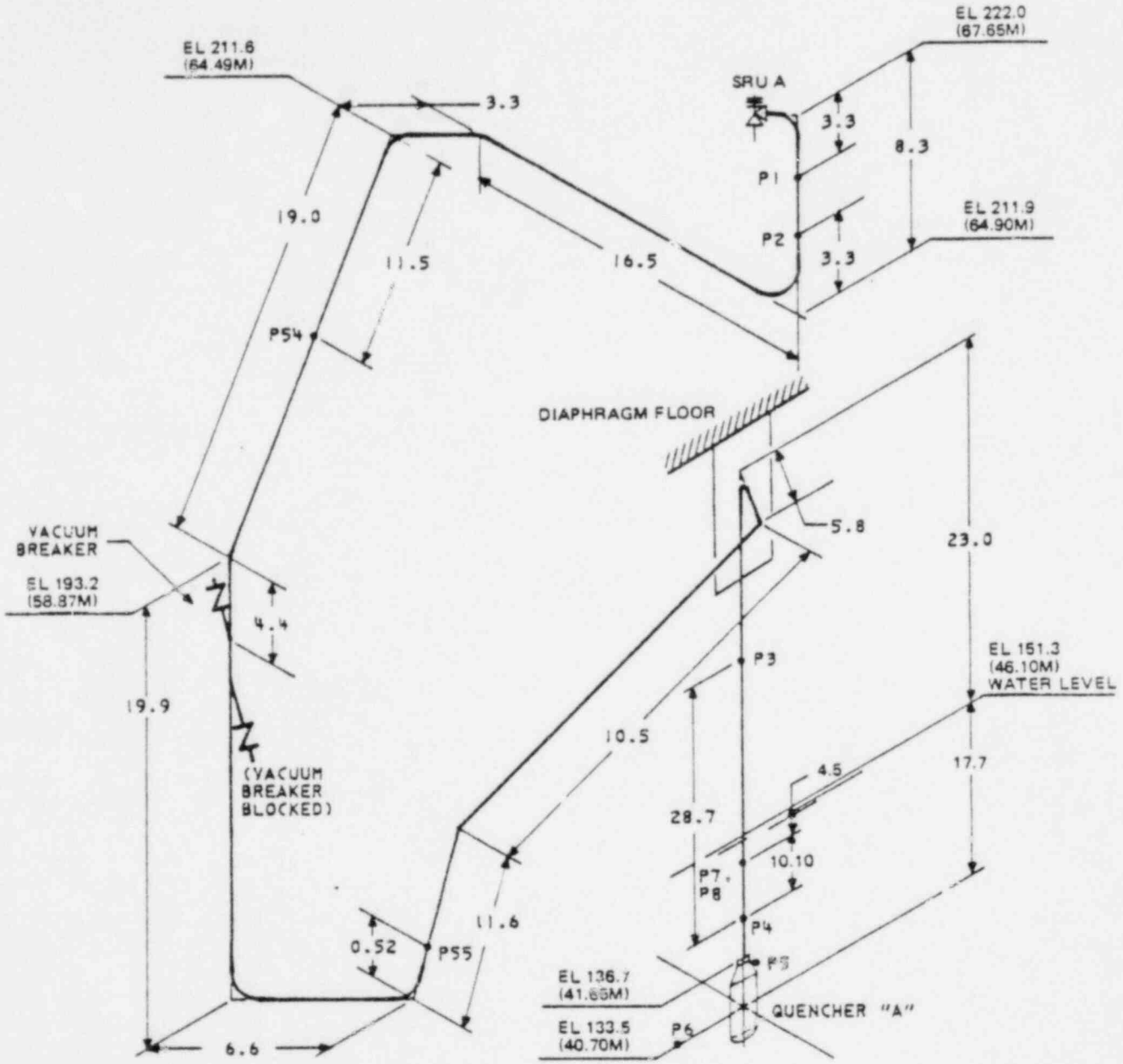

NOTE: ALL MEASUREMENTS ARE IN FEET UNLESS OTHERWISE NOTED.

Figure 7-1. SRV A Discharge Line and Quencher Configuration

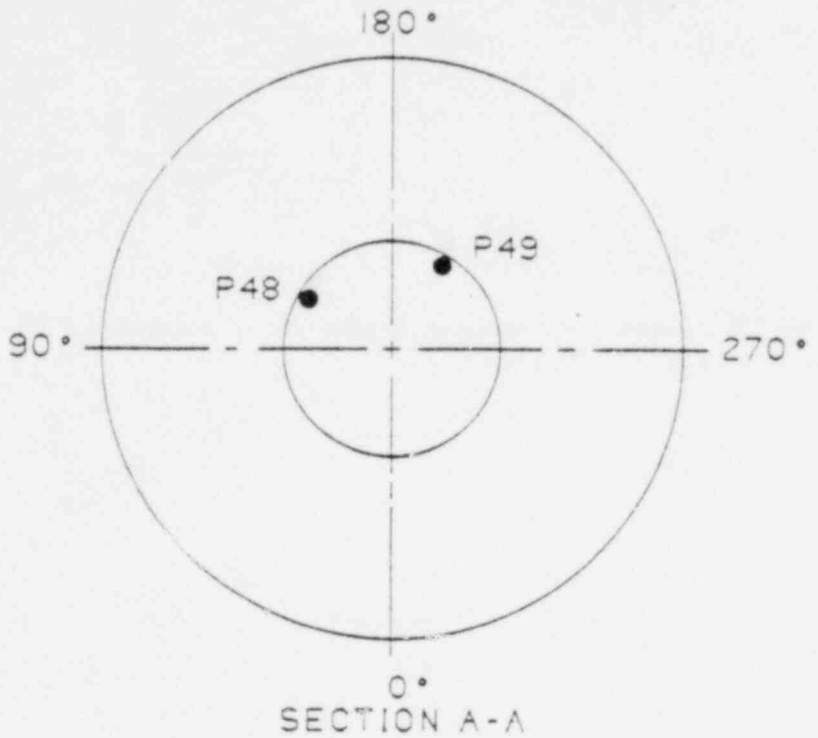

NOTE: PRESSURE SENSORS TO READ PRESSURE WITHIN PEDESTAL SUPPORT.

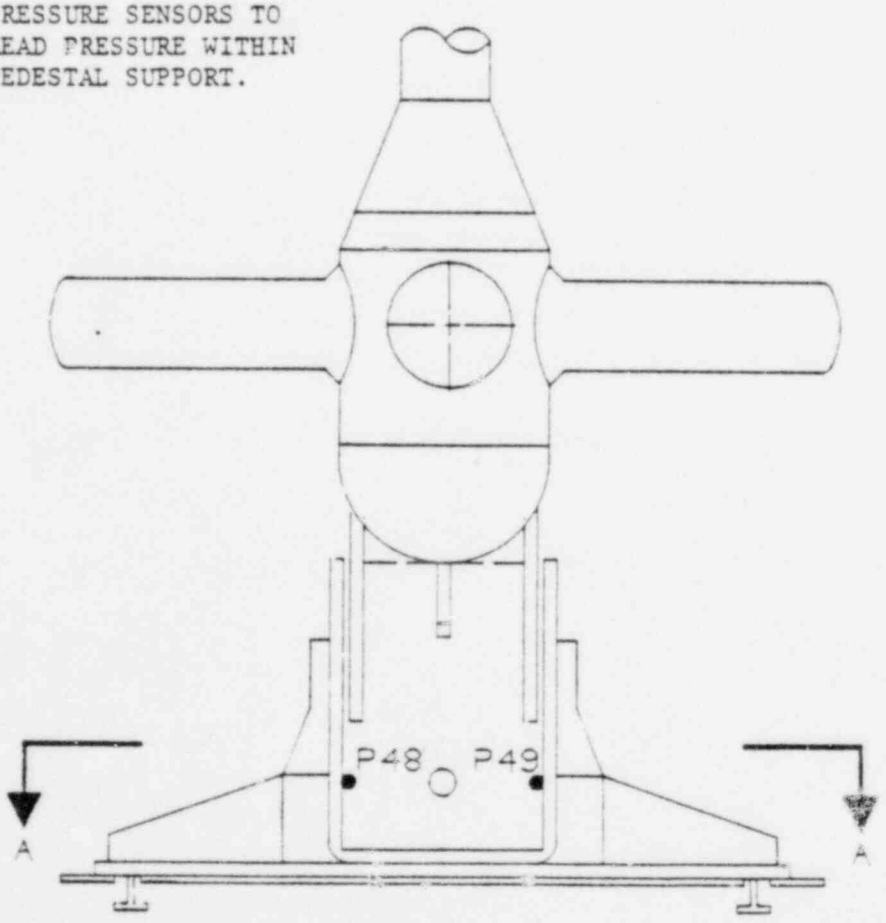

Figure 7-2. Pressure Sensors in Quencher Support

The following Figures are GENERAL ELECTRIC COMPANY PROPRIETARY and have been removed from this document in their entirety.

Figure 7-3 Description of Stresses Measured by SG33 and SG35

Figure 7-4 Description of Stress Measured by SG33 and SG35

Figure 7-5 Data Time Histories, Sensors SG33, SG35 and and SG36, Test 39

Figure 7-6 Data Time Histories, Sensors P1, P4, P5 and SG35, Test 24

Figure 7-7 Data Time Histories, Sensors SG1, SG33, A6Z and A15Z, Test 24

Figure 7-8 Data Time Histories, Sensors SG37, SG38, SG39 and SG40, Test 24

Figure 7-9 Data Time Histories, Sensors SG1, SG33, A6Z and A15Z, Test 26

Figure 7-10 Data Time Histories, Sensors SG1, SG33, A6Z and A15Z, Test 27

Figure 7-11 Data Time Histories, Sensors SG1, SG33, A6Z and A15Z, Test 31

Figure 7-12 Data Time Histories, Sensors SG1, SG33, A6Z and A15Z, Test 32

Figure 7-13 Data Time Histories, Sensors SG1, SG33, A6Z and A15Z, Test 33

Figure 7-14 Data Time Histories, Sensors SG1, SG33, A6Z and A15Z, Test 36

Figure 7-15 Data Time Histories, Sensors SG1, SG33, A6Z and A15Z, Test 4401

Figure 7-16 Data Time Histories, Sensors SG1, SG33, A6Z and A15Z, Test 4402

Figure 7-17 Thrust Load and Quencher Displacement (LVDT1) Time Histories, Test 24

Figure 7-18 Thrust Load and Quencher Displacement (LVDT1) Time Histories, Test 26

The following Figures are GENERAL ELECTRIC COMPANY PROPRIETARY and have been removed from this document in their entirety.

Figure 7-19 Thrust Load and Quencher Displacement (LVDT1) Time Histories, Test 27

Figure 7-20 Thrust Load and Quencher Displacement (LVDT1) Time Histories, Test 31

Figure 7-21 Thrust Load and Quencher Displacement (LVDT1) Time Histories, Test 32

Figure 7-22 Thrust Load and Quencher Displacement (LVDT1) Time Histories, Test 33

Figure 7-23 Thrust Load and Quencher Displacement (LVDT1) Time Histories, Test 36

Figure 7-24 Thrust Load and Quencher Displacement (LVDT1) Time Histories, Test 4401

Figure 7-25 Thrust Load and Quencher Displacement (LVDT1) Time Histories, Test 4402

Figure 7-26 Linear Thermal Gradient Stress Transient at Quencher Arm

Figure 7-27 Acceleration Response Spectrum/0.02 Damping, Sensor A15X,Test 45-1

Figure 7-28 Acceleration Response Spectrum/0.02 Damping, Sensor A15Y,Test 45-1

Figure 7-29 Acceleration Response Spectrum/0.02 Damping, Sensor A15Z, Test 45-1

8. CONTAINMENT DYNAMIC RESPONSES

8.1 INTRODUCTION

Accelerometers A1 through A14 were installed for the purpose of measuring containment dynamic responses. The responses measured during Phase I single valve tests have been discussed in the Phase I Test Report. Further studies on the scattering of data and the effect of subsequent actuations for Phase I data are included in this section. However, the majority of this section concentrates on the interpretation and discussion of Phase II test data. The specific topics discussed in this section are the repeatability of the tests, the comparison of MVA and SVA tests, the effects of valve actuation time phasing on MVA tests, and the effects of a leaking valve.

8.2 DATA REDUCTION AND EVALUATIONS METHODS

8.2.1 Time Histories and Response Spectra

The acceleration time histories were recorded at 1-millisecond intervals. Wild points were partially removed by discarding unreasonably high values. The time histories were filtered through a 100 Hz low-pass filter. The resulting time histories were plotted and maximum values tabulated. Response spectra were calculated for 1.4 seconds of the time history which included approximately the first 1.2 seconds of the SRV bubble oscillation. A critical damping ratio of two percent was used in the response spectra calculations.

8.2.2 RPV Data

Accelerometer A11 located on the RPV at the top flange is physically composed of 3 piezoelectric accelerometers with a sensitivity of 220 picocoulomb/g. The high sensitivity enables the sensors to easily saturate and block the passage of data through the remote charge converter. This problem was corrected by installing a low-pass filter between the accelerometer and the remote charge converter during the break between Phase I and Phase II testing. A shortage

of 100 Hz low-pass filters permitted the installation of only one 100 Hz filter on Accelerometer A11Z, while 1000 Hz low-pass filters were used on A11X and A11Y. Consequently, the saturation problem for A11Z was solved, but A11X and A11Y still showed partial saturation. Therefore, only A11Z data will be used in this discussion.

The data were recorded on FM tapes, and then processed by an HP Fourier Analyzer 5451B. The time histories were first processed through an anti-aliasing filter and then digitized at 5-millisecond intervals using 5.12 seconds of the time history to generate response spectra.

8.3 SCATTERING OF DATA

Fifteen Phase I tests had similar test conditions, i.e., first actuation of Valve A, CP, NWL, and reactor pressure varying from 924 to 937 psig, which included Tests 1 through 4, 501, 601, 7 through 10, 1101, 1301, 1401, 21 and 2201. Accelerations measured during these tests showed significant scattering due to environmental noise, uncontrolled sources of vibrations, and other parameters. The means, standard deviations and coefficients of variation for the maximum accelerations of six accelerometers at various locations are given in Table 8-1. The coefficient of variation defined as the ratio between the standard deviation and the mean varies from 0.13 to 0.25. The accelerations at the top of biological shield wall had the greatest scattering. Histograms for some of these maximum accelerations are shown in Figures 8-1(a) through (d), in terms of Z variable, defined as

$$Z = \frac{X - m}{s}$$

where X, m and s are the individual maximum acceleration, the mean maximum acceleration and the standard deviation, respectively. A large cell width of one standard deviation was used in the plot because of the small sample size. In Figure 8-1(e) these four histograms were lumped into a composite which exhibits a reasonably normal distribution.

8.4 REPEATABILITY OF TESTS

In view of the scattering of the data, the repeatability of the tests needs to be investigated. "Repeatability" is defined as the quality of being able to produce similar results, in terms of response magnitudes and frequency contents, if the test is repeated after some significant elapsed time.

Tests 1401 and 1402 from Phase I, and Tests 2311 and 2312 from Phase II were selected for comparison. These tests represent typical first and second actuations of Valve A and their repetitions in Phase II. Figures 8-2 through 8-13 compare the response spectra from these tests. The responses agree reasonably well in both frequencies and magnitudes. Therefore, it is concluded that the repeatability of the tests is reasonably good.

8.5 COMPARISON OF FIRST AND SUBSEQUENT ACTUATIONS

Pressure oscillations in the pool from a first actuation with NWL started with a high initial pressure peak, followed by some lower amplitude low frequency oscillations. Those from a subsequent actuation with DWL had a relatively low initial pressure peak and high subsequent low frequency oscillations. In order to study the difference in structural responses caused by these two types of pressure oscillations, acceleration data from Tests 7 and 2202 were compared, except for A11. Acceleration data from Tests 22A01 and 22A02 were compared for A11Z.

The comparisons of response spectra from the two tests shown in Figures 8-14 through 8-19 indicate that the second actuation response spectra generally appears to envelope the first actuation response spectra. Differences in the shapes of the spectra indicate that different structural modes were excited by the two types of actuations. Note that the peak pool pressures measured for Tests 7 and 2202 are 5 psi and 7.5 psi, respectively. If the response spectra from the two tests are normalized to the same pressure amplitude, the first actuation response spectra will exceed the second actuation response spectra at some higher frequencies. Also note that responses on the diaphragm floor that were mainly caused by quencher vibrations did not show any significant difference (see Figure 8-16).

8.6 COMPARISON OF MULTIPLE VALVE AND SINGLE VALVE TESTS

In order to study the multiple valve effect on structural responses, accelerations from Tests 7, 32 and 45-1 were selected for comparison, including one, eight and four-valve actuations, respectively. Since Test 7 data was not available for the RPV responses, Test 22A01 data was used. The maximum accelerations and the ratios between multiple and single valve test accelerations are shown in Tables 8-2 and 8-3. Response spectra were also compared for the differences in frequency content.

8.6.1 RPV Response

Data given in Table 8-2 (Accelerometer A11Z) shows the acceleration increased when multiple valves were actuated. However, the greatest acceleration occurred during Test 45-1 when four adjacent valves were actuated. The increase in accelerations was substantially less than proportional to the number of valves actuated due primarily to differences in spatial distributions of the pressure loads (see Table 8-3, Accelerometer A11Z). The comparison of response spectra is shown in Figure 8-20.

8.6.2 Pedestal and Biological Shield Wall Response

The radial accelerations measured at the top of the biological shield wall were about 0.05g for both the four-valve Test 45-1 and the eight-valve Test 32 (see Table 8-2, Accelerometer A1Y). The accelerations from both of these tests were higher than those observed for Test 7 (see Table 8-3, Accelerometer A1Y). The comparison of response spectra is shown in Figure 8-21.

Radial and vertical accelerations at the top of the pedestal (accelerometers A3Y and A4Z) are given in Table 8-2. Both the radial and vertical accelerations for Tests 32 and 45-1 were higher than those observed for Test 7 (see Table 8-3, Accelerometers A3Y and A4Z, respectively). The comparison of response spectra at the top of the pedestal is shown in Figure 8-22.

8.6.3 Containment and Basemat Response

The maximum radial accelerations on the containment were 0.069g and 0.088g, for Tests 32 and 45-1, respectively (see Table 8-2, Accelerometer A12Y). This indicates that the containment responded more to the actuation of four adjacent valves than to the eight uniformly distributed valves. The responses for both tests were higher than those observed during Test 7 (see Table 8-3, Accelerometer A12Y).

Maximum vertical accelerations on the basemat are given in Table 8-2 (see Accelerometers A13 and A14). The accelerations for the MVA tests were higher than those observed for Test 7 (see Table 8-3, Accelerometers A13 and A14).

By the comparison of response spectra for the three tests at both the containment and the basemat (see Figures 8-23 and 8-24), apparently different structural modes were excited by the different tests.

8.6.4 Operating Floor Response

The eight-valve test (Test 32) produced the highest horizontal and vertical accelerations on the operating floor (see Table 8-2, Accelerometers A5Y and A5Z). The horizontal accelerations had a greater increase when more valves were actuated than the vertical accelerations did (see Table 8-3). The vertical accelerations on the operating floor were lower than those on the basemat which indicates no overall building amplification during the eight-valve test.

8.6.5 Diaphragm Floor Response

Because the quenchers are supported vertically by the diaphragm floor, high vertical accelerations caused by quencher vibrations were observed on the diaphragm floor (see Table 8-2, accelerometer A6Z). These accelerations did not increase relative to the single valve test responses for the four-valve (Test 45-1) and the eight-valve (Test 32) tests (see Table 8-3). This indicates that the vibrations are localized and non-additive when more valves open.

Data in Table 8-3 also shows that radial accelerations on the diaphragm floor in both MVA tests increased over those of Test 7. Figure 8-25 shows that the diaphragm floor responded in roughly the same predominant vibration mode.

8.7 TIME PHASING EFFECT FOR MULTIPLE VALVE TESTS

Tests 27 through 30 and 45-1 and 45-2 included actuation of the same four valves (Valves A, E, F and U), with CP and NWL. The reactor pressure only varied from 969 psig to 982 psig. The only key variable was the time lag between actuations of valves. Figure 8-26 shows the maximum acceleration measured in the tests as a function of the time lag between the actuations of the first and the last valves. The accelerations appear to be affected by the time phasing. However, if the ratios of standard deviation over mean for those four-valve tests are compared with the coefficients of variation for single valve tests (see Table 8-4), the time phasing effects are small.

8.8 EFFECT OF LEAKING VALVE

Pool pressure during the first actuation of a leaking valve tends to oscillate at higher frequencies than those of non-leaking single valve first actuations. Figures 8-27 through 8-32 show the comparison of response spectra from Tests 4401 and 7 which were leaking and non-leaking valve tests, respectively. Except for the diaphragm floor response, the leaking valve actuation generally caused higher responses than the non-leaking single valve first actuations. However, the responses observed on the diaphragm floor are about the same (see Figure 8-17). It is further noted that the responses from the single leaking valve test (Test 4401) were in general bounded by those from the four-valve or eight-valve tests (Tests 45-1 or 32, respectively).

The following Tables are GENERAL ELECTRIC COMPANY PROPRIETARY and have been removed from this document in their entirety.

Table 8-1	Scattering of Maximum Accelerations
Table 8-2	Measured Maximum Accelerations
Table 8-3	Ratios of Maximum Accelerations Between Multiple and Single Valve Tests
Table 8-4	Time Phasing Effect for Four-Valve Tests

The following Figures are GENERAL ELECTRIC COMPANY PROPRIETARY and have been removed from this document in their entirety.

Figure 8-1 Histograms of Maximum Acceleration (SVA, CP, NWL, Valve A)

Figure 8-2 Phase I and Phase II Response Spectra/0.02 Damping, Sensor A1Y, Test 1401 and 2311

Figure 8-3 Phase I and Phase II Response Spectra/0.02 Damping, Sensor A2Y, Test 1401 and 2311

Figure 8-4 Phase I and Phase II Response Spectra/0.02 Damping, Sensor A3Y, Test 1401 and 2311

Figure 8-5 Phase I and Phase II Response Spectra/0.02 Damping, Sensor A4Z, Test 1401 and 2311

Figure 8-6 Phase I and Phase II Response Spectra/0.02 Damping, Sensor A12Y, Test 1401 and 2311

Figure 8-7 Phase I and Phase II Response Spectra/0.02 Damping, Sensor A14, Test 1401 and 2311

Figure 8-8 Phase I and Phase II Response Spectra/0.02 Damping, Sensor A1Y, Test 1402 and 2312

Figure 8-9 Phase I and Phase II Response Spectra/0.02 Damping, Sensor A2X, Test 1402 and 2312

Figure 8-10 Phase I and Phase II Response Spectra/0.02 Damping, Sensor A3Y,Test 1402 and 2312

Figure 8-11 Phase I and Phase II Response Spectra/0.02 Damping, Sensor A4Z, Test 1402 and 2312

Figure 8-12 Phase I and Phase II Response Spectra/0.02 Damping, Sensor A12Y, Test 1402 and 2312

Figure 8-13 Phase I and Phase II Response Spectra/0.02 Damping, Sensor A14, Test 1402 and 2312

Figure 8-14 Phase I and Phase II Response Spectra/0.02 Damping, Sensor A1Y, Test 1402 and 2312

Figure 8-15 Phase I and Phase II Response Spectra/0.02 Spectra/0;02 Damping, Sensor A4Z, Tests 2202 and 7

Figure 8-16 First and Subsequent Actuations Response Spectra/0.02 Damping, Sensor A6Z, Tests 2202 and 7

The following Figures are GENERAL ELECTRIC COMPANY PROPRIETARY and have been removed from this document in their entirety.

Figure 8-17 First and Subsequent Actuations Response Spectra/0.02 Damping, Sensor A12Y, Tests 2202 and 7

Figure 8-18 First and Subsequent Actuations Response Spectra/0.02 Damping, Sensor A14, Tests 2202 and 7

Figure 8-19 First and Subsequent Actuations Response Spectra/0.02 Damping, Sensor A11Z, Tests 22A01 and 22A05

Figure 8-20 SVA and MVA Response Spectra, Sensor A11Z, Tests 32, 22A01 and 45-1

Figure 8-21 SVA and MVA Response Spectra/0.02 Damping, Sensor A1Y, Tests 7, 32 and 45-1

Figure 8-22 SRV and MVA Response Spectra/0.02 Damping, Sensor A4Z, Tests 7, 32 and 45-1

Figure 8-23 SRV and MVA Response Spectra/0.02 Damping, Sensor A12Y,Tests 7, 32 and 45-1

Figure 8-24 SRV and MVA Response Spectra/0.02 Damping, Sensor A14, Tests 7, 32 and 45-1

Figure 8-25 SRV and MVA Response Spectra/0.02 Damping, Sensor A6Z,Tests 7, 32 and 45-1

Figure 8-26 Effects of Time Phasing for Four-Valve Tests

Figure 8-27 Leaking and Non-Leaking Valve Actuations Response Spectra/0.02 Damping, Sensor A1Y, Tests 7 and 4401

Figure 8-28 Leaking and Non-Leaking Valve Actuations Response Spectra/0.02 Damping, Sensor A4Z, Tests 7 and 4401

Figure 8-29 Leaking and Non-Leaking Valve Actuations Response Spectra/0.02 Damping, Sensor A6Z, Tests 7 and 4401

Figure 8-30 Leaking and Non-Leaking Valve Actuations Response Spectra/0.02 Damping, Sensor A12Y, Tests 7 and 4401

The following Figures are GENERAL ELECTRIC COMPANY PROPRIETARY and have been removed from this document in their entirety.

Figure 8-31 Leaking and Non-Leaking Valve Actuations Response Spectra/0.02 Damping, Sensor A14, Tests 7 and 4401

Figure 8-32 Leaking and Non-Leaking Valve Actuations Response Spectra/0.02 Damping, Sensor A11Z, Tests 7 and 4401

APPENDIX A

INSTRUMENTATION ACCURACY COMPARISON

CAORSO PHASE I AND PHASE II TESTS

A.1 SUMMARY

A representative sample of the data obtained during Phase II of the Caorso SRV Test Program was reviewed. The magnitude and response characteristics of this data and the testing conditions were compared with equivalent Phase I data and conditions to determine if sufficient differences existed between the two phases of testing to warrant a separate Phase II accuracy evaluation.

The documentation of each sensor replaced or repaired after termination of Phase I testing was reviewed to determine if each instrument could be identified by serial number.

The conclusions from this investigation are presented in Section A.2. A description of the comparisons is presented in Section A.3.

A.2 CONCLUSIONS

The end-to-end instrumentation accuracies reported in Appendix B of the Phase I Test Report are also valid for Phase II tests. Although some measurements were of greater magnitude in Phase II than the corresponding measurements in Phase I, the increase did not result in significant accuracy differences.

A.3 DISCUSSION

The same phenomena were investigated during both phases of SRV Tests. The primary difference between the two test series was that during Phase II more than one SRV was actuated simultaneously. Thus, the conditions which the sensors were subjected to and the frequency response characteristics of the measured variables were essentially identical in Phase I and Phase II. The magnitudes of some measurements, most notably building accelerations, showed increases in Phase II due to the simultaneous multiple SRV actuations.

The Phase II tests which differ significantly from those conducted during Phase I are discussed in this report. These tests include the multiple valve tests affecting the response of the accelerometers, and the leaking valve tests affecting the strain gage data. All other tests and data similar to Phase I will not be discussed in detail.

Appendix B of the Phase I Test Report established a basis for determining the accuracy of any data obtained from the Data Acquisition System. As long as the data obtained does not change significantly in magnitude, the accuracy described in Appendix B will apply.

Table A-1 shows various pressure, strain gage and accelerometer data for the conditions existing during both Phase I and Phase II testing. The mean values measured for each condition (SVA and CVA for Phase I, and SVA, CVA, MVA, LP and LV for Phase II), and the maximum value measured during each phase are shown for each sensor listed in the table. The values shown were obtained from the Caorso Test Plan and the Phase I Test Report. This table compares the Phase I and Phase II data and shows that instrumentation accuracy presented in the Phase I Test Report is valid for both phases.

A.3.1 ACCELEROMETERS

The Entran accelerometers, excluding those mounted on the quencher, showed the largest magnitude changes between the Phase I and Phase II tests. However, the maximum values are still in the ranges discussed in Appendix B of the Phase I Test Report, so the total instrument error previously calculated remains valid. Example: Table A-1, the value obtained from Sensor A6Y doubles from Phase I (0.04g) to Phase II (0.08g).

Possible error due to non-linearity = 0.01* x 0.08g = 0.0008g

Possible error due to transverse sensitivity = 0.03* x 0.08g = 0.0024g

Possible error due to data acquisition system** = 0.0160g

TOTAL ERROR = $\sqrt{a^2+b^2+c^2}$ = 0.016g

This error is identical to the error given for Phase I in the Phase I Test Report appendix, and as a percentage of the measured value, the error is actually less than that measured in Phase I (40 percent in Phase I versus 20 percent in Phase II).

As a percentage of measured value, the error decreases as the measured value increases until full scale is approached, because the error introduced by the data acquisition system is much greater than that of the individual sensor, if the magnitude of the parameter measured is somewhat below full scale. In the example, the largest single error in A6Y was ±0.016g, which was calculated as a fraction of the sensor full scale. Therefore, this error did not increase from Phase I to Phase II although the actual reading may have increased. This is generally true for all sensors in the Caorso tests.

*Error contributions discussed in Appendix B to the Phase I Test Report.
**Error due to data recording system and signal conditioning equipment = 0.16 percent of full scale value.

A.3.1.1 The Accuracy of the Endevco Model 2236 Accelerometer

Accelerometer A11 was not discussed in Appendix B to the Phase I Test Report because this sensor was inoperable during the entire first phase of testing. On completion of Phase I testing, Accelerometer A11 was repaired but only the Z axis remained operable throughout the remainder of the test program. The accuracy of this accelerometer is discussed below.

With the exception of temperature sensitivity, the significant sources of error for the Entran accelerometer are identical to those of the Endevco accelerometers:

a. Error due to non-linearity = 1 percent of full scale value

b. Error due to transverse sensitivity = 3 percent of sensitive axis

c. Error due to Data Acquisition System = 0.16 percent of full scale value.

In addition to these errors, the Endevco accuracy was affected by the high temperature environment. During the Caorso test program the temperature at the reactor flange where Accelerometer A11 is mounted ranged from 400° to 500°F. At these temperatures the Endevco unit can be in error by ±18 percent of the reading.

Also contributing to the total error of this Triaxial Endevco Accelerometer are zero shifts in the Z axis. The uncertainty in identifying the shifted zero point in this case is approximately ±0.003g.

Table A-2 shows typical accuracy tabulations for Accelerometer A11.

A.3.1.2 Pressure Transducers

Data in Table A-1 shows that pressure measurements from Phase I and Phase II are essentially the same. As in the case of accelerometers, the major contributions to pressure sensor error are calculated as fractions of full scale. Therefore, although some few pressure sensors (P51 for instance) showed Phase II readings somewhat higher than their Phase I readings the expected errors for both test series are the same.

Zero shifts were also evident on some suppression pool sensors - P22, P42, P52, P9, and P57. These should be treated as recommended in the Phase I accuracy evaluation, i.e., data valid to ±1 psi. Readings from P1 and P2 still showed discrepancies. A difference of 50 psi was seen in Test 24. Sensor PT25 which measured the SRVDL pressure downstream of P1 and P2 sometimes showed higher values than P1 and P2, although the downstream location suggests that PT25 should have shown lower values.

A.3.1.3 All Other Sensors

The data from strain gages, water level sensors, flow elements, position indicators and temperature detectors were approximately the same in both phases. Since there was no change in their environment, the accuracy stated in the Phase I accuracy evaluation is valid for Phase II results.

Table A-1 is GENERAL ELECTRIC COMPANY PROPRIETARY and has been removed from this document.

Table A-2

ENDEVCO ACCELEROMETER ACCURACY

Component	
Typical Reading	0.06
Nonlinearity	±0.0006g
Transverse Sensitivity	±0.0018g
Temperature Sensitivity	±0.0100g
Zero Shift	±0.003g
Data Acquisition System	±0.016g
TOTAL ERROR $= \sqrt{a^2+b^2+c^2+\ldots}$	0.019g

APPENDIX B

HYDRODYNAMIC DATA

Tables B-1, B-2 and B-3 are GENERAL ELECTRIC COMPANY PROPRIETARY and have been removed from this document.

B.1 QUENCHER BOUNDARY PRESSURE OSCILLATION PHASING

B.1.1 INTRODUCTION

Because of the nonsymmetrical orientation of the quencher arms and films from small scale tests showing different size bubbles forming around the quencher, the phasing of the boundary pressure loads around a single quencher during water/air clearing was studied. Normal SVA and CVA responses were discussed in the Phase I Final Test Report.

The following cases are considered in this appendix:

a. Test 36 (LP, SVA). Reactor pressure of 400 psig

b. Test 43 (LV, SVA)

c. Test 30 (MVA, CP, NWL). Four valves actuated within 92 milliseconds

d. Test 26 (MVA, CP, NWL). Three valves actuated within 101 milliseconds

These four cases cover the different oscillating load cases seen during the Phase II tests. Case a (Figures B-1 and B-2) shows a characteristic pressure oscillation throughout the transient, similar to normal reactor pressure SVA tests. Case b (Figures B-3 and B-4) shows the erratic pressure oscillations for a LV test. Cases c and d (Figures B-5 through B-8) show the responses to MVA tests characterized by high magnitude pressure peaks followed by somewhat irregular pressure oscillations.

B.1.2 RESULTS

Figures B-9 and B-10 show the Power Spectral Density (PSD) for Sensor P19 during Test 36 and the phasing between P19 and P23. Figure B-10 shows the two pressures to be in phase at the dominant frequency. The lack of phase correlation at higher frequencies is irrelevant since there is essentially no pressure signal at these frequencies (see Figure B-9).

Figures B-11 and B-12 present the PSD for Sensor P19 during Test 43 and the phasing between P19 and P23. PSDs for these LV tests are unusual in that they show the pressure energy to be distributed over a wide range of frequencies. Even so, Figure B-12 shows the two pressure sensors to be essentially in phase at the dominant frequencies.

Figures B-13 through B-16 present PSDs and the phasing for MVA Tests 26 and 30. In general, the MVA pressures were in phase. This can be seen in Figures B-13 and B-14, the PSD for Sensor P19 and the phasing between P19 and P50 for Test 30. Figure B-14 shows the two sensors to be in phase at the dominant frequencies. The PSD for sensor P19 and the phasing between P19 and P51 are shown in Figures B-15 and B-16 for Test 26. Examination of the PSDs for these MVA tests shows two significant peaks, one in the prevailing range of the bubble oscillation frequency between 5 and 10 Hz, and one of somewhat lower frequency. The two pressure signals are shown as being in phase at the lower dominant frequency, however, they are approximately 30 degrees out of phase at the higher frequency.

Figures B-1 through B-16 are GENERAL ELECTRIC COMPANY PROPRIETARY and have been removed from this document.

APPENDIX C

STRUCTURAL DYNAMIC DATA

I. MAXIMUM ACCELERATIONS	Test Number
Table C-1	22A01
	22A02
	22A03
	22A04
	22AC5
	2301
Table C-2	2302
	2303
	2304
	2305
	2311
	2312
	2313
Table C-3	2314
	2315
	2321
	2322
	2323
	2324
	2325
Table C-4	24
	25
	26
	27
	28
	29
	30
Table C-5	31
	32
	33
	34
	35
	36
	37
Table C-6	38
	39
	40
	41
	42
	43
	4401

	Test Number
Table C-7	4402
	4403
	4404
	4405
	45-1
	45-2
	501X

II. ACCELERATION RESPONSE SPECTRA

Test Number	Figure
7	C-1 thru C-26
2202	C-27 thru C-52
32	C-53 thru C-78
4401	C-79 thru C-104
45-1	C-105 thru C-130

Tables C-1 through C-7 are GENERAL ELECTRIC COMPANY PROPRIETARY and have been removed from this document.

Figures C-1 through C-130 are GENERAL ELECTRIC COMPANY PROPRIETARY and have been removed from this document.

APPENDIX D

SENSOR INDEX

This index cross references all sensors to the sections of the report where discussions of the sensor or sensor data are included.

Sensor	Report Section Presenting Results
P1	4.2, 6.3, 7.2, App. A
P2	4.2, 6.3
P3	4.2, 6.3
P4	4.2, 6.3, 7.2, App. B
P5	3.3, 4.2, 6.3, 7.2, App. A, App. B
P6	4.2, 6.3, App. B
P7	4.2
P8	4.2
P9	4.2, 6.5, 6.7, 6.8, App. B
P10	4.2, 6.5, 6.7, App. B
P11	4.2, 6.5, 6.7, App. B
P12	4.2, 6.5, 6.7
P13	4.2, 6.5, 6.7, 6.8, App. B
P14	4.2, 6.5, 6.7, 6.8, App. B
P15	4.2, 6.5, 6.7, 6.8, App. B
P16	4.2, 6.5, 6.7
P17	4.2, 6.5, 6.7, 6.8, App. B
P18	4.2, 6.5, 6.7, App. B
P19	4.2, 6.5, 6.7, 6.8, App. A, App. B
P20	4.2, 6.5, 6.7
P21	4.2, 6.5, 6.7
P22	4.2
P23	4.2, 6.5, 6.7, 6.8, App. A, App. B
P24	4.2, 6.6, App. B
P25	4.2, 6.5, 6.7, 6.8, App. B
P26	4.2, 6.5, 6.7, 6.8
P27	4.2, 6.5, 6.7, 6.8, App. B
P28	4.2, 6.5, 6.7

Sensor	Report Section Presenting Results
P29	4.2, 6.5, 6.7
P30	4.2, 6.5, 6.7
P31	4.2, 6.5, 6.7, 6.8, App. B
P32	4.2, 6.5, 6.7, App. B
P33	4.2, 6.6, App. B
P34	4.2, 6.6, App. B
P35	4.2, 6.5, 6.7, 6.8, App. B
P36	4.2, 6.5, 6.7, 6.8, App. B
P37	4.2, 6.5, 6.7, 6.8, App. B
P38	4.2, 6.5, 6.7, App. B
P39	4.2, 6.6, App. B
P40	4.2, 6.6, App. B
P41	4.2, 6.6, App. B
P42	4.2, 6.6, App. B
P43	4.2
P44	4.2
P45	4.2
P46	4.2
P47	4.2
P48	4.2, 7.2
P49	4.2, 7.2
P50	4.2, 6.5, 6.7, 6.8, App. A, App. B
P51	4.2, 6.5, 6.7, 6.8, App. A, App. B
P52	4.2
P53	4.2, 6.6, App. B
P54	4.2, 6.3, App. B
P55	4.2, 6.3
P56	4.2, 6.5, 6.7, App. B
P57	4.2, 6.5, 6.7
PT25	3.3, 4.2, 6.3, App. A, App. B
T1	4.2
T2	4.2

Sensor	Report Section Presenting Results
T3	4.2, 6.4
T4	4.2
T5	4.2
T7	4.2
T8	4.2
T9	4.2
T10	4.2
T11	4.2
T12	4.2
T13	4.2
T14	4.2
T15	4.2
T16	4.2
T17	4.2
T18	4.2
T19	4.2
T20	4.2
T21	4.2
T22	4.2
T23	4.2
T24	4.2
T26	4.2
T27	4.2, 6.4
T28	4.2, 6.4
L1	4.2, 6.4
L2	4.2, 6.4
L3	4.2, 6.4
L4	4.2, 6.4
L5	4.2, 6.4
L6	4.2, 6.4
L7	4.2, 6.4
L8	4.2, 6.4

Sensor	Report Section Presenting Results
L9	4.2, 6.4
L10	4.2, 6.4
L11	4.2, 6.4
L12	4.2, 6.4
TL6	4.2
LVDT1	4.2, 7.2, 7.5
LVDT2	4.2, 7.5
VB1	4.2
VB	4.2
VAP	4.2
VEP	4.2
VFP	4.2
VIP	4.2
A1	3.3, 4.2, 8.2, 8.5, App. A, App. C
A2	4.2, 8.1, App. A, App. C
A3	3.3, 4.2, 8.1, 8.5, App. A, App. C
A4	3.3, 4.2, 8.1, 8.5, App. A, App. C
A5	4.2, 8.1, 8.5, App. A, App. C
A6	4.2, 7.2, 8.1, 8.5, App. A, App. C
A7	4.2, 8.1, App. A, App. C
A8	4.2, 8.1, App. A, App. C
A9	4.2, 8.1, App. A, App. C
A10	4.2, 8.1, App. A, App. C
A11	4.2, 8.1, 8.3, 8.5, App. C
A12	4.2, 8.1, 8.5, App. A, App. C
A13	4.2, 8.1, 8.5, App. A, App. C
A14	4.2, 8.1, 8.5, App. A, App. C
A15	4.2, 7.2, 7.5, App. A
A16	4.2, 7.5, App. A.
A17	4.2, 7.2, 7.3, App. A
A18	4.2, 7.2, 7.3, App. A

Sensor	Report Section Presenting Results
A19	4.2, 7.2, 7.3, App. A
A20	4.2, 7.2, 7.3, App. A
A21	4.2
A22	4.2
A23	4.2
SG1	4.2, 7.2, 7.3, App. A
SG2/SG6	3.3, 4.2, 7.3, App. A
SG3	4.2, 7.3, App. A
SG4/SG8	3.3, 4.2, 7.3, App. A
SG5	4.2, 7.3, App. A
SG7	4.2, 7.3, App. A
SG9	4.2, 7.3, App. A
SG10/14	4.2, 7.3, App. A
SG11	4.2, 7.3, App. A
SG12/16	4.2, 7.3, App. A
SG13	4.2, 7.3, App. A
SG15	4.2, 7.3, App. A
SG17	4.2, 7.3, App. A
SG18/22	4.2, 7.3
SG19	4.2, 7.3
SG20/24	4.2, 7.3
SG21	4.2, 7.3, App. A
SG23	4.2, 7.3, App. A
SG25	4.2, 7.3, App. A
SG26/30	4.2, 7.3
SG27	4.2, 7.3, App. A
SG28/32	4.2, 7.3
SG29	4.2, 7.3, App. A
SG31	4.2, 7.3, App. A
SG33	3.3, 4.2, 7.2, 7.4, App. A
SG34	4.2, 7.4

Sensor	Report Section Presenting Results
SG35	3.3, 4.2, 7.2, 7.4, App. A
SG36	3.3, 4.2, 7.4, App. A
SG37	4.2, 7.5, App. A
SG38	4.2, 7.5, App. A
SG39	4.2, 7.5, App. A
SG40	4.2, 7.5, App. A
SG41	4.2
SG42	4.2
SG43	4.2
SG44	3.3, 4.2
SG45	4.2
SG46	3.3, 4.2
SG47	4.2
SG48	3.3, 4.2
SG49	4.2
SG50	4.2
SG51/53	3.3, 4.2
SG52/54	3.3, 4.2
SG55	4.2
SG56	4.2
SG57	4.2
SG53	4.2